University of Alberta

MIXED METAL OXIDE AND MIXED METAL OXIDE SUPPORTED -ION EXCHANGED ZEOLITE SORBENTS FOR HOT GAS DESULFURIZATION

by

SAGAR NARENDRA LUNAWAT

A thesis submitted to the Faculty of Graduate Studies and Research
in partial fulfillment of the requirements for the degree of

Master of Science
in
Chemical Engineering

Chemical and Materials Engineering

Fall 2012
Edmonton, Alberta

Dedicated to my father, late **Shri. Narendra Dagduram Lunawat**

His words of inspiration and encouragement

in pursuit of excellence, still linger on.

ABSTRACT

This study describes the evaluation of the mixed metal non-supported and supported ion exchanged sorbents for hot gas desulfurization capable of withstanding a wide temperature range and multiple sulfidation-regeneration cycles. Copper-cobalt, copper-cerium mixed metal oxide and mixed metal oxide supported- ions exchanged on natural zeolite (MMS-IZ) sorbents are studied in this work. Copper-cobalt mixed system is a good candidate for low temperature desulfurization while copper-cerium exhibits the high temperature stability and high performance. The reduced form of cerium oxide (CeO_n) in copper-cerium reduced the H_2S concentration to sub-ppmv level. The MMS-IZ sorbents also showed the high performance in desulfurization by surface interaction. Various combinations of these sorbents exhibited the high efficiency in H_2S removal. The thermodynamic analysis of the single metal oxide systems and H_2S concentration in equilibrium shows that the sulfidation is a strong function of temperature and can be calculated using Factsage 6.1 (GTT technologies).

Keyword: desulfurization, sorbent, regeneration, thermodynamic

ACKNOWLEDGEMENT

First, I would like to express my deep and sincere gratitude to my adviser, Dr. Rajender Gupta for his invaluable guidance, encouragement and all his experiences that he shared with me, not only pertaining to research but also about various other facets of life. Working with him exposed me to many invaluable experiences that I will deeply cherish for the rest of my life.

I would also like to thank Dr. Arunkumar Samanta for providing valuable suggestions and comments in this research study. This research is supported by the Canadian Center for Clean Coal/Carbon and Mineral Processing Technology (C^5MPT) and Alberta Innovates Technology Futures (AITF). I am also grateful to Mr. Allan Chambers and Mr. Juan Segura who shared the research facility at AITF and helped throughout the project. I would also like to thank Dr. Jingli Luo for sharing the research facility at NINT and Dr. Yoshihiko Ninomiya (Chubu University, Japan) for his guidance and help in thermodynamic analysis.

Most importantly, I would like to thank My Mother, My brother and Sister for unconditional support and encouragement. Finally, I would like to thank GOD for carrying me when everything else failed.

TABLE OF CONTENTS

LIST OF TABLES

LIST OF FIGURES

CHAPTER - 1

INTRODUCTION

In the last few decades, there has been almost 25-fold increase in the world energy demand. The increasing energy demand as well as the rapid economic development has to be met by the available current sources, fossil fuels as well as the renewable energy sources. Coal and natural gas are still the most promising sources of energy for coming decades. Among all the fossil fuels, coal reserves exceed that of the oil and gas and seem to have the highest potential as an energy carrier. In 2011, coal was the fastest growing form of energy outside renewables. The share of coal as an energy source in global primary energy consumption increased to 30.3% - the highest since 1969 (World Coal Association).

The role of coal in electricity production as well as the production of chemicals is expected to become more and more important as the world reserves of the other fossil fuels are diminishing. The world demand of electricity will increase by a factor of 2.5 in the near future and there is huge market for new and clean coal technologies to be developed. Conventional coal fired fire plants generate the electricity from coal where, almost two-third of the heating value is lost during generation of electricity. Hence, there is a huge opportunity for technologies with improved efficiency and utilization of coal.

However, the development and the growth in the utilization of coal cannot take place on the account of detrimental effect on the environment as well as human health. Use of large amount of coal causes various environmental problems such as SO_x, NO_x emission and emission of other several pollutants. Coal is playing important role in the new civilization but its use is raising many environmental concern and the stringent environmental regulations are set for emissions from coal gasification and combustion. In order to comply with this restriction there is a need of new advanced and environmental technologies.

The newer approach is the integrated gasification combined cycle (IGCC) which promises the higher thermal efficiency, superior performance and economics as compared to the conventional coal based power plants. The coal gasification is one of the practical examples of gas-solid reaction. Coal constitutes different contaminants such as sulfur, nitrogen, alkali and halogens that are released in the process of gasification in the form of syngas. According to the 2010 world gasification database the total world syngas output has grown to 70817 MW from 144 operating plant and 412 gasifiers. Syngas is one of the important building blocks and serve as a feedstock in chemical, oil, and energy industries. In order to use the syngas in downstream processes the contaminants present in the coal or other feedstocks must be removed to low levels. These contaminants may cause the erosion, corrosion, and loss of strength in the turbine blades, may act as a poison to the downstream catalyst. Furthermore, even trace amounts of sulfur in the feed gas can poison the anode catalysts in fuel cells.

Table 1.1 indicates the typical fuel gas composition and the H_2S concentrations in particular from various gasification systems

Table 1.1: Typical fuel gas composition (Haupt et al., 1995; ETSU, 1998)

Fuel Gas Properties Analysis, %v/v	**Shell**	**Texaco**	**BGL**	**ABGC**
CO	61-63	39-73	53-57	16-18
H_2	29-30	27-29	27-29	18-20
CO_2	1	12-14	1-2	9-10
N_2	4	1	3-4	44-46
CH_4	0	0	5-7	<2
H_2O	3	16-19	3-5	7-10
Impurities (ppmv)				
H_2S/COS	1000-10000	1000-9000	4500-14000	300-2000
NH_3/HCN	1800-2000	1800-2000	5000	1000-1500
HCL	40-600	40-500	50-700	20-300

New emerging technologies for highly efficient and clean generation of electric power from syngas demand sub-ppmv concentration of sulfur compounds. For IGCC power plant, a sulfur level of below 100 ppmv is required while for SOFC and MCFC applications, the sulfur content level of fuel gas should be limited to less than 1 ppmv and 0.5 ppmv, respectively. In order to achieve these stringent limits the cleaning of the gas to remove the particulate matter as well as sulfur compounds is necessary. The conventional as well as hot gas cleaning technologies are explained below.

1.1 CONVENTIONAL CLEAN-UP TECHNOLOGIES VERSUS HOT GAS CLEAN-UP

To achieve zero-gas emission in the gas cleaning technology is a crucial task with maintaining the gasification performance and cost targets. To improve the plant efficiency as well as simplifying the cycle configuration hot gas clean up using regenerable metal oxide received more attention. The conventional wet gas cleaning technology involves series of processes such as carbonyl sulfide hydrolysis, hydrogen sulfide stripping, and amine scrubbing followed by Clause and Scott processes (Atimtay and Harrison, 1998). The conventional method operates at lower temperature and the streams again heated for downstream hydrogen production and other applications, which adversely affect the thermal efficiency of the plant. These processes are of significant part to the capital as well as operating cost.

High temperature syngas cleaning technologies therefore offer potential economic advantages over the conventional technologies by allowing gasification, gas cleaning and downstream processes to be operated at similar process temperatures. This subject forms the basis of this research work. Over the years various metal oxides, mixed metal oxides and supported oxides were investigated as the desulfurization sorbents. The sorbent development, sorbent choice, contacting method, regeneration gas are outlined in this work.

The objectives for this research study are as follows:

- Thermodynamic analysis of single metal oxides using Factsage 6.1
- Preparation and characterization of mixed metal oxide as well as mixed metal oxide supported-ion exchanged zeolite (MMS-IZ) sorbents
- Study the performance of the synthesized sorbents at various operating conditions such as adsorption/regeneration temperature, initial gas composition, gas flow rate, the effect of particle size, and composition of the mixed metal oxide sorbent and mixed metal oxide supported-ion exchanged zeolite (MMS-IZ) sorbents

This thesis is comprised of various sections, starting with an introduction, which gives an overview about the need of new technologies for coal utilization and importance of hot gas clean up. A broad literature review section gives an overview about the research work done in the area of hot gas desulfurization. The literature review chapter also contains the focus of this research work. The thermodynamic analysis chapter contains Factsage 6.1 analysis and corresponding sulfidation performance of single metal oxide. The experimental section describes the preparation and characterization methods used in this work for synthesizing sorbents. The results and discussion chapter constitutes the important results obtained in this work and finally the conclusion.

CHAPTER 2

LITERATURE REVIEW

Over the past decades, a significant effort has been made to the development of regenerable sorbents for the intensive desulfurization of syngas streams at mid- to high- temperature. First-generation sorbents developed for these applications are not capable of meeting the new desulfurization levels established. The main limitations are the low sorbent structural stability, decay in sulfidation reactivity, loss of sorbent efficiency in multi-cycle operations.

All first-generation leading desulfurization sorbents undergo significant loss of sulfidation reactivity and capacity with cycling, as much as 50% or greater loss in only 25-50 cycles. Stability of the hot-gas desulfurization sorbents over one hundred cycles is essential for improved IGCC economics over conventional power plants. Robust and reliable technology has not yet been developed especially for gas cleaning over 600 °C to achieve higher efficiencies and meet the specifications for all kinds of applications. The hot gas cleanup is attracting various researchers throughout the world because of its impact on process and environment. This technology is primarily concentrated on particulate removal and further extended to desulfurization.

Two different types of sorbents have been used for desulfurization, one is disposable and other one is regenerable (Gangwal et al., 1995). The disposable sorbents are cheap materials and can be used once and then disposed of (e.g. dolomite). Their application is by direct injection technique where these materials are injected into the combustion chamber. It has been observed that they tend to give low sulfur capture efficiency and the waste generation in this process is high (Atimtay and Harrison, 1998). The other category of sorbent is regenerable sorbent. The regenerable sorbent is generally used in an external reactor. The regenerable sorbents are mostly metal oxides and sometimes the product produced by them is of commercial value (e.g. elemental sulfur etc.) (Atimtay and Harrison, 1998).

2.1 THERMODYNAMICS OF DESULFURIZATION

The desulfurization process is governed by many parameters:

- Types of metal oxide: Different metal oxides have different sulfidation performance hence the selection of metal oxide is an important step. Moreover, the single or combination of metal oxides will also affect the desulfurization process.
- Thermodynamic stability: The sorbent should have favorable thermodynamics for the desulfurization in the temperature range of application.
- Behavior in the reaction environment: The sorbent should have more affinity towards H_2S over other species in the gas stream and should have minimum undesirable reactions.

- Net surface area available for adsorption: The surface area available affects the desulfurization performance hence the net surface area available for adsorption should be high.
- Equilibrium constant: Equilibrium constant can be expressed as the ratio of gas phase concentration by assuming that the activity of the solid phase is constant

  $K_{eq} = [H_2O] / [H_2S]$

  Considering the surface sites on the acceptor the above expression can be written as

  $K^{i}_{eq} = [H_2O] / [H_2S] \times$ [sulfided surface sites] / [free surface sites]

  To have good desulfurization performance K_{eq} should be high.

In order to maintain the economy of the process, the metal oxide sorbent should be regenerable.

The general sulfidation-regeneration reaction of metal oxide is quiet simple and non-catalytic one and it can be represented as follows

$$MeO (s) + H_2S (g) \rightarrow MeS(s) + H_2O(g) \qquad (1)$$

The regeneration reaction is represented as follows

$$MeS(s) + 1.5\ O_2(g) \rightarrow MeO(s) + SO_2 (g) \qquad (2)$$

The sulfidation capacity for the metal oxide is generally described as g of S per 100 g of sorbent. A selective comparison of different single metal oxide sorbents based on sorption capacity is summarized in Table 2.1.

Table 2.1 Comparison of sulfidation capacity of single metal oxide sorbent materials

No	Sorbent type	Chemical formula	Theoretical sorption capacity (g S/100 g of sorbent)
1	Zinc oxide	ZnO	39.51
2	Copper oxide	Cu_2O	22.38
3	Manganese oxide	MnO Mn_2O_3	40.03 40.54
4	Iron oxide	FeO Fe_2O_3 Fe_3O_4	44.54 40.08 41.46
5	Cerium oxide	CeO_2	9.3
6	Limestone Dolomite Lime	$CaCO_3$ $CaCO_3.MgCO_3$ CaO	32 17.39 57.14

The early search for the sorbent started in 1970's. Westmoreland and Harrison (1976) studied the sulfidation thermodynamic analysis of 28 potential metal oxide candidates. A figure 2.1 shows the comparison of desulfurization performance of the potential metal oxides. They concluded that 17 elements out of 28 were not thermodynamically suitable for sulfidation and rejected for further application. Some of them were rejected due to the formation of unstable solid, inadequate desulfurization, stable and unreactive oxides.

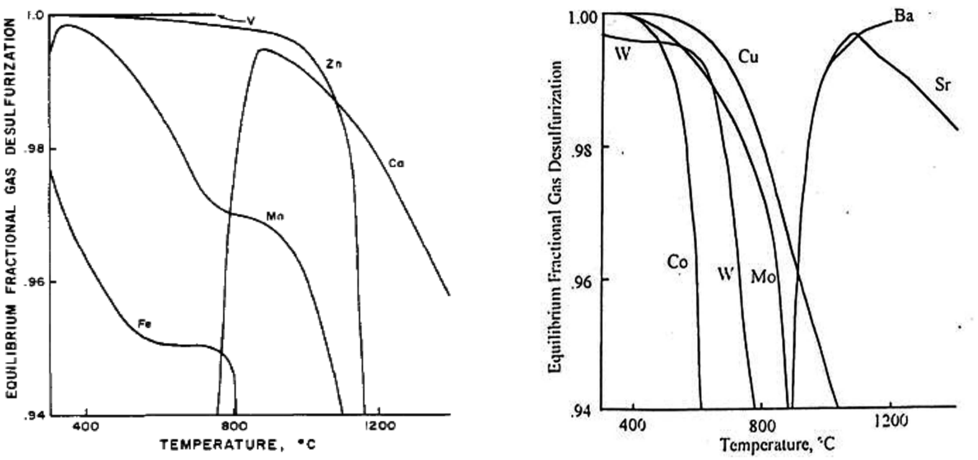

Figure 2.1: Desulfurization potential of candidates (Westmoreland and Harrison, 1976)

They also identified that the oxides of 8 different metals (Co, Cu, Fe, Mn, Mo, V, W, and Zn) as the possible candidates and having capacity to reduce down the concentration of H_2S in flue gas from 1 mol % to below 100 ppmv level at the reaction conditions of the hot gas desulfurization process (Westmoreland and Harrison, 1976).

The above thermodynamic assessments were also well supported by the thermodynamic simulations using Factsage by different other researchers. Meng et al. (2009) reported desulfurization simulation analysis using Factsage simulator for various metal oxides. They used different syngas compositions obtained from typical gasifiers. The results showed that the effluent H_2S concentration is a strong function of temperature.

The oxides of Cu, Zn, and Mn showed the most favorable thermodynamic properties for desulfurization at temperature lower than 650 °C whereas, dolomite, limestone showed quiet different sorption tendency as compared to other sorbents. However, they concluded that other parameters such as evaporation, sintering, and temperature rise during regeneration as well as mechanical disintegration may affect the sorbent performance negatively and need systematic experimental evaluation.

2.2 SORBENT SELECTION CRITERION

The main challenge in the sorbent development area is to produce a sorbent having high sulfidation capacity, superior sulfidation-regeneration kinetics, sufficient chemical and mechanical stability in order to withstand the multiple sulfidation-regeneration cycles. The followings are the criteria for selecting hot gas desulfurization sorbents (Westmoreland and Harrison, 1976; Zeng et al., 1999; Bakker et al., 2003):

1. Favorable thermodynamics: Sorbent material must be thermodynamically favorable to enable > 99% removal of H_2S at the required temperature and pressure conditions.
2. Sulfidation capacity: Sorbent material should have good working capacity. This will help to reduce both the requirement of sorbent quantity and the size of the process equipment.
3. Sulfidation kinetics: The sorbent sulfidation kinetics should be rapid to reduce the overall cycle time.
4. Stability: The sorbent should have the high thermal stability in order to withstand the high temperature conditions. The sorbent should also have mechanical and chemical stability to minimize the loss of sorbent during sulfidation-regeneration cycle and in reducing gas environment.

5. Regeneration: Feasibility and ease of complete conversion of metal sulfide back to metal oxide without generation of undesired products (e.g. sulfates). Generally, the regeneration reaction is exothermic and requires high temperature. The temperature control is required to prevent the sintering of sorbent material.
6. Low cost: The sorbent materials should be available at low cost.

2.3 REGENABLE METAL OXIDES

Over the last few decades, a number of studies reported on high temperature H_2S removal, primarily using various regenerable metal oxide sorbents that were considered as the potential candidates based on the thermodynamic analysis (Jalan and Wu**,** 1980; Grindley and Steinfeld, 1981). The first sorbent development was concentrated on the oxides of transition elements. Mostly, the oxides of Fe, Zn, Cu and Mn in different forms were evaluated under various experimental conditions (Jalan and Wu**,** 1980; Ayala et al., 1995). A comprehensive performance analysis of various metal oxides – single or mixed are discussed in details in the following sections based on available literature.

2.3.1 Transition metal oxides

2.3.1.1 Iron oxide

The early sorbent development work was mainly concentrated around iron oxide. (Ryu et al., 1998). Different iron based sorbents were investigated on various scales due to its favorable thermodynamics, high desulfurization capacity, low cost and ease of regeneration over the temperature range 350 – 600 °C (Kobayashi et al., 1990; Ayala et al., 1995). The stable forms of iron oxides are

Fe_2O_3, Fe_3O_4, FeO or elemental Fe depending on temperature and partial pressure of gaseous species present in the gas stream and on the kinetics of the reduction reactions. Iron oxide reacts with H_2S as follows (Atimtay and Harrison, 1998):

$$Fe_xO_y + x\,H_2S + y\text{-}x\,H_2 \rightarrow x\,FeS + y\,H_2O \qquad (3)$$

Or $$Fe_xO_y + x\,H_2S + y\,CO \rightarrow x\,FeS + y\,CO_2 \qquad (4)$$

Or $$Fe + H_2S \rightarrow FeS + H_2 \qquad (5)$$

In reducing atmosphere (for example, 39% H_2, 27% CO, 12% CO_2 and 2000-3000 ppm H_2S) at 500 °C, the desulfurization capacity was reported as 20-24 mg S/g of sorbent and showed the same capacity for consecutive 5 cyclic runs (Fan et al., 2005). However, it is observed that in reducing atmosphere around 700 °C Fe_3O_4 is reduced to FeO which resulted into slow sulfidation reaction kinetics (Gasper-Galvin et al., 2000). The iron oxide was also reported to form Fe at high temperature, which ultimately makes it more unsuitable for cyclic sulfidation-regeneration tests (Ryu et al., 1998). The application of iron oxide eventually reduced in 1980's due to the instability and low sulfidation capacity of iron oxide at high temperatures. Researchers also reported the iron carbide formation, severe sorbent disintegration at a temperature higher than 550 °C (Gangwal et al., 1988; Meng et al., 2010). It is also observed that formation of Fe_2O_3 reduces the sulfidation performances as compared to other forms of iron oxides. (Ayala et al., 1995).

2.3.1.2 Zinc oxide

The ZnO is found to have superior thermodynamic properties and the ability to reduce down the H_2S concentration as low as 10 ppmv (Lew et al., 1989; Ayala et al., 1995). The applicability of ZnO for desulfurization was studied over a wide temperature range and the most applicable temperature for sulfidation is found below 550 °C. The reaction between ZnO and H_2S is shown below (Atimtay and Harrison, 1998):

$$ZnO + H_2S \rightarrow ZnS + H_2O \quad (6)$$

The main problem with ZnO arises at high temperature. The gasifier temperature is typically in between 500–800 °C and ZnO based sorbents are not suitable for temperature above 550 °C. The reduction of ZnO to elemental zinc at high temperature and in highly reducing environment followed by vaporization of elemental zinc leads to substantially low sulfidation capacity (Garcia et al., 2000; Zeng et al., 2000; Ko et al., 2005). Moreover, it is found that ZnS is very stable in oxygen environment and temperature up to 720 °C (Garcia et al., 2000). At low temperature and high oxygen partial pressure environment, the regeneration product formed is $ZnSO_4$ (White et al., 1998). It was reported that ZnS, $ZnSO_4$ have the bigger volumes than ZnO and the sorbent pores cannot occupy this bigger volume products, which leads to the sorbent structure breakdown, hence there is a need to increase the pore size for the sorbent at various experimental conditions.

2.3.1.3 Copper oxide

The later research was concentrated around copper oxide and related sorbents. Copper oxide based sorbents, due to their favorable thermodynamics and high sorption capacity in reducing as well as oxidizing environment has been studied predominantly (Meng et al., 2010). Copper oxide can be used at elevated temperatures than ZnO and do not suffer from the vaporization problems as with ZnO (Gavalas et al., 1987; Patrick et al., 1993). The operation without volatilization is ensured by low vapor pressure of copper oxide and copper metal. In case of copper oxide based sorbents the reaction kinetics are observed to be fast when copper is in +2 or +1 oxidation states (Swisher et al., 2000). In all metal oxides, copper oxides (CuO and Cu_2O) have the highest sulfidation constants (Li and Flytzani-Stephanopoulos, 1997). At 627 °C, $K_s = 6.3\times10^{17}$ and 8.9×10^{8}, respectively for CuO and Cu_2O (Barin et al. (1973, 1977); Li and Flytzani-Stephanopoulos, 1997; Vamvuka et al., 2004) sulfidation reaction as shown below:

$$2CuO + H_2S + H_2 \rightarrow Cu_2S + 2H_2O \qquad (7)$$

$$Cu_2O + H_2S \rightarrow Cu_2S + H_2O \qquad (8)$$

Copper oxide can reduce the H_2S concentration to sub-ppmv levels (Li and Flytzani-Stephanopoulos, 1997). For copper oxide the optimum range for sulfidation should be around 600 °C (Abbasian and Slimane, 1998). In highly reducing environment the CuO can readily be reduced to metallic copper, which has slow kinetics for H_2S removal (Kyotani et al., 1989; Wang and Flytzani-Stephanopoulos, 2005). The sulfidation equilibrium constant of CuO is 10 times higher in magnitude than that of metallic Cu (Li and Flytzani-Stephanopoulos, 1997). The metallic copper has even inferior sulfidation capacity than ZnO (Focht, 1988). The metallic copper reacts with H_2S in following way:

$$2\,Cu + H_2S \rightarrow Cu_2S + H_2 \qquad (9)$$

One of the disadvantages of copper oxide is at high temperature its utilization is low due to the thermal sintering, which causes the crystal growth. The onion like sulfide layer increases the diffusion resistance and causes the structure breakdown of the pallet (Sick et al., 1987; Kalakota, 2008). It is necessary to keep Cu in its +2 or +1 oxidation state and keep it in highly dispersed form to utilize it efficiently (Li and Flytzani-Stephanopoulos, 1997; Alonso et al, 2000).

2.3.1.4 Manganese oxide

Another good candidate with comparatively good sulfidation performance is manganese oxide. The manganese oxide is stable at temperature around 700 °C and noted for high sulfur capacity between 600-700 °C (Ben-Slimane and Hepworth, 1994; Ayala et al., 1995). At high temperature above 1000 °C, desulfurization had been studied by Westmoreland et al. (1977) and reported that MnO allowing the flexibility in its operating temperatures without loss of sorbent material. Yoon et al. (2003) reported that at higher temperatures, there was an increase in the rate of sulfidation with increase in the H_2S content. However, MnO does not decompose to elemental manganese readily in reducing gas environment. They reported that that the sulfidation of MnO was faster than iron or zinc based sorbents. The reduction reactions are as shown below (Kalakota, 2008).

$$3\ Mn_2O_3\ (s) + H_2\ (g) \rightarrow 2\ Mn_3O_4\ (s) + H_2O\ (g) \qquad (10)$$

$$Mn_3O_4\ (s) + H_2\ (g) \rightarrow 3\ MnO\ (s) + H_2O\ (g) \qquad (11)$$

MnO reacts with H_2S to form MnS.

$$MnO + H_2S \rightarrow MnS + H_2O \tag{12}$$

In reducing environment, higher oxides of manganese can easily be reduced to MnO causing lower sulfidation performance (Ben-Slimane and Hepworth, 1994). The thermodynamics of MnO sulfidation is not as favorable as some other metal oxides such as zinc oxide and copper oxide. The disadvantage is that manganese oxide based sorbents are prone to sulfate formation and have to be regenerated at a very high temperature. Decrease in the sulfidation capacity of Mn based oxides has been observed with increasing Mn content, which forms MnO_x clusters during calcination (Liang et al., 1999).

2.3.2 Rare earth metal oxides (REO)

Most of the transition metal oxides were reported to be incompatible for high temperature and highly reducible gaseous environment application. The requirement of sub-ppmv sulfur level in few applications lead to the studies focused on the application of the rare earth metal oxide elements as one of the promising candidates for hot gas desulfurization in the last few years. Recently, oxides of cerium, lanthanum, and zirconium have been evaluated for hot gas desulfurization and reported as the potential candidates high temperature processes, for example SOFC application due to their favorable equilibrium in reducing environment as well as stability at elevated temperatures.

Cerium oxide is found to be one of the promising candidates for high temperature syngas clean up and regeneration of the sulfided sorbent Ce_2O_2S using SO_2 can produce elemental sulfur directly which has commercial value (Zeng et al., 2000). At 287 – 627 °C, cerium oxide (CeO_2) can be reduced to non-stoichiometric oxide, CeO_n ($1.7<n<2$) (Kay et al., 1993; Trovarelli, 1996; Rogemond et al., 1997; Ferrizz et al., 2003; Wang and Flytzani-Stephanopoulos, 2005; Kalakota, 2008). Zeng et al. (2000) reported that CeO_2 alone cannot reduce the H_2S concentration below 20 ppm but CeO_n can bring down the H_2S concentration to sub ppm level.

According to the phase diagram of cerium oxide the cerium oxysulfide (Ce_2O_2S) formation at high temperature and in reducing environment was reported. The formation of other sulfides of cerium such as CeS, Ce_3S_4, Ce_2S_3 was also reported by Zeng et al. (2000), Ferrizz et al. (2003), Yi et al. (2005). Thermodynamic calculations for typical syngas composition showed that the reaction of CeO_2 with H_2S is endothermic and that with Ce_2O_3 is exothermic. The entire sequence of possible sulfidation reactions is shown below (Zeng et al., 2000; Kalakota, 2008):

Reduction of cerium oxide

$$CeO_2 + (2-n)\ H_2 \rightarrow CeO_n + (2-n)\ H_2O \tag{13}$$

Sulfidation of Cerium Oxide

$$CeO_2 + 1/2\ H_2S + 1/2\ H_2 \rightarrow 1/2\ Ce_2O_2S + H_2O \tag{14}$$

$$Ce_2O_3 + H_2S \rightarrow Ce_2O_2S + H_2O \tag{15}$$

$$CeO_2 + 3/2\ H_2S + 1/2\ H_2 \rightarrow 1/2\ Ce_2S_3 + 2\ H_2O \tag{16}$$

$$Ce_2O_3 + 3\ H_2S \rightarrow Ce_2S_3 + 3\ H_2O \tag{17}$$

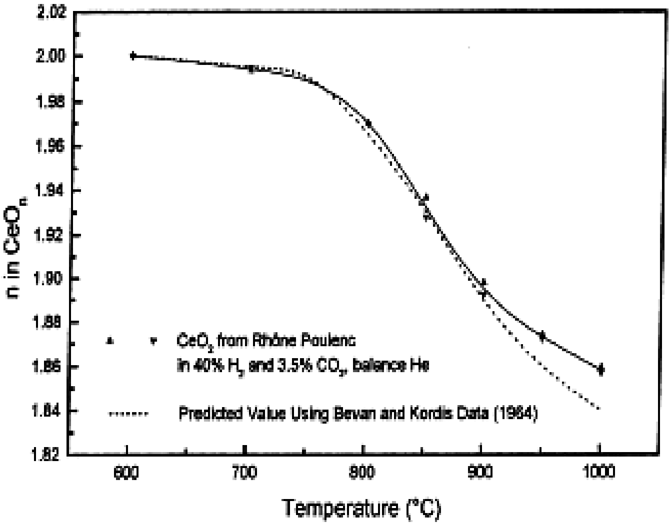

Figure 2.2: Reduction of CeO2 to CeO$_n$ (n<2) (taken from Zeng et al., 2000)

Zeng et al. (2000) reported that the average value of n in CeO$_n$ is a function of temperature. Initially the CeO$_2$ is maintained in the original form but the oxygen is removed during the reduction leading to the formation of CeO$_n$ at the temperatures above 685 °C. Researchers have tested both the cerium oxide as well as its reduced form, which showed that the reduced cerium oxide has superior efficiency for H$_2$S removal. A slight difference has been observed in the sulfidation of prereduced cerium oxide and simultaneous sulfidation-reduction of cerium oxide (Zeng et al., 2000). The problem of using CeO$_2$ alone for sulfidation is its slow desulfurization kinetics and hence researchers studied the combination of cerium oxide with other transition and rare earth metal oxides.

2.3.3 Mixed metal oxide sorbents

Single metal oxide is not enough to achieve the higher sulfidation kinetics so when two or more metal oxides mixed together the desulfurization performance was found promising hence, the hot gas desulfurization research has been conducted by using mixed metal oxides. The mixed metal oxide research for hot gas desulfurization sorbent started in late 1980's by Grindly and Steinheld (1981) and Flytzani-Stephanopoulos (1985) where they showed that mixed metal oxides have superior properties over single metal oxides.

Mixed metal oxides have been studied in past by combination of vanadium, copper, manganese, cobalt and others. The initial mixed metal oxide research was concentrated around zinc titanate and zinc ferrite. In pilot scale experiments, zinc titanate showed more promising results as compared to zinc ferrite but Ayala et al. (1995) reported that zinc titanate suffered from gradual loss in its reactivity with H_2S over multiple cycles.

The zinc and iron oxide formed the next mixed metal oxide based research where good thermodynamic properties of ZnO and the high sulfidation capacity of iron oxide were combined together in zinc ferrite form. The reaction of zinc ferrite with H_2S is as shown below (Atimtay and Harrison, 1998).

$$ZnFe_2O_4 + 3\ H_2S + H_2 \rightarrow ZnS + 2\ FeS + 4\ H_2O \qquad (18)$$

Zinc ferrite showed the ability to reduce the H_2S concentration down to sub-ppmv level (< 20 ppm) at 550 – 800 °C and 15 bar (Focht et al., 1988; Abbasian et al, 1995; Ayala, 1995; Vamvuka et al., 2004). The disadvantage of zinc ferrite is the reduction of its components at higher temperatures (above 700

°C) (Li and Flytzani-Stephanopoulos, 1997) and sulfate formation upon regeneration which reduced the sulfidation efficiency of zinc ferrite and caused decomposition (Focht, 1988; Vamvuka at al., 2004). The durability was found to be affected when the multiple sulfidation cycles were studied (Gangwal et. al., 1989; Harrison, 1998; Kwon et al., 1997).

In Mid 1980's the zinc titanate research was proposed. The ZnO and TiO_2 mixture formed the zinc titanate, where ZnO reacts with H_2S and TiO_2 acted as a stabilizer. The reaction of zinc titanate with H_2S is as shown below.

$$Zn_2TiO_4 + 2\ H_2S \rightarrow 2\ Zns + TiO_2 + 2\ H_2O \qquad (19)$$

The theoretical capacity reported was in between 17 to 26 wt % (Atimtay et al., 1998). Zinc titanate was suffered with gradual loss in the sulfidation capacity after multiple cycles of sulfidation-regeneration (Mojtahedi et al., 1994; Ishikawa et al., 1999; Atimtay et al, 2001).

Though zinc titanate was proven mix metal oxide sorbent but it was suffered with many disadvantage such as spalling, loss of reactivity over time, and cracking (Jun et al., 2001). The formation of sulfates was also reported during regeneration (Gangwal at al., 1989; Mojtahedi et al., 1994; Ishikawa at al., 1999; Atimtay at al., 2001).

The thermodynamic equilibrium study and the industrial requirements for the H_2S removal at higher temperatures limited the research towards only few metal oxide elements (Ayala et al., 1995). The copper as well as cobalt based sorbents gained attention from researchers. Later research was concentered with various mixed transition metal oxides. Researchers investigated various mixed oxides of ZnO, CuO, CuO-Fe_2O_3 as well as CuO-Fe_2O_3-Al_2O_3 as the regenerable mixed metal oxide sorbents (Tamhankar et al., 1986). The reported sulfidation efficiency trend is as shown below (Li and Stephanopoulos, 1997).

CuO, Cu_2O > $CuAl_2O_4$, $CuAlO_2$ > $CuFe_2O_4$, $CuFeO_2$ > > Cu >> Fe_3O_4 > $FeAl_2O_4$

These combined forms of mixed metal oxide were found to be more promising for hot gas desulfurization. High adsorption capacity, minimal pore blockage, stability and regenerability are few of the advantages of this family of sorbents (Tamhankar et al., 1986).

Few researchers focused on the ternary mixed metal oxides such as Cu-Fe-Al-O. It was observed that aluminum oxide acts as a stabilizer. These kind of ternary systems were proven to have more stable properties than two mixed metal oxide sorbent. Li and Stephanopoulos (1997) reported that the advantage of iron in the ternary system is to increases the sulfur loading capacity of the sorbent

Studies related to the role of one metal oxide as an additive to other metal oxide sorbent were also performed. Jun et al. (2001) reported that the addition of cobalt to the zinc titanate based sorbent showed the improvement in the sulfur capacity as well as the multiple sulfidation-regeneration capacity. Another study by Alonso et al. (2002) was done with graphite as an additive to zinc ferrite doped with TiO_2. It was reported that the graphite acted as a pore-forming agent. The most research based on mixed metal oxide is still limited to the lab scale experiments and there is necessity to evaluate their performance on pilot scale.

2.3.3.1 Mixed rare earth metal oxide and transition metal oxide sorbents

Investigation using rare earth metal oxides combined with transition metal oxides as a potential desulfurization sorbent was also performed recently (Li and Flytzani-Stephanopoulos, 1997). The main rare earth element metal oxides explored are cerium and lanthanum oxide. The high desulfurization and low deactivation was reported for Ce-Mn oxide system (Yaryesli et al., 2008). The CeO_2 reducibility as well as the sulfur removal capacity can be greatly increased with addition of CuO (Kobayashi et al., 2002).

More studies were carried out with copper and cerium oxide together. Li and Flytzani-Stephanopoulos (1997), Akyurtlu and Akyurtlu (1999) reported that CuO and CeO_2 are two immiscible oxides where CeO_2 acts as a dispersing agent for CuO and keeps it in a highly dispersed form that leads to the proper utilization of CuO. It was observed that the sulfidation product of Cu-Ce system as Cu_8S_5, Ce_2S_3, Cu_xS, and unreacted CeO_2 instead of only Cu_2S and CeO_2. With various proportions of Cu-Ce, the utilization of CuO was reported to be higher with more Ce ratio. Reduction of Cu-Ce system was observed to be independent of temperature as it has lower activation energy and easy to reduce. Copper-cerium oxide has shown high sulfidation efficiency as well as the good reversibility of the sorbent. Crystal size increment for copper was recorded at high temperature as the narrower peaks recorded in XRD that affected the performance at elevated temperature (Rong et al., 2009).

Recently the lanthanum oxide was also studied widely with copper, cerium, manganese, cobalt oxides. It was reported that La-Mn system has the highest sulfidation efficiency as well as capacity among all other combinations (Rajagopalan et al., 1999). Praseodymium-doped lanthanum oxide study showed that these sorbents are highly efficient and promising at high temperature application sulfur removal from hot reformate gas streams (Valsamakis and Flytzani-Stephanopoulos, 2010).

Though metal and mixed metal oxides can work for removal of H_2S at higher temperatures (300 – 700 °C) and give higher sulfidation capacity but they suffer from poor H_2S adsorption selectivity in the presence of other species (e.g. Co, CO_2 and H_2O) hence metal oxide supported sorbents were investigated and are discussed in details below.

2.3.4 Metal oxide with support

In general, the supported sorbents have advantage over unsupported sorbents at higher temperatures because of the higher rates of reaction but the capacity is less as compared to the bulk sorbents (Gasper-Galvin et al., 1998). The supports have the large surface area and hence the metal oxides distribute uniformly on the surface and ultimately lead to the proper utilization of metal oxides. The desulfurization efficiency as well as the sorbent utilization is improved in case of supported sorbents (Jalan et al., 1983). Researchers studied SiO_2, Al_2O_3, synthetic and natural zeolites as a support for metal oxide. The study with the unsupported and supported metal oxide showed following trend towards the desulfurization (Atimtay and Harrison, 1998).

Unsupported metal oxide < supported on SiO_2 < supported on Al_2O_3 < supported on zeolite

The development started with SiO_2 and Al_2O_3 as a support. Supported copper oxide has shown the better utilization and sulfidation efficiency than the unsupported one. The capacity and efficiency was reported to be high with zeolite than SiO_2 and Al_2O_3 (Jalan et al., 1983). It was also reported that supported copper oxide almost has the same breakthrough as CuO with proper utilization of Cu (Kyotani et al., 1989; Gasper-Galvin et al., 1998). Another study evaluated the mixing with support and palletizing with support, where CuO and Al_2O_3 were used and no difference in its capacity was recorded. (Sick and Schwerdtfeger, 1987). The supported zeolites can withstand the multiple cycles at higher temperature without sintering effect (Gasper-Galvin et al., 1998). The sorbents of copper, molybdenum and manganese supported on zeolite showed better utilization of oxides and reversibility (Jalan, 1983; Gasper-Galvin et al., 1998).

Gasper-Galvin et al. (1998) studied Cu-Mn-Mo based supported sorbents on a SP – 115 zeolite to prevent metal migration. They studied the sulfidation at 871 °C and reported that CuO was more effective in desulfurization over Mo and Mn acted as a promoter (Desai et al., 1990; Voecks et al., 1993) and reported less volatilization of Mo due to presence of Cu and Mn. SBA-15 and MCM-41 are the most studied synthetic zeolites as a support. Cu supported SBA-15 showed promising results over temperature range 523–573 °C. The sulfidation capacities of 21.97 wt % and 40.22 wt % Cu were reported as 0.63 and 1.57 g S/ 100 g of sorbent. The multiple sulfidation-regeneration cycle reduced the capacity for high Cu content sample. The preparation method and sulfidation tests were reported to have no effect on the support (Karvan et al., 2008). Mureddu et al., (2012) studied the Zn supported SBA-15 as potential candidate for low temperature desulfurization. Zn supported SBA-15 sorbents have good sulfidation capacity and multiple cyclic performance and reported that the preparation method does not affect the performance of the sorbent.

Wang et al. (2007) studied the combined mesoporous and microporous SBA-15 loaded with ZnO nanoparticle for low temperature desulfurization. Distribution of mesopores and micropores was an important factor as ZnO loading was in the mesopores only which lead to proper utilization of ZnO nanoparticles and high desulfurization efficiency. Mn-Cu/SBA-15 showed good sulfidation capacity around 13.8 g S/100 g of sorbent at high temperature around 800 °C. After 9 cycles of sulfidation-regeneration at 800 °C, 74% sulfidation capacity was maintained (Zhang et al., 2012).

The natural zeolites are also investigated for desulfurization application due to their availability and low cost. Rong et al. (2009) studied the copper and cerium exchanged zeolite-Y as well as copper-cerium exchanged zeolite-Y. In case of Cu-zeolite-Y the copper metal formation was observed at 800 °C resulted in reduced surface area while in case of Ce-zeolite-Y and Cu-Ce-zeolite-Y no reduction in the surface area was observed. The sulfidation capacity was also observed to be same over multiple cyclic tests and no sintering was reported. It is noticed that ion exchanged zeolite have surface interactions with H_2S

Praveen Kumar and others (2011) tested Cu and Ag exchanged faujasite for H_2S adsorption. The preparation was done with vapor phase ion exchange method to get Cu^{1+} phase. It was reported that the higher temperature is required for activation of cation site and ultimately higher sulfidation capacity. The capacity increase was recorded due to variation in Cu^{+1}/Cu^{+2} ratio. The Ag-faujasite showed the strongest affinity toward H_2S at room temperature as well as at 150 °C while others were suffered by the presence of other gaseous species.

The natural and synthetic zeolites are attracting many researchers. However, they have high surface area, uniform pore distribution as well as active cation sites but still many natural and synthetic zeolites are yet not studied as a support for hot gas desulfurization sorbent so it is necessary to evaluate them for hot gas desulfurization.

The thermodynamic study showed that the metal oxide sorbent have good sulfidation thermodynamic equilibrium at lower temperature (300 - 500 °C). Researchers suggested that IGCC should be operated at lower temperature (348 – 538 °C) in order to be more economical and reduce down the cost significantly (Droog et al., 1993; Chung et al., 2004). It is observed that as temperature is decreased the sulfidation kinetics of metal oxides slows down but leads to the use of sorbent material for multiple cycles. Thermodynamically, the lower temperature application will lead to more cost effective operation of IGCC but no significant steps are taken in order to develop the low temperature desulfurization sorbents.

Table 2.2: Overview of sulfidation and regeneration conditions of various sorbents

Sorbent type	Particle diameter preparation method	Absorption condition	Gas composition	Purification degree or capacity	Regeneration Reactor type,	Reference
Pure iron	0.15 mm grinded ore	420 - 480 °C 16 - 20 bar	1500 ppm	< 80 ppm	4-8% O_2/N_2 600-800 °C Two stage fluid bed reactor	Kobayashi (1990)
Fe_2O_3 on FCC	0.1 mm deposition precipitation of iron oxide on FCC	300-600 °C 1 Bar	1000 - 7000 ppm	< 10 ppm	400 - 500 °C 1 bar Packed bed reactor	Van der Ham et al. (1994)

Fe_2O_3 on alumina-silica carrier	1 mm spherical shape	400 °C 1 Bar	3000 - 4000 ppm	< 20 ppm	450 °C 1 bar 10-12 % O_2/N_2 Cross flow moving bed reactor	Ishikawa (1993)
Fe_2O_3 - TiO_2 honeycomb structure	Honey comb structure	300- 500 °C 16 Bar	1000 ppm	< 100 ppm	650 °C 16 bar 2% O_2/N_2 Fixed bed reactor	Suehiro et al. (1993)
Zinc ferrite	0.2 mm granulation Zn-Fe= 1:1	550 - 800 °C 15 bar	4500 ppm	< 20 ppm	700 °C 2% O_2/N_2 High pressure fluidized bed	Jain et al. (1991)

ZnO in porous matrix with nickel oxide	0.1 - 0.3 mm	540 °C 20 atm	5000 ppm	< 50 ppm	650 °C 20 bar fluidized bed reactor	Khare et al. (1995)
Zinc titanate	0.1 - 0.3 mm granulation Zn/Ti: 1/5	750 °C 15 bar	11000 ppm	< 20 ppm	780 °C 15 bar 2.5 %O_2/N_2 fluidized bed reactor	Gupta et al. (1992)
Zinc ferrite and vanadium oxide	20/40 mesh zinc ferrite impregnated withV_2O_5 and calcination	600 - 700 °C 1 bar	10000 ppm	< 1 ppm	700 °C 1 bar 10 % O_2/N_2 Packed bed reactor	Akyurtlu and Akyurtlu (1992, 1995)
Zinc titanate	Zn/Ti: 1.5	600 °C 24 bar	Oxygen blown syngas	> 99 % removal	700 °C 15 bar 10 % O_2/N_2 Packed bed reactor	Robin et al. (1993)

Zn/Ti: 1.5	0.38 mm and 0.27 mm	600 °C	1500 ppm	< 50 ppm	750 °C , 20 bar fluidized bed reactor	Mojtahedi and Abbasian (1995)
Zinc titanate and 50% excess TiO_2	0.1 - 0.3 mm agglomeration and calcination	15 bar 650 °C	10000 ppm	< 100 ppm	720 °C 15 bar Fluidized bed reactor	Swisher et al. (1995)
Zinc titanate and molybdenum oxide	5 - 6 mm rounded calcined pellets of Zno, TiO_2, MoO_3, Zn-Ti: 2 Mo: 1.7 wt %	540C 1 bar	10000 ppm	< 10 ppm	700 °C 1.21% O_2/N_2 Packed bed reactor	Ayala et al. (1992)
Copper manganese oxide	Co-precipitation	Atm pressure 550-700 °C	10 000 ppm	< 100 ppm (few cases < 20ppm)	650- 750 °C	Fixed bed reactor
Cu-Cr-O	Co-Precipitation molar ratio of 1:3, 1:1, 3:1	600-750 °C	20000 ppm	< 10 ppm	700-800 °C	Li and Flytzani-Stephanopoulos (1997)
				Surface area: 0.6-3.7 m^2/g Loading: 3.0 - 12.2 g S/100 g Packed bed reactor		

Cu-Ce-O	Co-precipitation Molar ratio of 1:3, 1:1, 3:1	650 °C	20000 ppm	< 20 ppm	700-800 °C	Li and Flytzani-Stephanopoulos (1997)
				Surface area: 1.1-5.8 m^2/g Loading: 2.7 - 17.7 g S/100 g Packed bed reactor		
Cu- alundum	Molar ratios (Cu-Al) 1.41, 2.23, 2.61	600 °C	20000 ppm	< 1 ppm	725 °C	Karayilan et al. (2005)
				Loading: 9.03 - 10.23 g S/100 g Packed bed reactor Packed bed reactor		
Cu-SBA-15	Wet impregnation method Cu content 20 % to 40 %	525 °C	2000 ppm	< 20 ppm	600 °C	Karvan et al. (2008)
				Surface area: 376- 556 m^2/g T Loading :5.54 - 10.15 g S/100 g A Loading :0.67 - 1.54 g S/100 g Fixed bed reactor		
Pure clinoptiolite	Naturally available (Gordes Region, Turkey) 250 µm	100 – 600 °C	1.06%H_2S/ He	NA	Fixed bed reactor	Yasyerli et al. (2002)
CuO-SBA-15 1. Cu = 18.66 % 2. Cu = 13.11%	Wet impregnation method	515 °C (100 kPa)	2044 ppm	1. 20 ppm (0.63 g S) 2. 20 ppm (1.72 g S)	5% O_2/N_2 Fixed bed reactor	Gasper-Galvin et al. (1998)

Pure zeolite-Y	Zeolite –Y	800 °C	0.1 % H_2S, 50% H_2, 10% H_2O, bal. He	0.26 g S % H_2S = 99	50% H_2, 10% H_2O, balance He Fixed bed reactor	Rong et al. (2009)
Cu-zeolite Ce-zeolite Cu-Ce-zeolite	Ion exchange method	800 °C	0.1 % H_2S, 50% H_2, 10% H_2O, balance He	1.80 g S % H_2S = 87 1.04 g S % H_2S = 98 1.58 g S % H_2S = 98	50% H_2, 10% H_2O, balance He Fixed bed reactor	Rong et al. (2009)
Ag,Cu exchanged faujasite	Vapor phase ion exchange	Room temp – 150 °C	10 ppm, balance He 10 and 100 ppm , balance N_2	1. NaX = 0.5^* 2. AgY = 1.4^* 3. AgX = 1.8^* 4. CuX = 0.8^* 5. CuY = 0.6^* * g S/100 gm sorbent	NA Fixed bed reactor	Parveen Kumar et al. (2011)

2.4 REGENERATION FOR HOT GAS DESULFURIZATION SORBENTS

The sorbent should perform very well for multiple sulfidation-regeneration cycles in order to be a good sorbent. The regeneration step is equally important as the sulfidation step and it is more difficult to carry out accurately. Regeneration requires a good combination of thermodynamic as well as experimental parameters in order to achieve complete regeneration of the sorbent material. The general regeneration reactions are as shown below:

Generally, air or $O_2 + N_2$ mixture is used for regeneration of sulfided sorbent.

$$(x)\ MeS + (x+y/2)\ O_2 \rightarrow Me_xO_y + SO_2 \qquad (20)$$

In order to get elemental sulfur as a product SO_2 is used as a regeneration gas.

$$2\ MeS + SO_2 \rightarrow MeO + 2\ S_2 \qquad (21)$$

In order to get H_2S back steam is used as a regeneration gas.

$$MeS + H_2O \rightarrow MeO + H_2S \qquad (22)$$

It is necessary to use the perfect experimental conditions with regeneration gas or else the regeneration will lead to the formation of unwanted byproducts as shown below:

$$MeS \rightarrow MeSO_4 \qquad (23)$$

The sulfates formed are quiet stable and it is difficult to convert them back to the oxide form. This unwanted side reaction is as shown below:

$$MeS + 2\ O_2 \rightarrow MeSO_4 \qquad (24)$$

Meng et al (2009) carried out thermodynamic analysis for regeneration of Mn based as well as Fe based sorbents by phase stability diagram. From phase stability diagram it is clear that for Mn based sorbents the regeneration should be carried out at around 900 °C with required partial pressure of oxygen in order to get oxide form as a regenerated product while for Fe based sorbent regeneration temperature should be above 900 °C (Meng et al., 2009).

Copper-based sorbents can be regenerated in the temperature range of 600 to 900 °C. Thermodynamically CuO will be formed as product at elevated temperature of 900 °C despite of different partial pressure of O_2. At high temperature, it is observed that copper undergo sintering so regeneration conditions should be selected carefully or copper oxide should be combined with other metal oxides (Meng et al., 2009)

The general regeneration reactions for copper oxide are as shown below.

$$Cu_2S + 2\ O_2 \rightarrow 2\ CuO + SO_2 \qquad (25)$$

However, in actual the regeneration forms an undesirable sulfate product.

$$2\ Cu_2S + 5\ O_2 \rightarrow CuSO_4 + 4\ CuO + SO_2 \qquad (26)$$

The CeO_2 was observed to have the easy regeneration pattern at higher temperature due to the highly mobile oxygen vacancies (Zeng et al., 2000; Kempegowda et al., 2007). It was reported that the CeO_2 oxide due to the high oxygen mobility and modification ability gives the different regeneration performance (Kempegowda et al., 2007). The general regeneration reaction is reported as follows:

$$Ce_2O_2S + O_2 \rightarrow CeO_2 + SO_2 \qquad (27)$$

The regeneration for various combinations of Cu/Ce mixed metal oxide was carried out at various temperatures and the sulfate formation was recorded as the main product formation. The regeneration path was reported as (Li et al., 1997).

$$Cu_2S \rightarrow CuSO_4 + CuO \rightarrow CuO \tag{28}$$

2.5 FOCUS OF THIS WORK

From literature review, it is clear that the transition (Cu, Co and others) as well as rare earth elements (Ce and others) possess the ability to desulfurize the syngas over a wide range of temperatures. The metal supported on various supports as well as ion exchange zeolite improves the sulfidation efficiency and there is a need to explore various natural zeolites as the potential supports for metal oxides. An effort is made in this work to include the various possibilities of combination of transition and rare earth metal oxides in various proportions as well as the mixed metal oxide supported - ion exchanged zeolites as the potential sorbents for desulfurization over a wide temperature range.

In this work based on the literature, we selected two transition metal oxides (copper and cobalt oxide) and one rare earth metal oxide (cerium oxide). This study describes the evaluation of the copper-cobalt, copper-cerium mixed metal oxide sorbents for hot gas desulfurization capable of withstanding the wide temperature range of application and multiple sulfidation-regeneration cycles. Copper-cobalt mixed oxide system is a good candidate for low temperature desulfurization while copper-cerium exhibits the high temperature stability and high performance.

It is also of interest to study mixed metal oxide supported –ion exchanged zeolite sorbents such as zeolite-Y, Ca-chabazite and clinoptiolite. It is important to know how the metal ions can be incorporated in this zeolite and their utilization in subsequent sulfidation cycles. The most interesting thing is to observe how the H_2S interact with this kind of sorbent.

The various combinations of these metal oxides exhibited the high efficiency in H_2S removal. The thermodynamic analysis of the metal oxide systems and H_2S concentration in equilibrium shows that the sulfidation is a strong function of temperature and calculated with Factsage 6.1 (GTT technologies). The kinetic study of sulfidation is performed by packed bed micro reactor test with feed gas mixture containing H_2S and N_2.

CHAPTER 3

THERMODYNAMIC ANALYSIS

This chapter mainly deals with the thermodynamic assessment of single metal oxides for their capability to reduce down the H_2S concentration in syngas to low levels by using the software package Factsage 6.1.

3.1 SULFIDATION SIMULATION ANALYSIS FOR SINGLE METAL OXIDE

The thermodynamic analysis of the single metal oxide was calculated with Factsage 6.1 (GTT technologies). H_2S concentration in equilibrium shows that the sulfidation is a strong function of temperature. The sulfidation simulation results of single metal oxide for standard syngas composition are discussed in details below. Figure 3.1 shows the thermodynamic analysis performed by using Factsage (6.1) for the potential metal oxide candidates identified from the literature for desulfurization performance.

The analysis was performed over a wide temperature range (300 – 1500 °C). Based on thermodynamic analysis it is clear that oxides of iron, manganese, zinc and copper are suitable candidates for desulfurization when the temperature is lower than 500 °C. The cerium oxide is suitable candidate up to a temperature of 900 °C. The desulfurization performance of calcium oxide sorbents mainly depends upon the contents of the gaseous environment and their application at higher temperature is favorable.

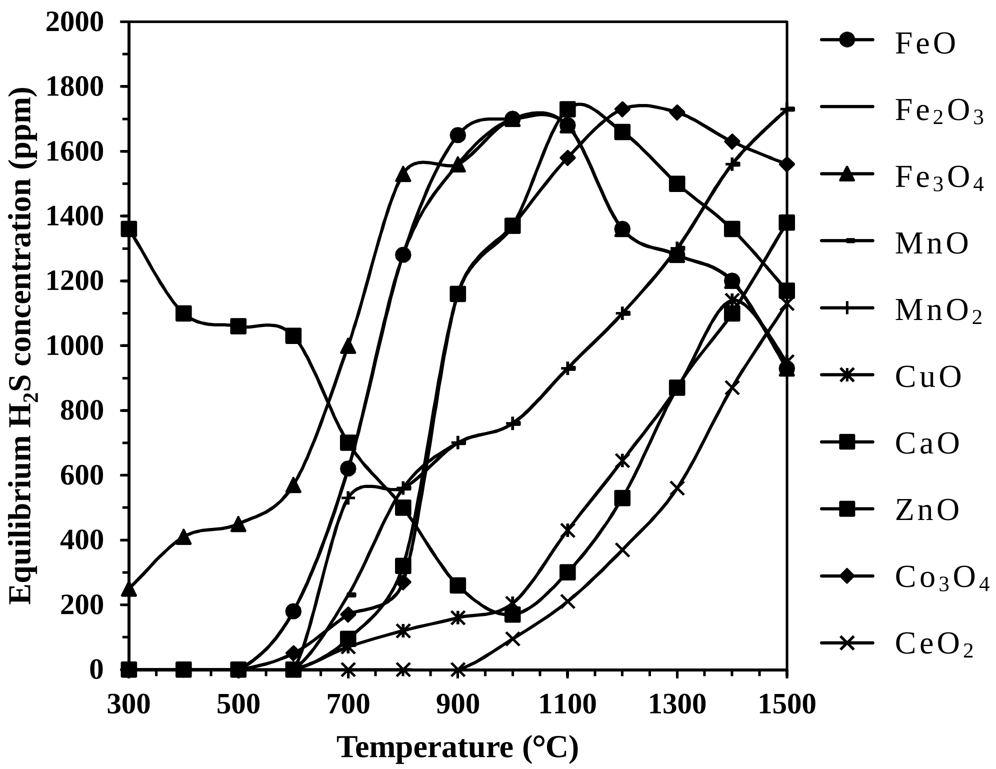

Figure 3.1: Factsage simulation analysis for single metal oxide for standard syngas composition as shown in Table 1.1

Manganese oxides (MnO_2 and MnO) showed capability to reduce the H_2S concentration down to about 80 ppm at 700 °C. This result is in agreement with literature, Ben-Slimane et al. (1994) reported that Mn based oxides are stable up to 700 °C and reported the high sorption capacity between 600 – 700 °C. Zinc oxide was capable to reduce the H_2S concentration down to low levels up to 700 °C but after that, sudden increase in the H_2S concentration was recorded which supports literature about the vaporization loss of zinc at higher temperature. The iron oxides (Fe_3O_4, Fe_2O_3, FeO) showed good performance over a wide temperature range but less desulfurization potential as compared to other single metal oxides. FeO and Fe_2O_3 showed capability to reduce down the H_2S

concentration down to 20 ppm at 500 °C. The all forms of iron oxide showed less capacity as compared to other oxides. This may be due to the reduction of higher oxides (Fe_3O_4, Fe_2O_3) of iron to lower oxide (FeO) and potential elemental Fe formation that have a detrimental effect on sulfidation performance as well as capacity. Copper oxide showed excellent performance up to a temperature of 700 °C by taking H_2S concentration to very low level (~10 ppm). At higher temperature, slow increase in the H_2S concentration was observed as compared to zinc, which confirms that the copper oxide is not prone to the vaporization loss as in case of zinc. The oxides of calcium showed different sulfidation behavior as compared to other oxides. They showed different sorption tendency as a function of temperature. Cerium oxide showed excellent capability to reduce down the H_2S concentration up to 20 ppm and high temperature stability. Zeng et al. (2000) reported that CeO_2 is capable of reducing the H_2S concentration down to 20 ppm but the reduced form (CeO_n) has more affinity towards H_2S and can reduce to even sub-ppm level. The cobalt oxide showed excellent behavior up to temperature of 600 °C and is capable take H_2S concentration to low levels. Based on the above thermodynamic analysis of single metal oxide copper oxide (excellent sulfidation behavior up to 700 °C), cerium oxide (up to 900 °C) and cobalt oxide (up to 600 °C) are selected for further experimental analysis in the form of mixed metal and mixed metal oxide supported-ion exchanged zeolite (MMS-IZ) sorbents.

CHAPTER 4

EXPERIMENTAL

This chapter describes sorbent synthesis, characterization and experimental equipment, procedures, used in this study. Materials characterization consisted of sorbent reduction, X-ray diffraction analysis, BET surface area measurement and thermogravimetric analysis. In order to achieve the objectives of this study the desulfurization tests were performed by using a packed bed reactor. A packed bed reactor system was designed and fabricated for sulfidation tests. The effect of various operating variables on the desulfurization capacity and desulfurization efficiency was studied.

4.1 SORBENT PREPARATION

The preparation process affects certain properties of synthesized sorbents such as the phase, particle size, surface area and oxygen storage capacity (in case of cerium oxide based sorbents). Currently, preparation methods are classified into three categories

1. Solid – Solid synthesis
    - Ceramic method
    - Mechanical milling
2. Solid – Liquid synthesis
    - Precursor method

- Precipitation and co-precipitation method
- Sol gel method
- Electrochemical method
- Ion exchange method

3. Solid – Gas synthesis
    - Gas condensation

Solid-solid synthesis has an advantage of low cost, but is not appropriate for ultra-pure materials. Liquid-solid synthesis is the easiest method because it occurs near ambient temperature, but in some cases solvent is consumed. Gas-solid synthesis is good for ultra-pure and extremely small size material preparation, but the cost is high. The following section deals with detailed aspects of the preparation methods used in this particular study.

The sorbents used in this research were prepared by following methods

1. Precursor method (Mecially et al., 1970; Adachiand Masui, 2001)
2. Ion exchange method

The mixed metal oxides were synthesized by precursor method. The citrate precursor method is a wet chemical method that has been applied to produce the sorbents by decomposition of its precursors such as hydroxides, nitrates, halides, sulfates, carbonates, formats, oxalates, acetates, and citrates because this method can make very fine (nano-sized grains) and amorphous powders with high chemical uniformity and homogeneity in grains from high purity materials. Moreover, it is simple and reproducible.

4.1.1 Precursor method

- **Materials:** Copper nitrate ($Cu(NO_3)_2.xH_2O$, purity $\geq$ 99.999%), cobalt nitrate ($Co(NO_3)_2.6H_2O$, purity > 98%), cerium nitrate ($Ce(NO_3)_3.6H_2O$, purity $\geq$ 99.99%), citric acid ($C_6H_8O_7$, purity 99.5+ %) were obtained from Sigma-Aldrich and used without further purification.
- The copper (Cu) and cerium (Ce), copper (Cu) and cobalt (Co) mixed metal oxides were prepared by amorphous citrate precursors. The solutions with the desired molar ratio as shown in Table 4.1 were prepared.
- In a typical synthesis procedure, for example 3:1 molar Cu:Ce mixed metal oxide, 1.76 g of Cu-nitrate, 0.63 g Ce-nitrate were taken and dissolved in 94 ml and 15 ml respectively of DI water. The aqueous nitrate solutions were mixed in room temperature under stirring for 5 minutes and clear solution of mixed metal nitrate was obtained.
- Approximately, 0.80 g of citric acid was dissolved in DI water to prepare the complexing agent. The molar ratio of citric acid to total metal in solution was 1:1.
- This aqueous nitrate solution was then added drop wise to the aqueous solution of citric acid. The solution was kept under continuous stirring at room temperature for one hour.
- The final aqueous solution was dehydrated rapidly on a hot plate at around 80 °C until a viscous liquid end point was achieved.

- This viscous liquid was then dried in an oven (Lindberg/blue) at 110 °C for 2 hrs and the solid foam was received.
- This foam was then calcined in a muffle furnace (Thermolyne/Barnstead 600 furnace) with 1 °C/min ramp at required temperature for 4 hrs in presence of flowing air. The product received after calcination was then crushed and sieved to the desired size (about 63 to 250 µm).
- The calcination temperature for Cu-Ce-O system was 650 °C while for Cu-Co-O system was 550 °C

Table 4.1: Composition of mixed metal oxide sorbent

Sorbent	**Molar Composition**	**Sorbent**	**Molar Composition**
Cu:Ce	3:1	Cu:Co	3:1
Cu:Ce	1:1	Cu:Co	1:1
Cu:Ce	1:3	Cu:Co	1:3

4.1.2 Ion exchange method

- **Materials:** Zeolite-Y (ZY) (Engelhard corporation), raw sedimentary chabazite (CC) (Bowie deposit, Arizona), clinoptiolite (CL) (Saint clouds deposit, New Mexico).
- The required molar aqueous solution of copper nitrate was prepared by dissolving the copper nitrate in DI water.

- The zeolite (about 2 g) was mixed with in the prepared solution of copper nitrate and then it was stirred at room temperature for 48 hrs.
- The aqueous solution was filtered by using filter paper. The filter cake was then washed with DI water and the final cake was then dried in an oven (Lindberg/blue) at 110 °C for 2 hrs.
- The dried product was then crushed (about 63 to 250 μm) and stored.
- The required molar aqueous solution of cobalt and cerium nitrate were prepared by dissolving the respective nitrate in D.I. water.
- The prepared Cu-zeolite was then placed in the prepared aqueous solution of cobalt as well as cerium nitrate with few drops of 0.1 M solution of HNO_3 and then it was stirred at room temperature for 48 hrs.
- After stirring the aqueous solution was then filtered by using filter paper and it was washed with DI water and the cake was then dried in an oven (Lindberg/blue) at 110 °C for 2 hrs.
- The dried cake was then calcined in a muffle furnace (Thermolyne/Barnstead 600 furnace) with 1 °C/min ramp at 650 °C for 4 hrs in presence of air. The product received after calcination was then crushed and sieved to the desired size (about 63 to 250 μm).

Table 4.2: Composition of mixed metal oxide supported–ion exchanged zeolite (MMS-IZ) sorbent

Sorbent	**Composition**	**Sorbent**	**Composition**
Cu-Ce-ZY	Cu-Ce = 1:1	Cu-Co-ZY	Cu-Co = 1:1
Cu-Ce-CC	Cu-Ce = 1:1	Cu-Co-CC	Cu-Co = 1:1
Cu-Ce-CL	Cu-Ce = 1:1	Cu-Co-CL	Cu-Co = 1:1

4.2 CHARACTERIZATION OF SORBENT

4.2.1 X-Ray diffraction (XRD)

The crystalline structure and phases in the sorbent were identified by using RIGAKU (Rigaku RU-200B) XRD system using Cu-Kά radiation (λ = 1.5415 Å) using an X-ray gun operated at 40 kV (voltage) and 200 mA (current). Data was collected from $2\theta = 10$ to 110° at a scan rate of 2° / min.

Quantification of crystalline compounds/phases present in weight % of the particular phases in the synthesized sorbents were carried by using Siroquant software from the XRD powder data. It uses Rietveld curve profile analysis of XRD data to calculate weight percentage of the component mineral phases. Firstly, a best fit was obtained for the diffraction pattern with refined models. The better is the fit more flat difference pattern can be obtained and for a perfect fit $\chi^2 = 1$. Quantitative results are normally based on 100 weight % and are in form of two results; the contrast corrected weight percentage and error percentage. Generally, the contrast corrected weight percentage is the quantitative result.

4.2.2 Surface area determination

The specific surface area of the synthesized sorbents were determined by 5-point BET using Quantachrome Autosorb I. In a typical analysis, the sample around 0.3 g was placed in the sample cell and degassed under vacuum at 150 °C overnight. A 20 point adsorption/desorption cycle was performed in order to analyze the pore size distribution (Density Function Test (DFT) or Barrett, Joyner and Halenda (BJH)). The system was controlled and pressure data was collected and stored in the computer and data was analyzed using custom software.

4.2.3 Scanning electron microscopy (SEM) analysis

In order to understand the surface morphology of desulfurization sorbents, Hitachi S-2700 scanning electron microscope (SEM) with accelerating voltage of 20 kV was used. The composition analysis was performed using energy-dispersive x-ray analyzer (EDX). EDX is an analytical technique used for the elemental analysis or chemical characterization of the sorbent based on the fact that that each element has a unique atomic structure allowing unique set of peaks on its X-ray spectrum.

The back scattered electron detector (BSE) system used to get more details about the sorbent. BSE detectors are commonly integrated into SEM. As heavy atoms with a high atomic number can scatter electrons strongly than light ones, images with back-scattered electrons (BSE) can give the compositional information. BSE images are very helpful for obtaining high-resolution compositional maps of a sorbent and for quickly distinguishing different phases.

4.2.4 Thermo gravimetric analysis (TGA)

The TGA analysis was performed to study thermal stability of sorbent and reduction kinetics for sorbents. The SDT Q-600 was used to perform the TGA of the prepared sorbents. The mixed metal oxide as well as mixed metal oxide supported-ion exchanged zeolite sorbents were studied for thermal stability. The thermal stability of sorbents was tested in the temperature range of 350 – 850 °C. About 10-15 mg of sorbent was heated with a heating rate of 20°C/ min in N_2 atmosphere at a flow rate of 100 ml/min.

It is important to study the behavior of the sorbent in the reducing environment. Tests were conducted over a wide temperature range of application (350 to 800°C). The reduction of the sorbents was studied in hydrogen and moist atmosphere. Various different combinations of reducing gaseous environment were used as per the level of reduction in the standard syngas. The moisture was passed into the TGA by using the PHD 4400 programmable syringe pump (Havard instruments). The reduction was carried out with 5%, 15%, and 40% of H_2 and rest N_2. The reduction was carried out with following different composition of gaseous environment.

a) 15 % H_2, balance N_2

b) 40 % H_2, balance N_2

c) 15 % H_2, 15% H_2O, balance N_2

In case of cerium based sorbents, formation of pre-reduced cerium oxide (CeO_n) is necessary. It is an important step in desulfurization, because it helps to reduce the outlet H_2S concentration. About 20 – 30 mg of sorbent was used and heated to the required temperature (550 to 850 °C). Once the temperature was reached, the sorbent was then exposed to desired level of reducing condition by switching to the reducing gas. Once the reduction was complete, the sample was then oxidized again switching from reducing gas to air to see the reverse behavior at flow rate of 100 ml/min.

4.2.5 Inductively coupled plasma mass spectrometry (ICP-MS) and X-ray fluorescence (XRF)

Nu-Plasma multi-collector ICPMS equipped with UP-213 laser ablation system was used to detect the metal composition in the mixed metal oxide supported-ion exchanged zeolite (MMS-IZ) sorbents. Perkin Elmer's Elan 6000 ICP-MS instrument (ICP RF power was 1300 W; Dual detector mode) was used to detect the metal composition in the MMS-IZ sorbents. The X-ray fluorescence (XRF) was also used to get the composition of prepared sorbents. XRF instrument was L-energy dispersive EDAX XRF microproble system. Power used was 40 kV/50 μamps with optics - 30-micron poly-capillary, 1mm and 2 mms collimator.

4.3 SULFIDATION TESTS

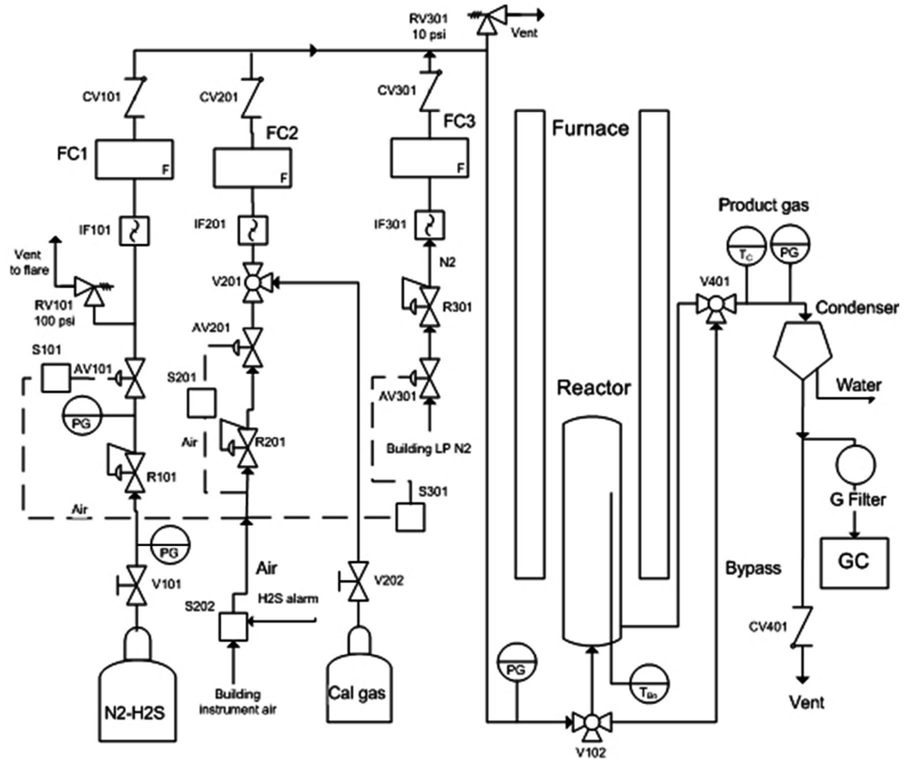

Figure 4.1: Packed bed experimental set up flow diagram (AITF, Devon)

Packed bed reactor system was used to perform the sulfidation test. The system is as shown in Figure 4.1. The quartz reactor was used to form the packed bed system. The quartz reactor had two different quartz tubes connected by Swagelok fitting. The inner reactor had a restriction where initially a layer of quartz wool was placed to form a base for the sorbent bed to sit on. The sorbent material was then inserted in to the inner quartz reactor tube and one more layer of quartz wool was placed on the sorbent bed to control fluidization of sorbent particle. A three-zone tube furnace (Lindberg/blue M) equipped with temperature controller was used to control the reactor temperature throughout the experiments.

A 10 m, PPU channel was used to determine the inlet and outlet concentration of H_2S using a micro gas chromatograph (GC model: Varian CP 4900). The PPU channel is capable of detecting the H_2S concentration to minimum of 20 ppm. The PPU channel was calibrated for H_2S and SO_2 gases and the details of calibration are mentioned in appendix A. The sulfidation tests were carried out using H_2S-N_2 (0.18% H_2S and remaining N_2) gas mixture (Praxair). The flow rate of gas was controlled by using the mass flow controllers (MFCs).

To perform the experiment the gas mixture was entered from the bottom of the inside reactor and sorbent bed was placed in the middle of reactor. The product gas exited from the bottom of the outside tube reactor. The exit gas was then passed to the gas chromatograph (GC) for analysis. Table 4.3 shows the list of equipment and their specifications used.

Table 4.3: List of equipment and their specifications

Component	**Specifications**
Packed bed	Material: Quartz Diameter: Inner tube: OD- 0.635 cm Outer tube: OD- 1.27 cm Height: Inner Tube: 45 cm Outer Tube: 60 cm Maximum temp: 900 °C Pressure: Atmospheric

Furnace	3 zone tube furnace Inside diameter: 13 cm Height of heater: 60 cm External dimensions: 43.2×88.9×40.6 cm 240V, 70 Amp
Flow controller	FC1 FC2 FC3 Omega mass flow controllers Flow range: 0-10 SLM Max pressure 500 psig
Valves	Check valves 316 SS CV101 CV201 CV301 CV401 Cracking pressure: 1/3 psig Maximum pressure: 3000 psig
	3 - way valves V401 V402 Maximum pressure: 2500 psig
	In-line filters 316 SS, 15 micron

	IF101 IF201 IF301 Maximum pressure: 3000 psig
	Relief valves RV101 RV201 Set point: 100 psi Maximum pressure: 6000 psig RV401 Set point: 10 psi Maximum pressure: 225 psig
	Ball valves V102 V202 V301 Maximum pressure: 3000 psig
	Air operating valve AV301 Maximum pressure: 3000 psig
Gas mixture	H_2S and N_2 H_2S = 1800 ppmv and balance N_2
Water condenser	SS 316

	Maximum pressure: 3000 psig
1/4 ″ SS Tubing (035 wall)	Pressure rating: 21,000 psi burst Temperature Rating : 232 °C
1/2 ″ SS Tubing (035 wall)	Pressure rating: 21,000 psi burst Temperature Rating : 232 °C

The product or feed gas was analyzed by using a micro gas chromatograph (GC Model: Varian CP 4900) containing two channels. The PPU column was installed. The PPU channel is capable of detecting the H_2S concentration to minimum of 20 ppm.

4.4 SORBENT REGENERATION

Once the sulfidation test was completed, the gas was switched to N_2. The temperature was set to the regeneration temperature. Once the regeneration temperature was reached, the flow of gas was switched to air (instrument grade). The outlet gas in regeneration was analyzed by micro GC for SO_2 concentration.

CHAPTER 5

RESULTS AND DISCUSSION

This chapter describes the characterization and performance results of high temperature desulfurization sorbents synthesized in this work. Copper-cerium and copper-cobalt mixed metal oxide and mixed metal oxide supported-ion exchanged zeolite sorbents (MMS-IZ) were evaluated over a wide temperature range of 350 to 850 °C using 0.18% H_2S and balance N_2 gas mixture under atmospheric pressure. The zeolites used were zeolite-Y, Ca-chabazite, clinoptiolite.

5.1 FRESH SORBENT CHRACTERIZATION RESULTS

5.1.1 BET surface area

The surface area of the synthesized sorbents was evaluated by using BET method. The Table 5.1 shows the surface area results for mixed metal oxide sorbents and Table 5.2 shows the surface area results for MMS-IZ sorbents. The surface area for mixed metal oxide sorbents was independent of the metal oxide ratios while in case of Cu-Ce mixed metal oxide sorbent higher surface area was recorded with increasing Ce content. In case of MMS-IZ sorbents, small reduction in the total surface area in case of zeolite-Y and chabazite, while more reduction in the surface area in case of clinoptiolite was observed. This reduction in surface area may be due to the different structure and ion-exchange capacity of individual zeolite.

Table 5.1: Surface area analysis for mixed metal oxide sorbent

Sorbent	**BET (m^2/g)**	**Sorbent**	**Surface Area (m^2/g)**
3CuO - CeO_2	7.86	3CuO - Co_3O_4	6.68
CuO - CeO_2	3.26	CuO - Co_3O_4	3.48
CuO - 3CeO_2	15.6	CuO - 3Co_3O_4	6.76

Table 5.2: Surface area analysis for mixed metal oxide supported-ion exchanged zeolite sorbents (MMS-IZ) sorbents

Sorbent	**BET of raw support (m^2/g)**	**BET after ion exchange (m^2/g)**	**Micropore Volume (cc/g)**
Cu-Ce-ZY	268	231	0.075
Cu-Ce-CC	412	379	0.150
Cu-Ce-CL	101	68.0	0.028
Cu-Co-ZY	268	241	0.075
Cu-Co-CC	412	392	0.150
Cu-Co-CL	101	78.2	0.028

5.1.2 X-Ray diffraction

The X-ray diffraction (XRD) analysis was performed in order to study the different phases formed in the prepared sorbents. In case of copper-cerium mixed metal oxide sorbents, the XRD was performed to confirm the different phases of copper and cerium oxide while to confirm the formation of copper-cobalt oxide in case of copper-cobalt mixed metal oxide. In case of natural zeolites, the XRD was performed on the raw zeolite samples to get the phases present in each of them. XRD was also performed on the MMS-IZ sorbents to know if any changes occurred in the zeolite structure. Table 5.3 shows the phases identified in the XRD analysis for copper-cerium and copper-cobalt mixed metal oxide sorbents.

Figure 5.1 shows the typical XRD spectra for copper-cerium mixed metal oxide (Cu-Ce=3:1 and Cu-Ce=1:3). The separate CuO and CeO_2 phases were observed. Figure 5.2 shows the typical XRD spectra for copper-cobalt mixed metal oxide (for equimolar (Cu-Co=1:1) mixture) and the formation of copper-cobalt oxide ($Cu_xCo_{(3-x)}O_4$) as well as excess copper or cobalt oxide were observed as individual phases.

Many researchers failed to report the formation of copper-cobalt oxide ($Cu_xCo_{(3-x)}O_4$), because the peaks are overlapping with the cobalt oxide but the copper-cobalt oxide is formed and is stable in certain temperature range based on the method of synthesis.

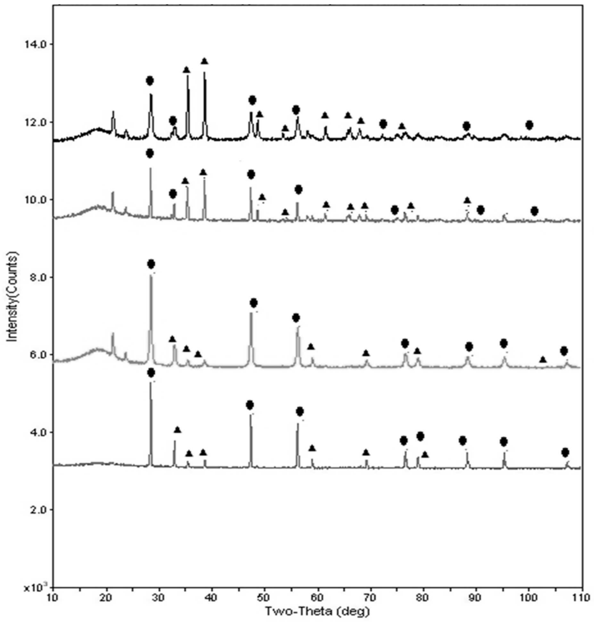

Figure 5.1: XRD spectra for copper-cerium mixed metal oxide (▲ = copper oxide, ● = cerium oxide) the first two spectra are for Cu-Ce (3:1) and lower two are for Cu-Ce (1:3)

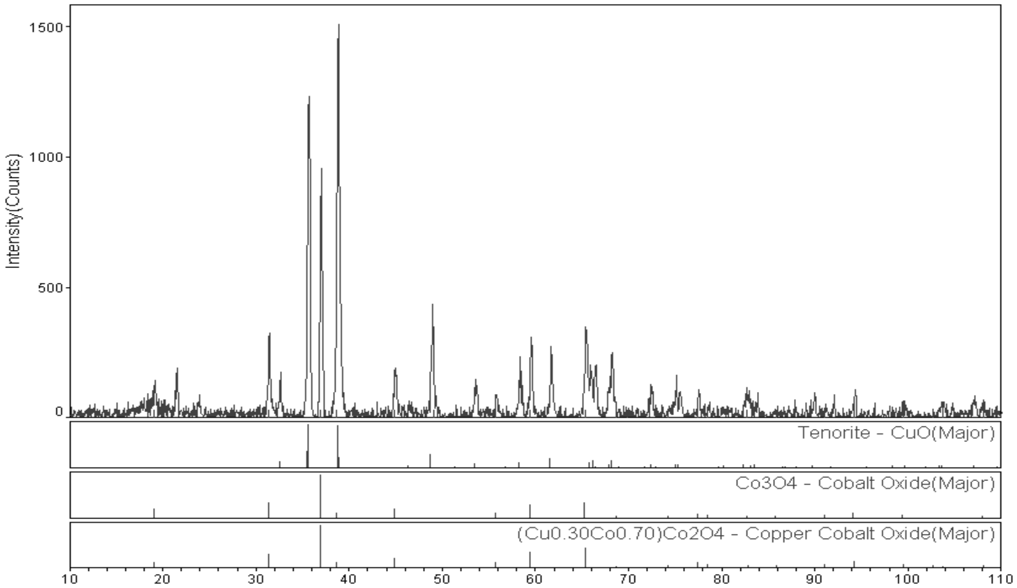

Figure 5.2: XRD spectra for copper-cobalt mixed metal oxide showing the formation of copper cobalt oxide ($Cu_xCo_{(3-x)}O_4$), x=0.30 for Cu-Co (1:1)

Table 5.3: Phases observed in the XRD for mixed metal oxide sorbents

Sorbent	**Crystalline phases (Fresh)**
3CuO - CeO_2	CuO, CeO_2
CuO - CeO_2	CuO, CeO_2
CuO - 3CeO_2	CuO, CeO_2
3CuO - Co_3O_4	$Cu_xCo_{3-x}O_4$, CuO, Co_3O_4
CuO - Co_3O_4	$Cu_xCo_{3-x}O_4$, CuO, Co_3O_4
CuO - 3Co_3O_4	$Cu_xCo_{3-x}O_4$, CuO, Co_3O_4

XRD peaks of various zeolites are shown in Figure 5.3 and the major phases are listed in the Table 5.4. The XRD of zeolite-Y mainly showed the presence of faujasite but some clinoptiolite was also recorded. In case of raw sedimentary chabazite the presence of Ca as well as Na chabazite was recorded on the XRD spectra. In case of clinoptiolite, the main phase observed was clinoptiolite but quartz and silica phases were also noted separately (Junaid et al., 2011).

Table 5.4: Phases observed in the XRD for mixed metal oxide supported-ion exchanged zeolite sorbents (MMS-IZ) sorbents

Zeolite	**Crystalline phases**
Zeolite -Y	Faujasite, Clinoptiolte
Raw Sedimentary Chabazite	Ca , Na forms of Chabazite
Clinoptiolite	Clinoptiolite, Quartz/Silica

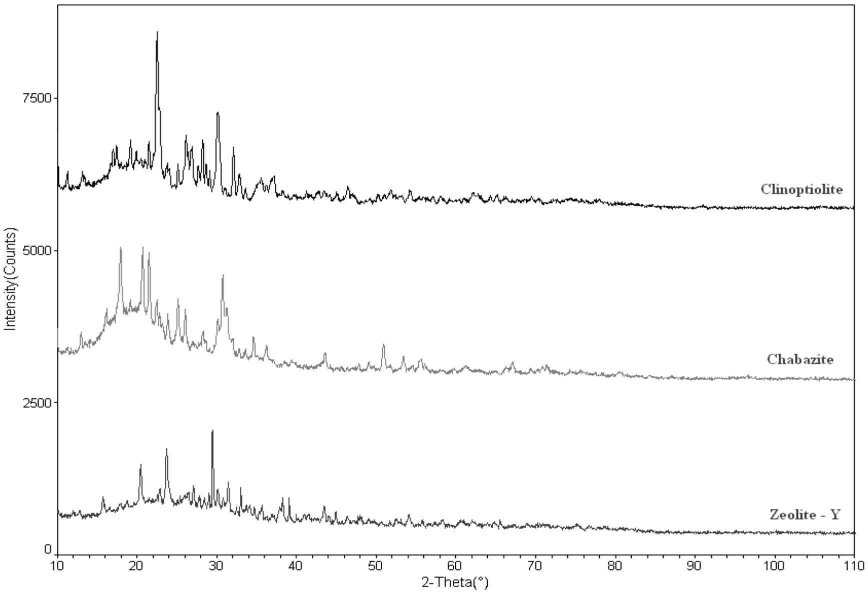

Figure 5.3: X-ray diffraction pattern of the mixed metal oxide supported-ion exchanged zeolite sorbents (MMS-IZ) sorbents

5.1.2.1 Quantitative analysis by Siroquant

The Siroquant analysis was performed to understand the various phases of metal oxides present in the synthesized mixed metal oxide sorbents and the zeolite phases in case of raw zeolite support. Figures 5.4 to 5.6 and Tables 5.5 and 5.6 show the results obtained from Siroquant analysis. The analysis showed that the major oxide phases (CuO, Co_3O_4, and CeO2) were almost present in the same proportions as mixed while synthesizing the sorbents.

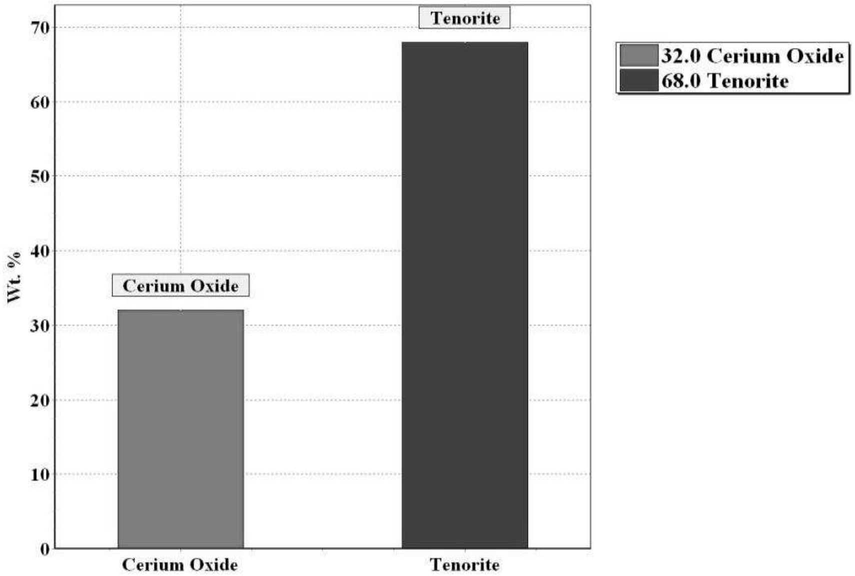

Figure 5.4: Siroquant analysis for Cu-Ce (3:1) mixed metal oxide sorbent (Teronite = CuO)

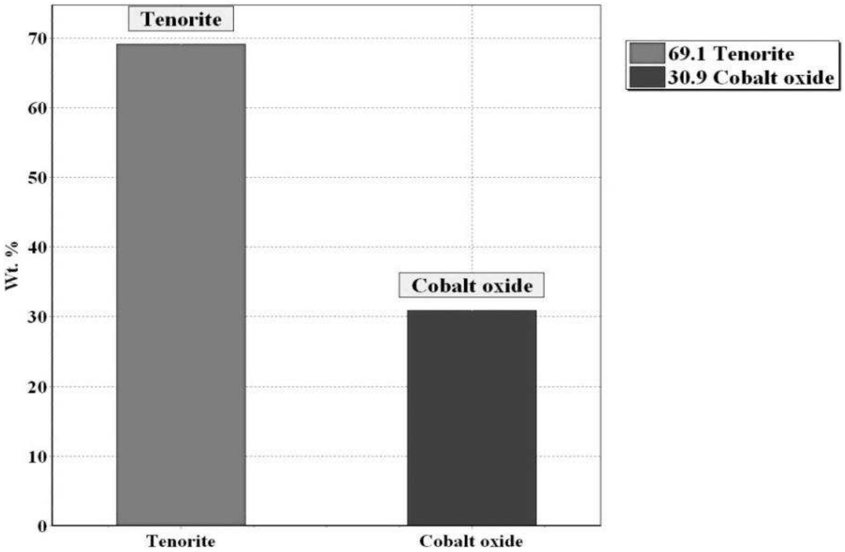

Figure 5.5: Siroquant analysis for Cu-Co (3:1) mixed metal oxide sorbent (Teronite = CuO)

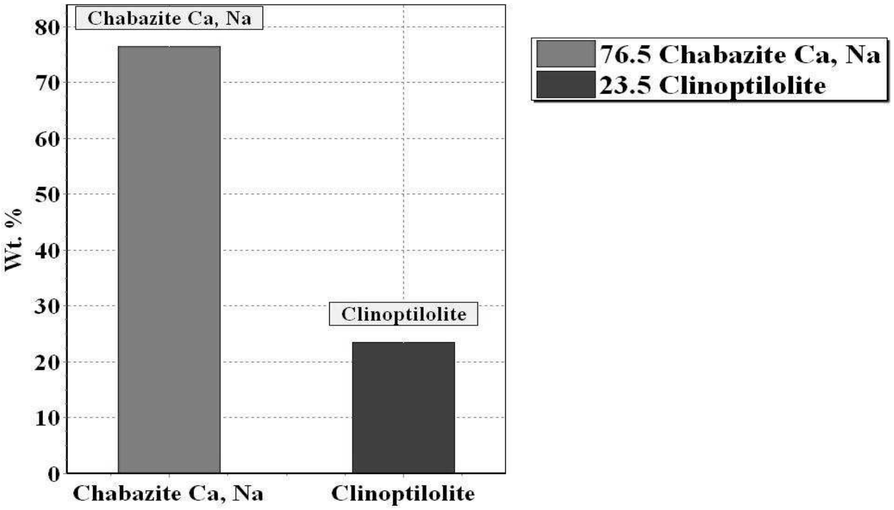

Figure 5.6: Siroquant analysis for raw sedimentary chabazite

Table 5.5: Quantitative analysis by Siroquant for mixed metal oxide sorbents

Sorbent Type	**CuO-CeO_2 (3:1)**	**CuO-CeO_2 (1:1)**	**CuO-CeO_2 (1:3)**	**CuO-Co_3O_4 (3:1)**	**CuO-Co_3O_4 (1:1)**	**CuO-Co_3O_4 (1:3)**
CuO Content (wt%)	68 (69.7)*	41 (31.6) *	13.4 (13.3) *	69.1 (49.7) *	25.5 (24.8)*	13 (9.9) *
Co_3O_4 Content (wt%)	N.A	N.A	N.A	30.9 (50.3) *	74.5 (75.2)*	87 (91.1) *
CeO_2 Content (wt%)	32 (30.3)*	58 (68.3) *	86.6 (86.7) *	N.A	N.A	N.A
χ^2	4.47	3.59	4.04	5.08	4.58	3.56
R	0.412	0.369	0.405	0.425	0.415	0.368

* *The weight % of oxide while synthesizing the sorbents*

Table 5.6: Quantitative analysis for raw zeolites by Siroquant

Sorbent Type	**Faujasite**	**Na-Al-Silicates**	**Chabazite**	**Clinoptiolite**	**Silica**
Zeolite Y	78.3	21.7	N.A	N.A	N.A
Chabazite	N.A	N.A	76.5	23.5	N.A
Clinoptiolite	N.A	N.A	N.A	88.2	11.8

5.1.3 Quantitative analysis by x-ray fluorescence (XRF) and inductively coupled plasma mass spectrometry (ICP-MS)

The analysis of MMS-IZ sorbents was carried out using XRF to determine quantitatively the degree of ion exchange in the zeolite during the synthesis process. XRF analysis was performed on raw as well as MMS-IZ to confirm the percentage exchange of mono positively charged ions with Cu and Ce. The SiO_2 as well as Al_2O_3 measurement performed to get the Si/Al ratio for zeolite. The Tables 5.7 and 5.8 show the typical XRF and ICP-MS analysis results for zeolite –Y exchanged with Cu-Ce and Cu-Co, respectively. From the XRF results, clinoptiolite has the highest Si/Al ratio (~ 5) than chabazite (~ 4.5) and zeolite-Y (~ 2.61). The presence of copper, cerium and cobalt confirmed the degree of ion exchange in the zeolites. ICP-MS also corroborates the XRF results.

Table 5.7: XRF analysis for raw zeolite-Y and Cu-Ce-ZY

Element	Weight % (Raw zeolite-Y)	Weight % (Cu-Ce-ZY)
NaK	13.61	3.960
MgK	0.91	0.760
AlK	17.03	22.76
SiK	48.06	59.48
TiK	-	1.370
CeK	-	5.100
FeK	2.82	1.690
CuK	-	4.060

Table 5.8: ICP-MS analysis for Cu-Ce-ZY and Cu-Co-ZY

Analyte	Na	Al	Cu	Ce	Co
Detection Limits	0.5	0.2	0.03	0.03	0.03
Units	ppm	ppm	ppm	ppm	ppm
Cu-Ce-ZY	14528	156051	17978	28271	N.A.
Cu-Co-ZY	18256	185463	25463	N.A.	50236

5.1.4 Scanning electron microscopy (SEM) analysis

Figure 5.7 (a) and Figure 5.7 (b) show a typical SEM images for equi-molar (1:1) copper-cerium and copper-cobalt mixed metal oxide sorbents respectively. Figure 5.7 (a) shows a different structure for the copper-cerium sorbent. No distinct phases of copper and cerium oxide were observed but the particles in the overall phase may be of copper on cerium. The similar morphologies were also found for Cu-Ce (3:1) and (1:3) mixed metal oxide sorbents. Li and Flytzani-Stephanopoulos (1997) and Zeng et al. (2000) also reported the similar observations. Figure 5.7 (b) shows SEM of copper-cobalt oxide. A formation of cluster was clearly visible for this class of sorbent. The cluster formation might be due to the presence of spinel as well as individual excess oxide phases. XRD results also support of formation of copper-cobalt oxide spinel form. Figures 5.7 (c to e) shows the surface morphology of MMS-IZ sorbents. The modified chabazite (Figure 5.7 (c)) and clinoptiolite (Figure 5.7 (d)) were showing the similar platy morphology with crystals and layers, as present in parent zeolites. While zeolite-Y shows the completely different structure (Figure 5.7 (e)) and no distinct change was observed in the modified zeolite-Y. Platy morphology of natural zeolites helps to achieve the surface interaction (Abu Junaid et al., 2011).

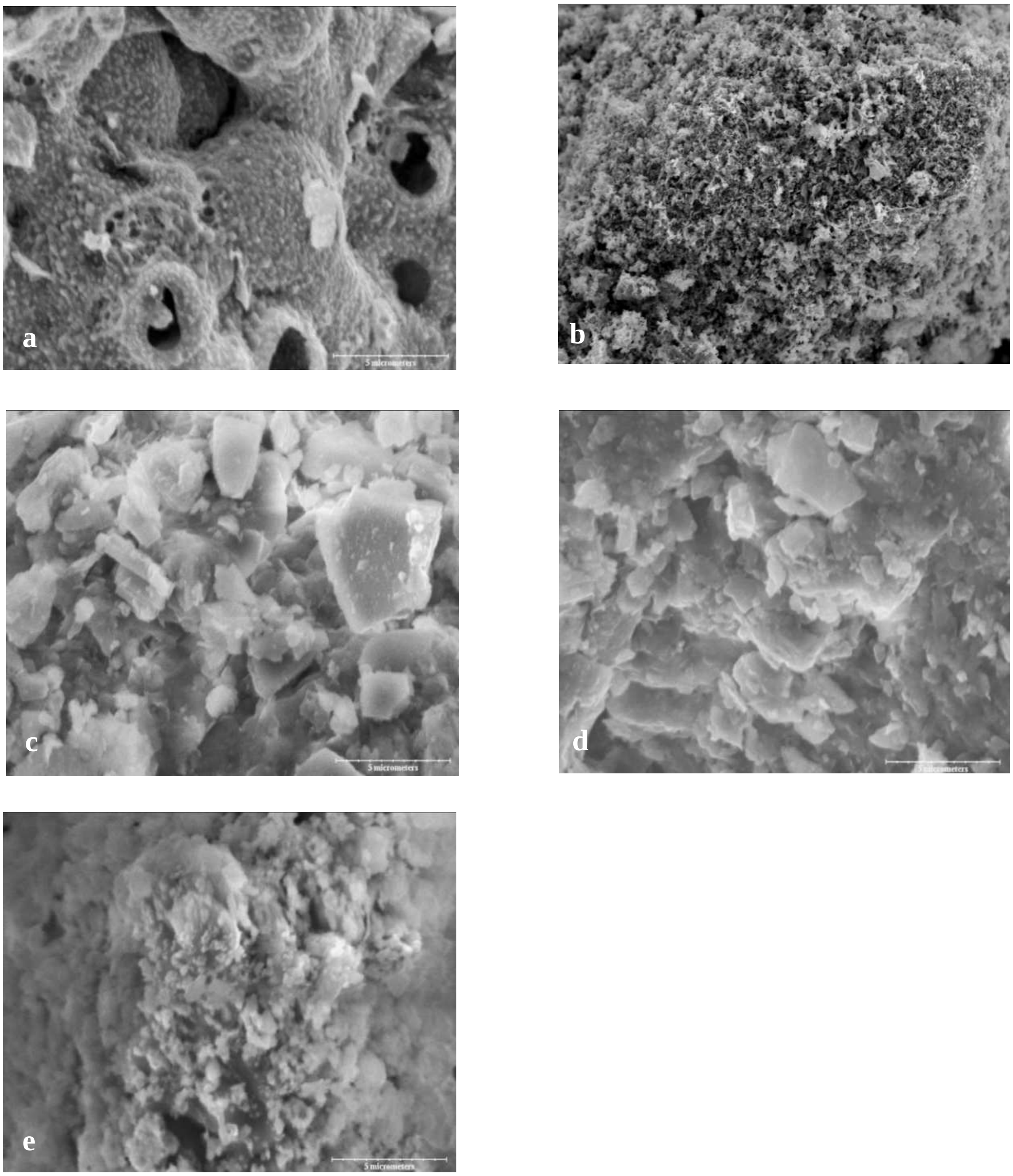

Figure 5.7: SEM analysis for mixed metal oxide sorbent (a = Cu-Ce (1:1), b Cu-Co (1:1)) and mixed metal oxide supported-ion exchanged zeolite sorbents (MMS-IZ) (c = chabazite, d = clinoptiolite, e = zeolite-Y) at magnification of 6000 (5 μm)

5.1.5 Thermogravimetric analysis (TGA)

5.1.5.1 Thermal stability of sorbent

In order to understand the thermal stability of sorbents at higher temperature the sorbents were heated to about 850 °C in N_2 atmosphere with 100 ml/min flow. Figure 5.8 and Figure 5.9 show the thermal stability trend for Cu-Ce and Cu-Co mixed metal oxide sorbents at various compositions, respectively and Table 5.9 lists the values of the corresponding weight loss of these sorbents**.** For all the sorbents, small weight loss was observed initially due to loss of adsorbed moisture and then there was negligible weight loss (< 1.0 %) up to 750 °C.

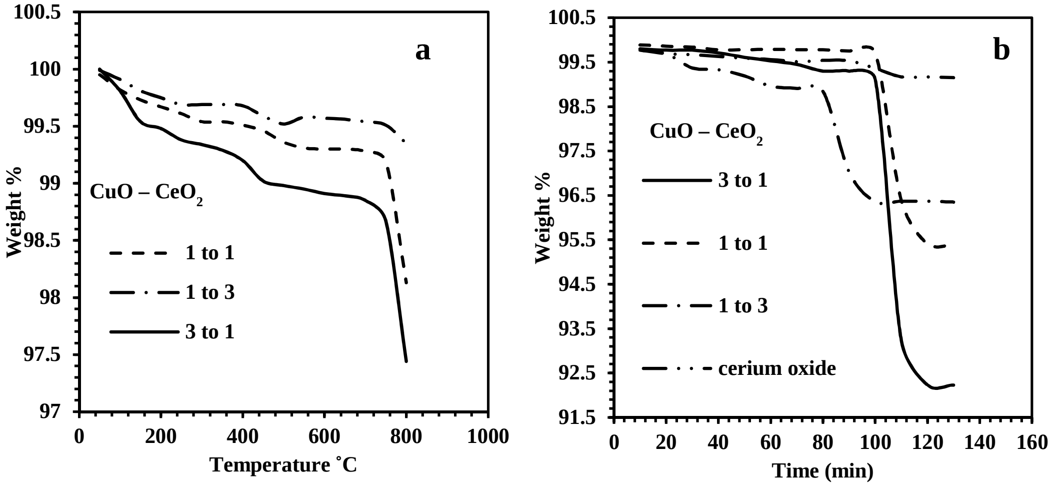

Figure 5.8: Thermal stability for Cu-Ce mixed metal oxide sorbents at 850 °C in N_2 atmosphere only

In case of Cu-Ce mixed metal oxide sorbents, the major weight loss was observed above 750 °C and there was a decrease in weight loss with increasing Cu-Ce ratio. This loss might be due to the changes in copper oxide. In case of only CeO_2 the weight loss was observed to be around 1% which confirms that the addition of CeO_2 increases the thermal stability of Cu-Ce mixed metal oxide sorbents. In case of Cu-Co mixed metal oxide sorbents, the same weight loss was observed for all Cu-Co ratios.

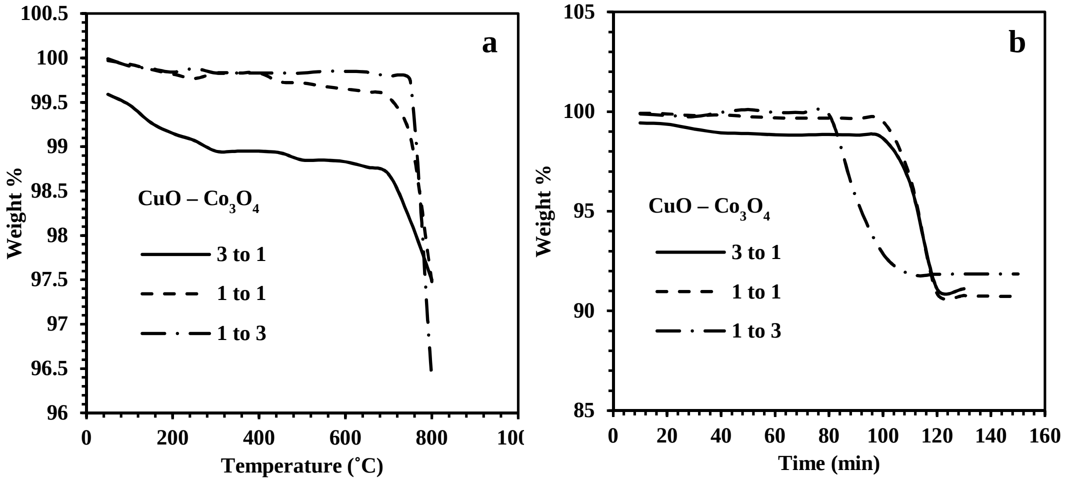

Figure 5.9: Thermal stability for Cu-Co mixed metal oxide sorbents at 850 °C in N_2 atmosphere only

Table 5.9: Weight loss results (TGA) for mixed metal oxide sorbents at 850 °C in N_2 atmosphere only

Sorbent	Weight Loss (%)	Sorbent	Weight Loss (%)
3 CuO – 1 CeO_2	7.77	3 CuO – 1 Co_3O4	9.14
1 CuO – 1 CeO_2	4.59	1 CuO – 1 Co_3O4	9.23
1 CuO – 3 CeO_2	3.64	1 CuO – 3 Co_3O4	9.33

Figure 5.10 show the thermal stability trend and table 5.10 lists the corresponding weight loss for Cu-Ce and Cu-Co MMS-IZ sorbents. The weight loss observed was less in case of zeolite-Y as compared to chabazite and clinoptiolite based MMS-IZ sorbents. The weight loss in case of Cu-Co MMS-IZ

was observed to be higher than that of Cu-Ce MMS-IZ. This thermal behavior may be due to the rare earth metal oxide in case of Cu-Ce MMS-IZ giving the extra thermal stability. MMS-IZ sorbents are observed to be thermally stable as compared to mixed metal oxides.

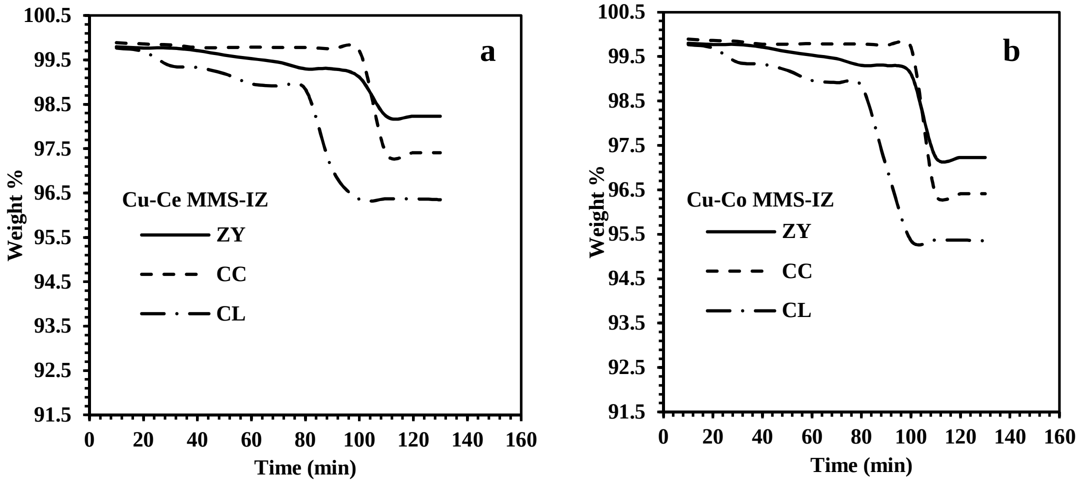

Figure 5.10: Thermal stability for (a) Cu-Ce and (b) Cu-Co mixed metal oxide supported-ion exchanged zeolite sorbents (MMS-IZ) sorbents at 850 °C in N_2 atmosphere only

Table 5.10: Weight loss results (TGA) for mixed metal oxide supported-ion exchanged zeolite sorbents (MMS-IZ) sorbents at 850 °C in N_2 atmosphere only

Sorbent	Weight Loss (%)	Sorbent	Weight Loss (%)
Cu-Ce-ZY	1.77	Cu-Co-ZY	2.77
Cu-Ce-CC	2.59	Cu-Co-CC	3.59
Cu-Ce-CL	3.63	Cu-Co-CL	4.63

5.1.5.2 Reduction Tests

In order to evaluate the effect of reducing gaseous environment on the sorbents, reduction tests were also performed at different reduction conditions by varying the concentration of hydrogen. The reduction study was performed with following compositions of gaseous environment.

d) 15 % H_2, balance N_2

e) 40 % H_2, balance N_2

f) 15 % H_2, 15% H_2O, balance N_2

40% H_2 is the most reducing gas composition, secondly 15% H_2 and then 15% H_2 and 15% H_2O. In case of 15% H_2 and 15% H_2O, the presence of H_2O can be a source of small quantity of oxygen at elevated temperature. As shown in Figures 5.12 and 5.13, total reduction for Cu-Ce mixed metal oxide sorbents was about 15%. However, when the temperature was increased from 350 to 800 °C, no significant change was observed in the reduction pattern and the effect of partial pressure of H_2 was less prominent on degree of reduction while Li and Flytzani-Stephanopoulos (1997) reported the bimodal reduction by hydrogen. The reduction for Cu-Ce mixed metal oxide sorbents was about 8% with the addition of 15% H_2O to the gas.

It is important to note that each oxide phase is less reducible as compared to the mixed metal oxide sorbent. The reduction behavior of CuO-CeO_2 mixed metal oxide sorbent is as shown in Figures 5.11, 5.12, and 5.13. Similar reduction behavior was also observed for Cu-Co mixed metal oxide sorbents and is shown in Figure 5.14. A fast reduction response was recorded in more reducing environment for Cu-Co mixed metal oxide sorbents as shown in Figure 5.15. For pure oxides, the slow reduction response was recorded at lower temperature than at higher temperature but in case of mixed metal oxide, the reduction rate was almost the same. Hence, the mixed metal oxide form is more reducible.

Reduction analysis was also carried out for MMS-IZ sorbents to observe their behavior in reducing atmosphere and over a wide temperature range. Figure 5.16 shows a typical reduction behavior of Cu-Ce-CC and Table 5.11 lists the reduction weight loss in case of Cu-Ce MMS-IZ sorbents in 15 % H_2 and balance N_2 environment. It was observed that MMS-IZ sorbents were less prone to reduction as compared to the mixed metal oxide sorbents. The reduction behavior of mixed metal oxide sorbents showed more reducibility nature in combination of metal oxides than individual oxide phases while different reduction pattern was observed in case of zeolite based sorbents.

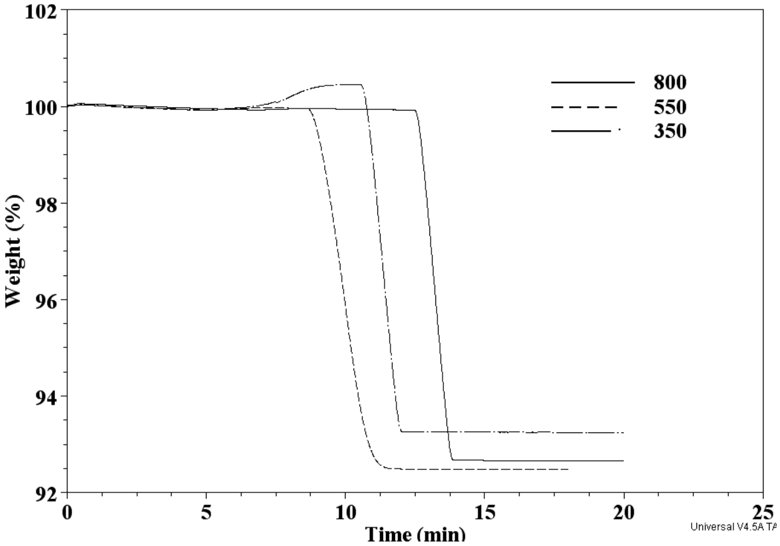

Figure 5.11: Reduction in 15 % H_2, 15% H_2O, balance N_2 for Cu-Ce mixed metal oxide sorbent

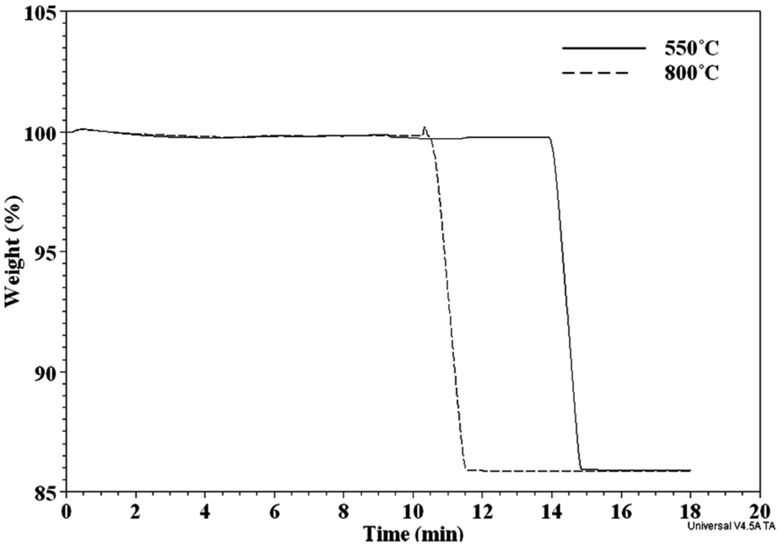

Figure 5.12: Reduction in 15 % H_2, balance N_2 for Cu-Ce mixed metal oxide sorbent

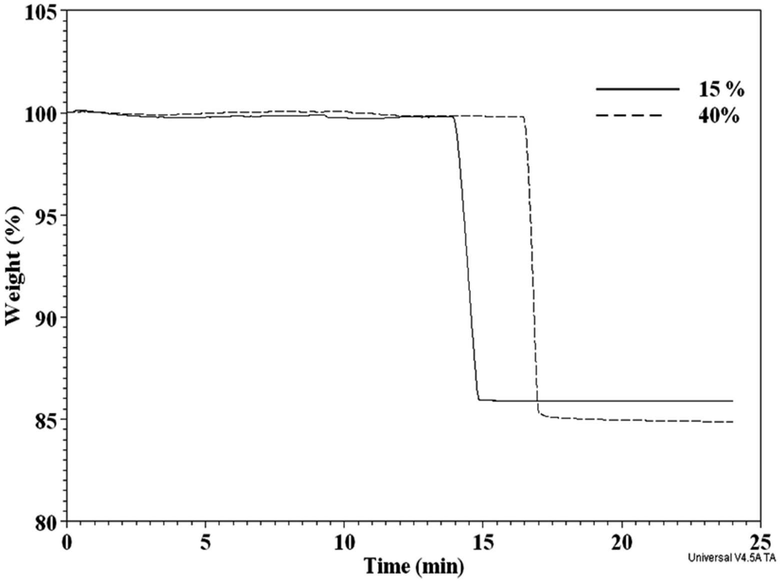

Figure 5.13: Reduction in 15 % H_2 and 40% H_2 with balance N_2 at T = 800 °C for Cu-Ce mixed metal oxide sorbent

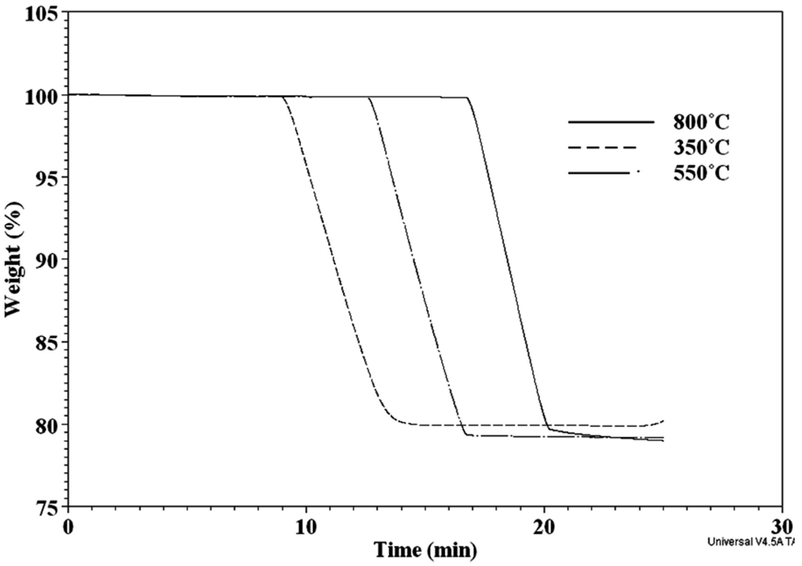

Figure 5.14: Reduction in 15 % H_2, balance N_2 for Cu-Co mixed metal oxide sorbent

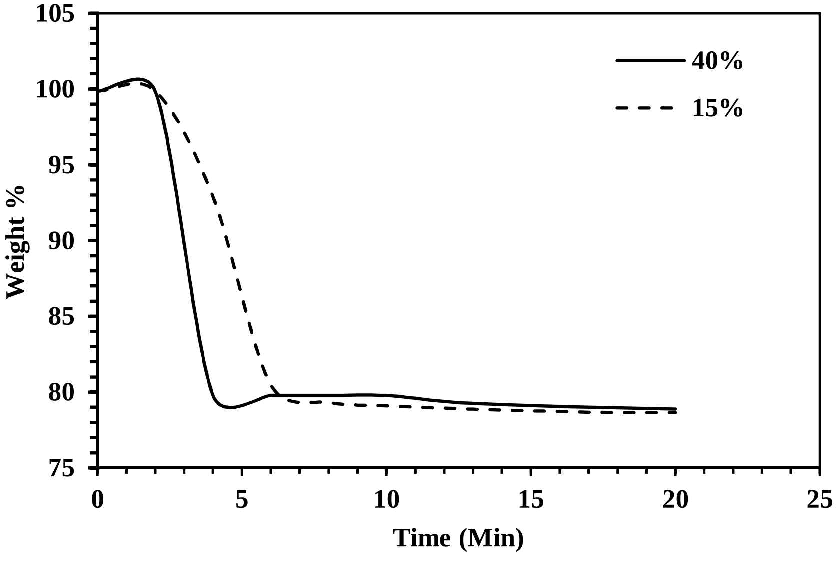

Figure 5.15: Reduction in 15 % H_2 and 40% H_2 with balance N_2 at T = 550°C for Cu-Co mixed metal oxide sorbent

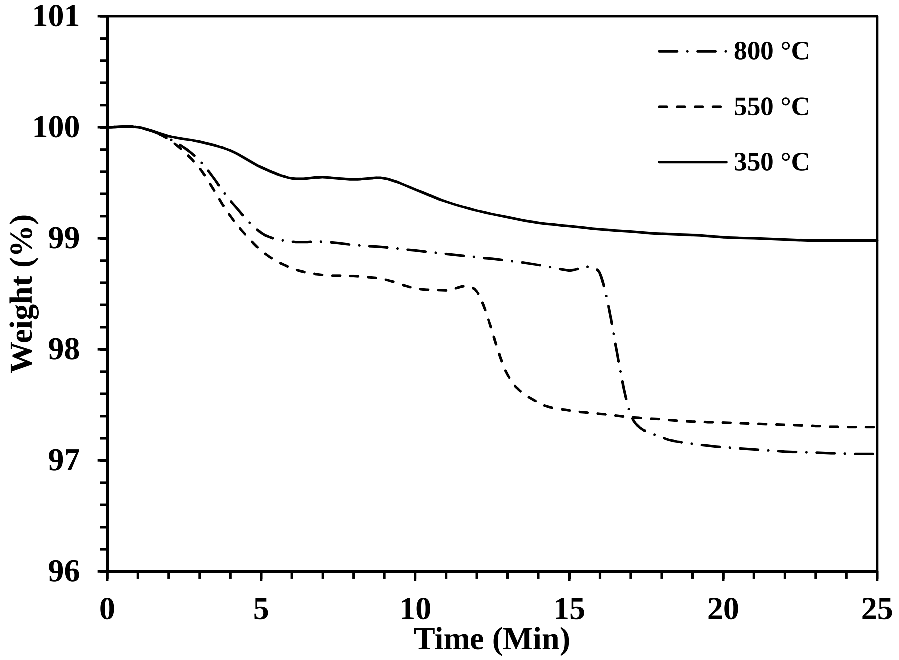

Figure 5.16: Reduction in 15 % H_2, balance N_2 for Cu-Ce-CC

Table 5.11: Reduction data for mixed metal oxide supported-ion exchanged zeolite (MMS-IZ) sorbents in 15 % H_2 and balance N_2 environment

Sorbent Type	Temperature (°C)	% Weight loss	Sorbent Type	Temperature (°C)	% Weight loss
Cu-Ce-ZY	350	0.5	Cu-Ce-CC	800	3.0
Cu-Ce-ZY	550	1.2	Cu-Ce-CL	350	0.3
Cu-Ce-ZY	800	1.9	Cu-Ce-CL	500	0.8
Cu-Ce-CC	350	1.3	Cu-Ce-CL	800	1.3
Cu-Ce-CC	550	2.7			

5.1.5.3 Reduction of CeO_2 in CuO-CeO_2 mixed metal oxide sorbent

In order to understand the reduction of CeO_2 to non-stoichiometric oxide, CeO_n and to calculate value of n, pure cerium oxide was reduced in the similar reduction conditions discussed in previous Section (5.1.5.2). The value of n is based on the reducing environment. Three blank runs were performed with empty sample pan for baseline correction. The actual weight loss was then corrected by subtracting the blank reduction data. The value of n in CeO_n was then calculated (See Appendix D-1). Table 5.12 shows the level of reduction observed and the value of n in CeO_n at various temperatures and various reducing environments. Figure 5.17 shows the average value of n in CeO_n is a function of temperature. A similar observation was also reported by Zeng et al. (2000).

Table 5.12: Reduction data for CeO_2

Gas Composition	**Temperature (°C)**	**% Weight loss**	**Value of n in CeO_n**
15% H_2, Remaining N_2	350	0.17	1.99
15% H_2, Remaining N_2	550	0.53	1.94
15% H_2, Remaining N_2	800	0.96	1.90
40% H_2, Remaining N_2	350	0.39	1.96
40% H_2, Remaining N_2	550	0.63	1.93
40% H_2, Remaining N_2	800	0.94	1.90

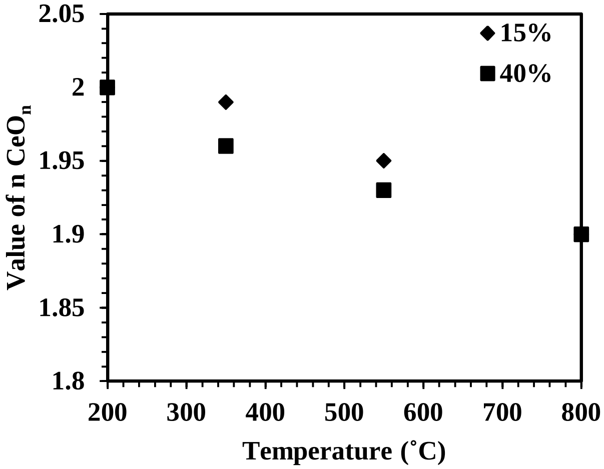

Figure 5.17: Comparison of reducibility in 15 % H_2 and 40% H_2

5.1.6 Conclusion from sorbent characterization and reduction tests

BET surface area measurement confirms that the mixed metal oxide sorbents have reasonably good value of surface area and there is no significant drop in surface area of zeolites after ion exchange. XRD analysis also confirms the presence of required phases of oxides for hot gas desulfurization. In case of $CuO\text{-}CeO_2$ the separate phases are observed while in case of $CuO\text{-}Co_3O_4$ the separate phases as well as the presence of $Cu_xCo_{3-x}O_4$ are observed. Siroquant analysis shows that the mixed metal oxide ratios are achieved as per the synthesis requirement.

XRF and ICP-MS analysis confirms the degree of ion exchange in case of zeolites. SEM analysis supports the results of XRD and shows the platy morphology of natural zeolites. TGA analysis confirms the thermal stability of sorbent while reduction tests shows that mixed metal oxide sorbents are more reducible than individual phases and zeolites are not prone to reduction. In case of CeO_2 the formation CeO_n has been achieved by reduction with a n value in the range of 1.9-2.0.

5.2 SULFIDATION TEST RESULTS FOR SORBENTS

5.2.1 Breakthrough analysis: Blank test

The breakthrough analysis using inert material was performed to check the response delay of the adsorption system. Initially, the sulfidation tests were performed using silica, which is a non-reacting material with H_2S. Silica material of the same amount (around 50 mg) was placed inside the packed bed reactor and the sulfidation test was performed. The results were obtained over a wide temperature range of application (350 - 800 °C). The similar flow conditions as for the sorbent bed were used for blank test. For each case, the first trace of H_2S was detected at about 137 sec. Figure 5.18 show the blank adsorption test for different temperatures.

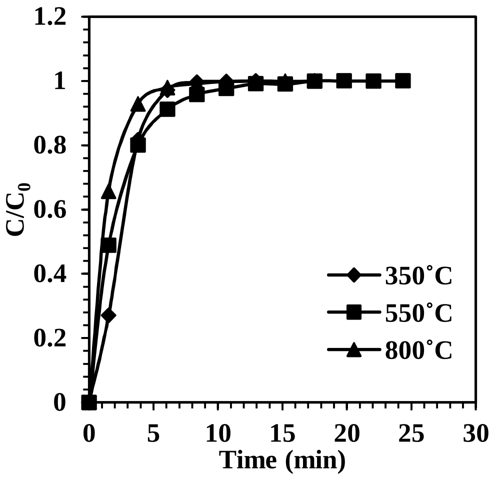

Figure 5.18: Breakthrough analysis for blank test by using inert material

5.2.2 Sulfidation performance study

5.2.2.1 Sulfidation tests for Cuo-CeO_2 sorbent system

Sulfidation tests were performed in a packed bed reactor with 0.18 % H_2S and N_2 (balance) as the feed gas mixture using fresh and without any prior reduction of the sorbent (the sulfidation performance of pre-reduced sorbent is discussed in Section 5.2.3). The gas flow rate used was 200 sccm and the tests were carried out at 550 °C. Figure 5.19 and Figure 5.20 show the breakthrough curve for sulfidation at 550 °C and 800 °C, respectively. The sulfidation breakthrough time is determined for 100 ppmv breakthrough point.

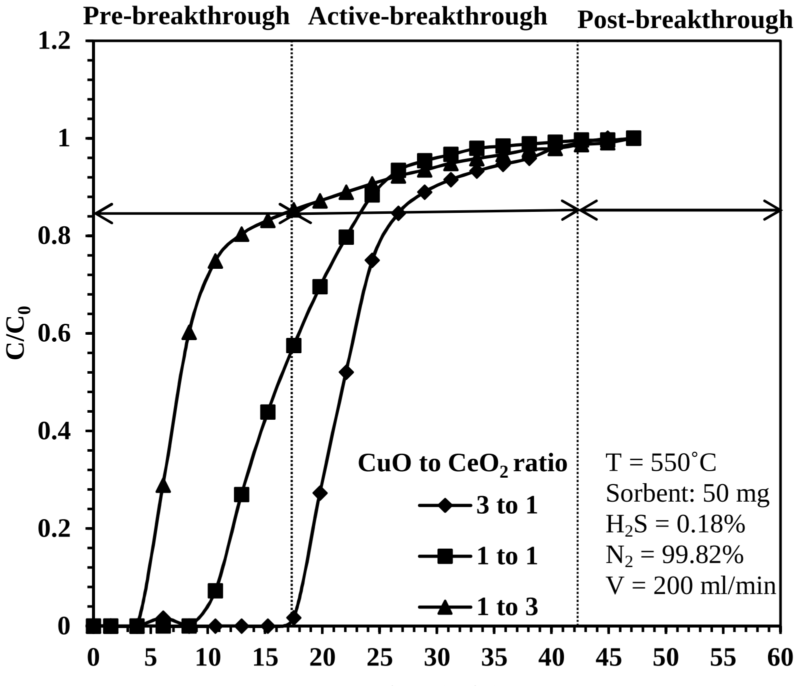

Figure 5.19: Sulfidation breakthrough curves for Cuo-CeO_2 mixed metal oxide sorbent at 550 °C (Breakthrough zones are shown for Cu-Ce (3:1))

The breakthrough Figures show a plot of normalized concentration, (C/C_0) versus time. The normalized concentration is defined as the ratio of H_2S concentration at the outlet to that of the inlet feed stream. The pre-breakthrough zone is the most important zone for sulfidation capacity determination. In this region, the main sulfidation reaction between H_2S and sorbent takes place. The product H_2S concentration reduced down significantly below the detection limit of the micro-GC, which was 20 ppmv. The reaction here is very fast and utilizes most of the sorbent bed.

In active breakthrough zone, the level of H_2S concentration goes up. This is the region where edge of sulfidation is reached for the sorbent bed and the concentration increases rapidly with time. The sulfidation kinetics in this region is relatively slow. The last region is post-breakthrough zone where the sorbent bed is saturated. There is no more sulfidation reaction taking place and the concentration reaches to the initial feed gas concentration.

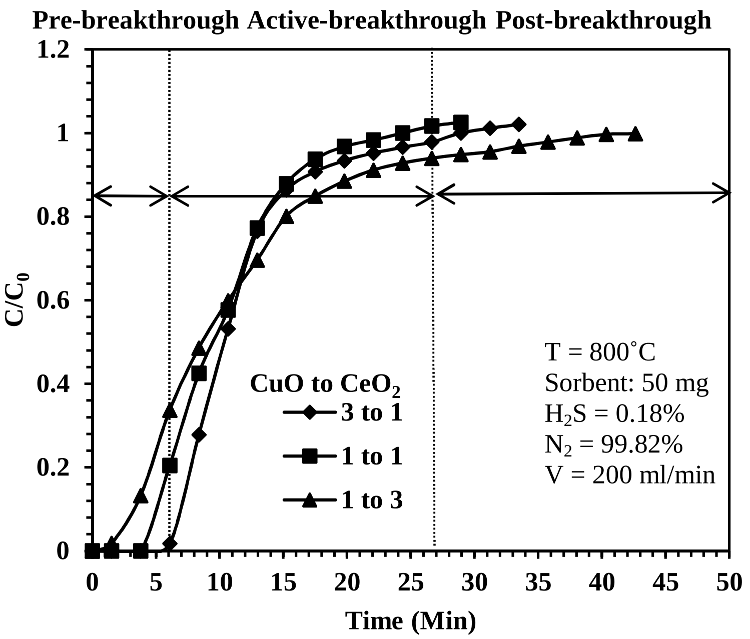

Figure 5.20: Sulfidation breakthrough curves for Cuo-CeO_2 mixed metal oxide sorbent at 800 °C (Breakthrough zones are shown for Cu-Ce (3:1))

Complete desulfurization of the feed stream was obtained using CuO-CeO_2 mixed metal oxide sorbents for both the sulfidation temperatures. The breakthrough was observed earlier when Cu-Ce ratio was increased which shows that CuO was utilized completely over CeO_2 at 550 °C and no pre-reduction. CeO_2 may or may not take part in the process of sulfidation but act as a dispersing agent for CuO. Zeng et al. (2000) reported that the Ce_2O_3 sulfidation reaction is exothermic while in case of CeO_2 the sulfidation reaction is endothermic. There are chances that CeO_2 participated in reaction at higher temperature and in order to establish that the characterization of sulfided sorbent was performed.

It is clear from Figures 5.19 and 5.20 that the H_2S breakthrough for CuO-CeO_2 mixed metal oxide sorbents occurred early at 800 °C than 550 °C, which means that the utilization of copper oxide has reduced at high temperature that may be due to increased resistance to sulfidation and increased crystal size at higher temperature. The reduced form of CeO_2 (CeO_n) has greater affinity toward H_2S than that of CeO_2 and the heat of reaction for CeO_n is intermediate to that of Ce_2O_3 and CeO_2 (Li and Flytzani-Stephanopoulos, 1997). The sorbents were prereduced to study the effect of reduction. The pre-reduced CeO_n was tested for sulfidation performance and discussed in details in Section 5.2.3.

5.2.2.2 Sulfidation tests for CuO-Co_3O_4 mixed metal oxide sorbent

The sulfidation for CuO-Co_3O_4 sorbent was studied in the range of 350 – 550 °C. Figures 5.21 and 5.22 show the breakthrough performance for Cuo-Co_3O_4 mixed metal oxide sorbents at 350 °C and 550 °C, respectively. It was observed that at 350 °C all the sorbents compositions had the good breakthrough performance (i.e. all sorbents produced pre-breakthrough H_2S levels below the detection limit of the micro-GC, which is below 20 ppmv) and Cu-Co (1:3) showed a relatively better pre-breakthrough zone but had extended active and post-breakthrough zones. As the CuO content increases the breakthrough occurs earlier which confirms the better sulfidation of Co_3O_4 at lower temperature. This observation is in good agreement with the thermodynamic analysis performed using Factsage and literature (Chung et al., 2005) which also suggest better sulfidation thermodynamics of Co_3O_4 at lower temperature. The sulfidation behavior at 550 °C is quite different. Sluggish behavior was observed and the sulfidation did not reach the 100% conversion. As the Co_3O_4 increases, the breakthrough observed earlier which shows the improper utilization of cobalt oxide at that temperature. To understand this behavior in details, the sulfided samples were analyzed and are discussed in details as below.

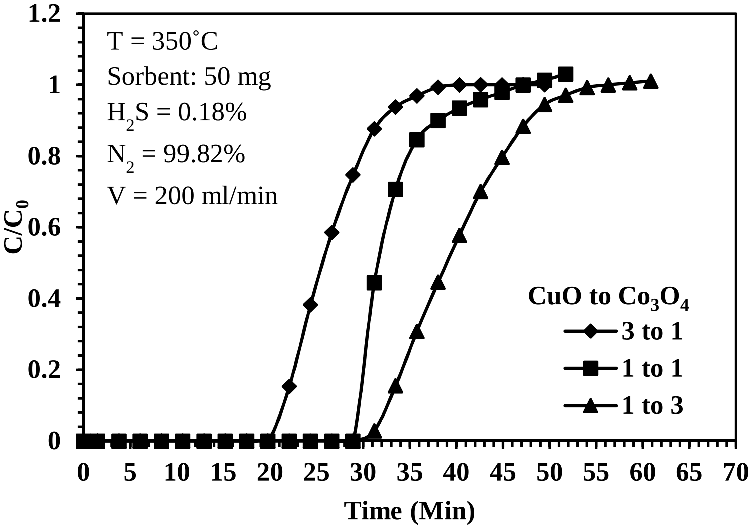

Figure 5.21: Sulfidation breakthrough curves for CuO-Co_3O_4 mixed metal oxide sorbent at 350 °C

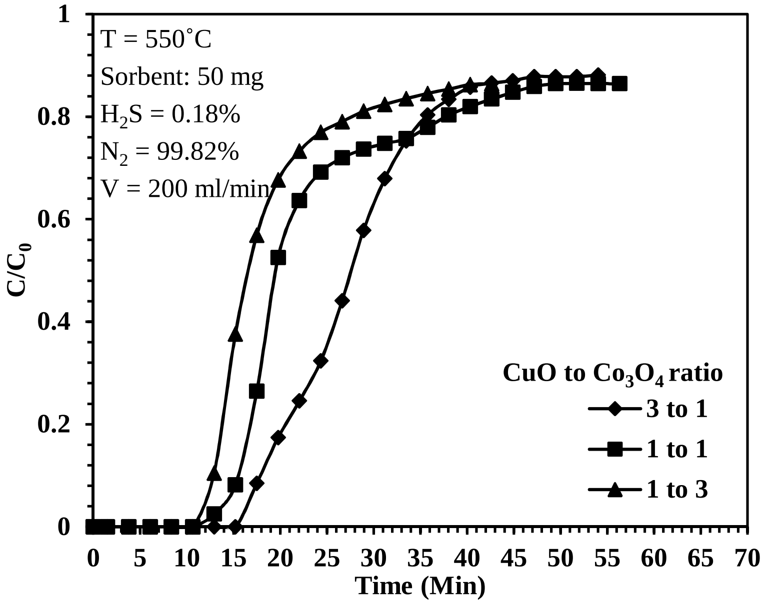

Figure 5.22: Sulfidation breakthrough curves for CuO-Co_3O_4 mixed metal oxide sorbent at 550 °C

5.2.2.3 Characterization of mixed metal oxide sulfided sorbents

The better understanding of the sulfidation reaction and its effect on the sorbent can be gained by characterizing the sulfided sorbents by XRD and SEM. Figure 5.23 shows the SEM analysis for the sulfided sorbents of (a) CuO-CeO_2 and (b) CuO-Co_3O_4 mixed metal oxide sulfided samples. As seen in Figure 5.23 (a) the sulfided CuO-CeO_2 sample shows quiet different structure than fresh sorbent. Li and Flytzani-Stephanopoulos (1997) observed the formation of smaller crystals of size about 0.4 μm. The CuO-Co_3O_4 sulfided sample as shown in Figure 5.23 (b) showed different crystal structure for the sulfided product. This may be due to the formation of different phases.

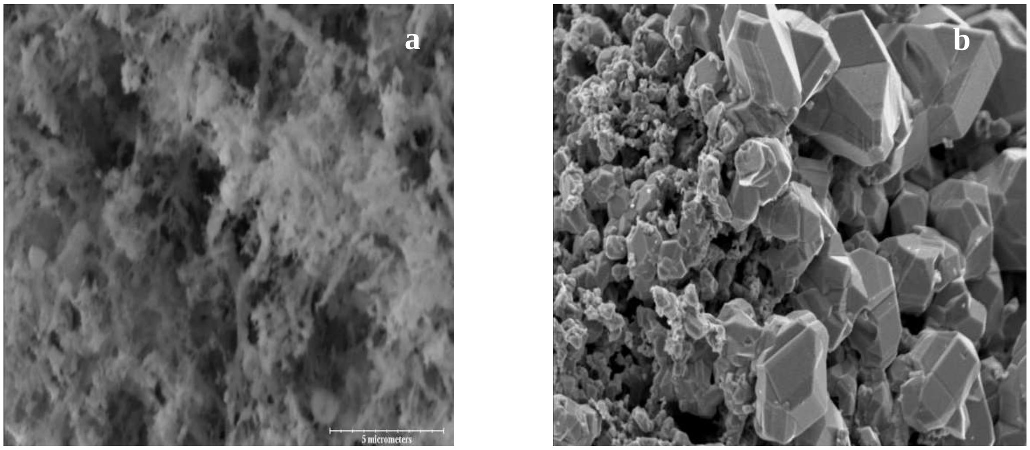

Figure 5.23: SEM of mixed metal oxide sulfided sorbents a. 1CuO-1CeO_2 b. 1CuO-1Co_3O_4 at magnification of 6000 (5 μm)

The formation Cu_8S_5 instead Cu_2S as main product was recorded in case of CuO - CeO_2 mixed metal oxide sulfided sorbents and different combination of sulfide was recorded in case of CuO - Co_3O_4 mixed metal oxide sulfided sorbents. Figures 5.23 and 5.24 show the XRD of 3CuO-1CeO_2 and 3CuO-1Co_3O_4 sulfided samples respectively and Table 5.13 lists the crystalline phases observed in sulfided samples.

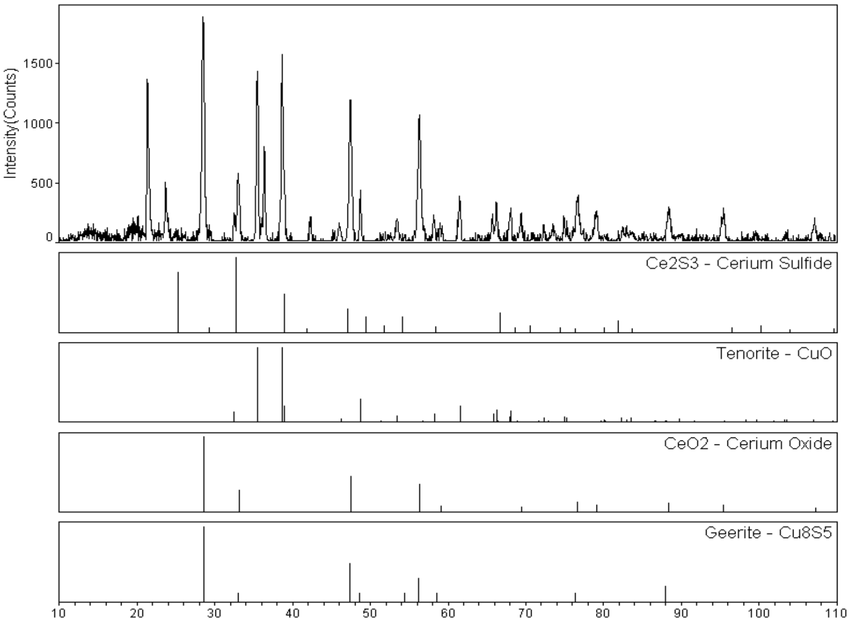

Figure 5.24: XRD of 3CuO-1CeO_2 sulfided sorbent

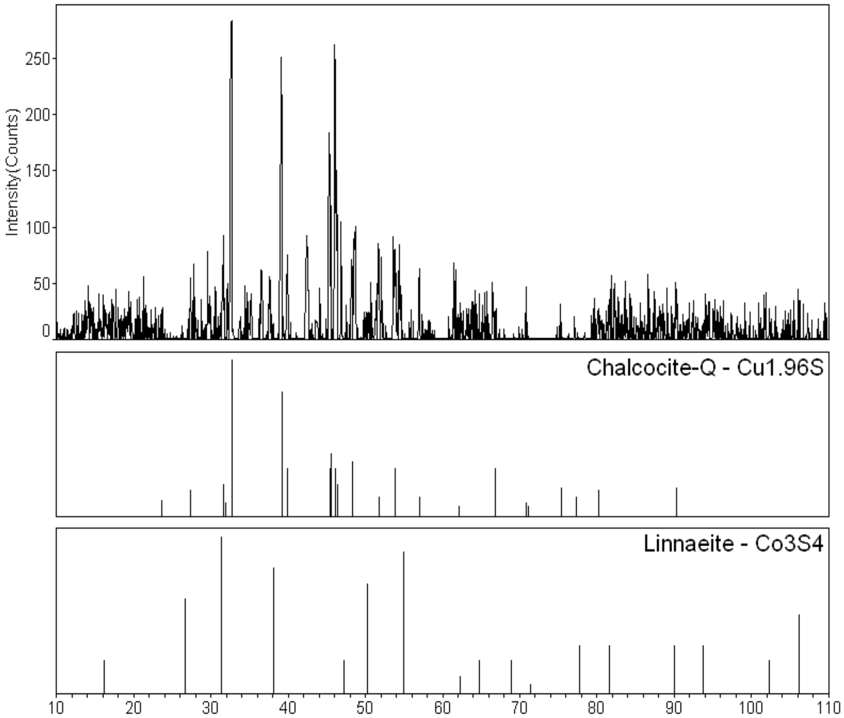

Figure 5.25: XRD of 3CuO-1Co_3O_4 sulfided sorbent

Table 5.13: Crystalline phases observed in mixed metal oxide sulfided sorbents

Sorbent	Sulfided Phases	Sorbent	Sulfided phases
3 CuO - 1 CeO_2	CeO_2, Cu_8S_5, CuO, Ce_2S_3	3 CuO - 1 Co_3O_4	$Cu_{1.96}S$, Co_3S_4
1 CuO - 1 CeO_2	CeO_2, Cu_8S_5, CeS, Ce_2S_3,	1 CuO - 1 Co_3O_4	$Cu_{1.96}S$, Co_3S_4, Co_9S_8
1 CuO - 3 CeO_2	CeO_2, Cu_8S_5, Cu_2S, CeS	1 CuO - 3 Co_3O_4	$Cu_{1.96}S$, Co_3S_4, Co_9S_8

5.2.2.4 Sulfidation tests for MMS-IZ sorbents

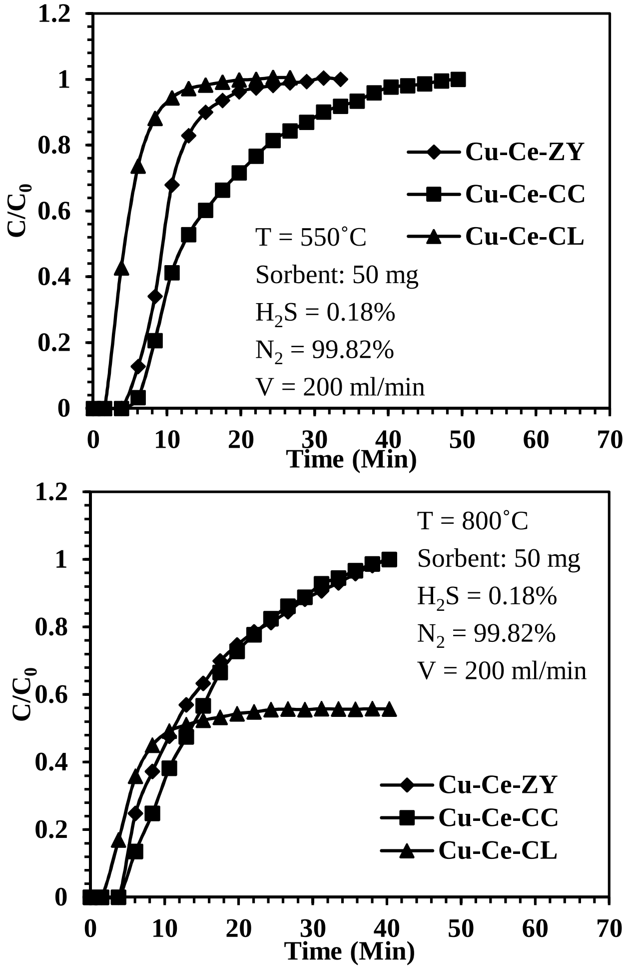

Figure 5.26: Sulfidation breakthrough curves for Cu-Ce mixed metal oxide supported-ion exchanged zeolite sorbents (MMS-IZ) sorbents

In case MMS-IZ sorbents, mono positively charged ions in zeolites were replaced with Cu^{2+} and Ce^{3+} in case of Cu-Ce and Cu^{2+} and Co^{+2} in case of Cu-Co MMS-IZ sorbents. The sulfidation results of these classes of sorbents are shown in Figure 5.26. Zeolite-Y and clinoptiolite showed fast breakthrough than chabazite at 550 °C. At 800 °C, the breakthrough performance was different, for zeolite-Y and chabazite the nature of breakthrough was same but the in case of clinoptilite the breakthrough was not complete. The breakthrough performance for MMS-IZ sorbents is lower as compared to that of mixed metal oxides.

In case of clinoptiolite, the structure might have broken down due to dealumination, as the water peak was observed in the chromatograph at that particular temperature. The same experiments were performed for Cu-Co exchanged zeolites and the corresponding sulfidation behavior and capacity was calculated. In order to understand the details, the sulfided samples were analyzed and discussed below.

5.2.2.5 Characterization of MMS-IZ sulfided sorbents

In case of MMS-IZ sorbents, the characterization helped to understand the changes occurred in the zeolite structure after sulfidation at various temperatures. At 800 °C, the zeolite structure remained intact in case of zeolite-Y but small changes in case of chabazite were observed. In case of clinoptiolite, significant structural change was observed at 800 °C. The high temperature may lead to the conversion of ions to metal and subsequent breakdown of zeolite structure.

Rong et al. (2009) observed that only copper exchanged zeolite was prone to structure breakdown of zeolite-Y due to sudden change in surface area while no sintering effect was observed in presence of REO for zeolite-Y. The application of clinoptiolite at lower temperature is favored due to the ease of regeneration at lower temperature. At higher temperature, detrimental effects were observed for clinoptiolite (Yasyerli et al., 2002). Figures 5.27 and 5.28 show the structure of clinoptiolite and zeolite-Y after sulfidation test at 800°C.

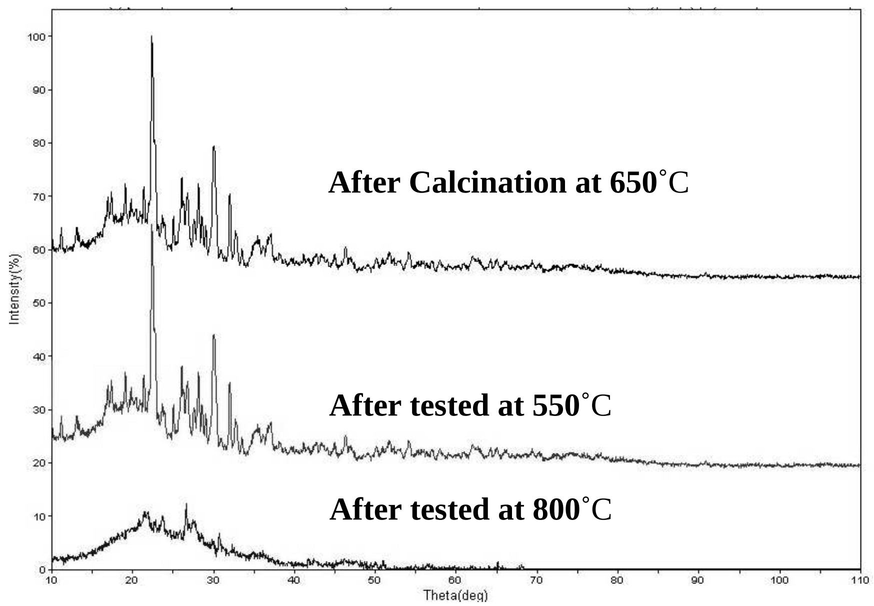

Figure 5.27: XRD of Cu-Ce on clinoptiolite

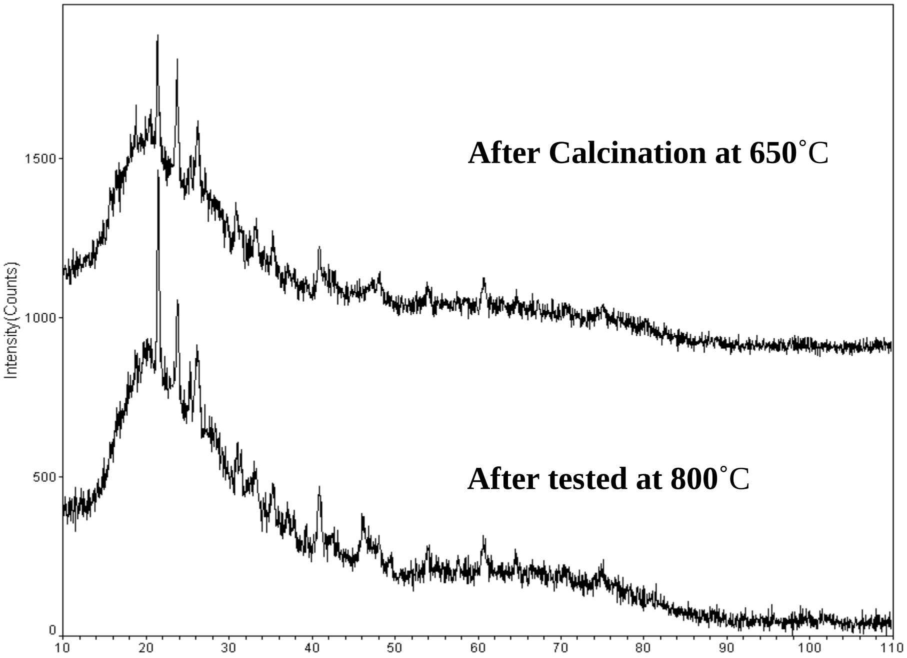

Figure 5.28: XRD of Cu-Ce on zeolite-Y

5.2.2.6 Sulfidation capacity

Based on the above breakthrough sulfidation experiments, the sulfidation capacity for various synthesized sorbents was calculated and listed in Table 5.14. The sulfidation capacity was calculated for 100 ppmv breakthrough point. The calculation was done using MATLAB tool (A typical sample calculations is shown in Appendix D-2). .

Table 5.14: Sulfidation capacity for sorbents

No	Sorbent type	Sulfidation capacity*	Temperature (°C)
1	3 CuO - 1 CeO_2	16.41	550
2	1 CuO - 1 CeO_2	7.503	550
3	1 CuO - 3 CeO_2	3.757	550
4	3 CuO - 1 Co_3O_4	17.82	350
5	1 CuO - 1 Co_3O_4	26.26	350
6	1 CuO - 3 Co_3O_4	29.08	350
7	3 CuO - 1 CeO_2	5.627	800
8	1 CuO - 1 CeO_2	4.221	800
9	1 CuO - 3 CeO_2	2.813	800
10	3 CuO - 1 Co_3O_4	15.01	550
11	1 CuO - 1 Co_3O_4	12.19	550
12	1 CuO - 3 Co_3O_4	10.31	550
13	Cu-Ce-ZY	3.752	550
14	Cu-Ce-CC	5.628	550
15	Cu-Ce-CL	3.752	550
16	Cu-Co-ZY	2.813	350
17	Cu-Co-CC	1.875	350
18	Cu-Co-CL	1.875	350
19	Cu-Ce-ZY	3.752	800
20	Cu-Ce-CC	3.752	800
21	Cu-Ce-CL	2.813	800
22	Cu-Co-ZY	2.813	550
23	Cu-Co-CC	1.875	550
24	Cu-Co-CL	1.875	550

* g of Sulfur/ 100 g of sorbent

Comparison of sorbent capacities

In the copper-cerium mixed metal oxide sorbent there was significant reduction in sulfidation capacity at various temperatures by increasing the concentration of CeO_2.The interesting point to note is that the sorbent were not pre-reduced for these tests so the cerium oxide was in the form of CeO_2 instead of CeO_n. CeO_n has more affinity towards H_2S than CeO_2. The capacities for CuO-CeO_2 mixed metal oxide sorbents are in the range of 16.41 to 3.757 g of S/100 g of sorbent at 550 °C and 5.627 to 2.813 g of S/100 g of sorbent at 800 °C. The capacities calculated here are comparable to the literature. For example, Li and Flytzani-Stephanopoulos (1997) carried out the sulfidation tests by varying Cu-Ce ratio in 2% H_2S, 20% H_2, 78% N_2 at 850 °C. The observed sulfidation capacity reported was in the range of 4.4 to 2.2 g of S/100 g of sorbent, while the theoretical capacity was in the range of 17.7 to 2.7 g of S/100 g of sorbent. The reducing environment converts CuO in metallic form and hence CeO_2 plays the major role to reduce the H_2S concentration to sub-ppmv level as the metallic Cu has inferior sulfidation efficiency (Li and Flytzani-Stephanopoulos, 1997; Wang and Flytzani-Stephanopoulos, 2005). Based on the analysis of the capacities, 3CuO-1CeO_2 is selected to carry out further effect of various parameters on the sulfidation behavior.

In case of CuO-Co_3O_4 system, the better sulfidation behavior was observed at lower temperature. The capacities for CuO- Co_3O_4 mixed metal oxide sorbents are in the range of 29.08 to 17.82 g of S/100 g of sorbent at 350 °C and 15.01 to 10.31 g of S/100 g of sorbent at 550 °C. Full utilization of Co_3O_4 was observed at lower temperature giving high sulfidation efficiency. The presence of Co_3O_4 or the reaction of spinel of copper-cobalt oxide with H_2S initiates different sulfidation behavior. Based on the results above 3CuO – $1Co_3O_4$ is selected for check the effect of various parameters.

In case of MMS-IZ sorbents, it was observed that at lower temperature all the sorbents have good sulfidation efficiency though the capacity is less as compared to mixed metal oxide system. It was observed that at 800°C the Cu-Ce exchanged clinoptiolite failed to give the required sulfidation performance due to structure breakdown.

The application of clinoptiolite is good up to the temperature of 600 °C after which there is a sudden drop in its capacity as well as structure breakdown was reported (Yasyerli et al., 2002). The clinoptiolite shows good sulfidation behavior at lower temperature. As compared to clinoptiolite, chabazite and zeolite-Y shows good performance at higher temperature. It is interesting to note that the sulfidation capacity was almost the same at 550 °C as well as 800 °C which confirms that the MMS-IZ sorbents are not prone to sintering while the sudden reduction in sulfidation capacity was observed in case of mixed metal oxide sorbents due to sintering of the metal oxide structure. The presence of REO in zeolite structure is giving the stability at higher temperature while only copper exchanged zeolite-Y was prone to sintering at higher temperature and highly reducing gas. The conversion of copper ion to copper metal leads to the structure breakdown of zeolite in case of copper exchanged zeolites while presence of REO reduce that effect significantly (Charles Rong et al., 2009).

5.2.3 Effect of pre-reduction CuO-CeO$_2$ mixed metal oxide sorbent

The effect pre-reduction of Cu-Ce mixed metal oxide sorbent on sulfidation is also studied in this work. The pre-reduction of sorbent was carried out for about 4 hrs at 550 °C in hydrogen environment prior to sulfidation. Sulfidation performance of the sorbent with or without pre-reduction is shown in the Figures 5.29 and 5.30.

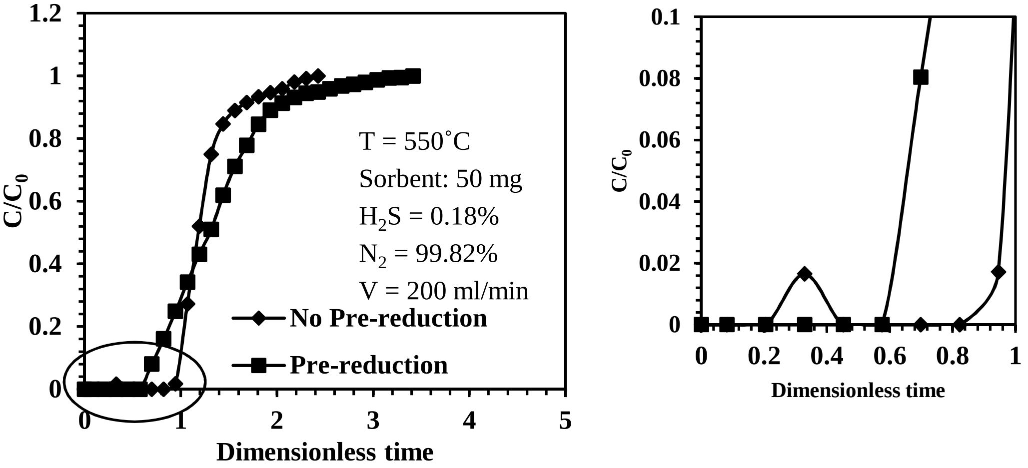

Figure 5.29: Effect of pre-reduction at 550 °C for Cu-Ce (3:1)

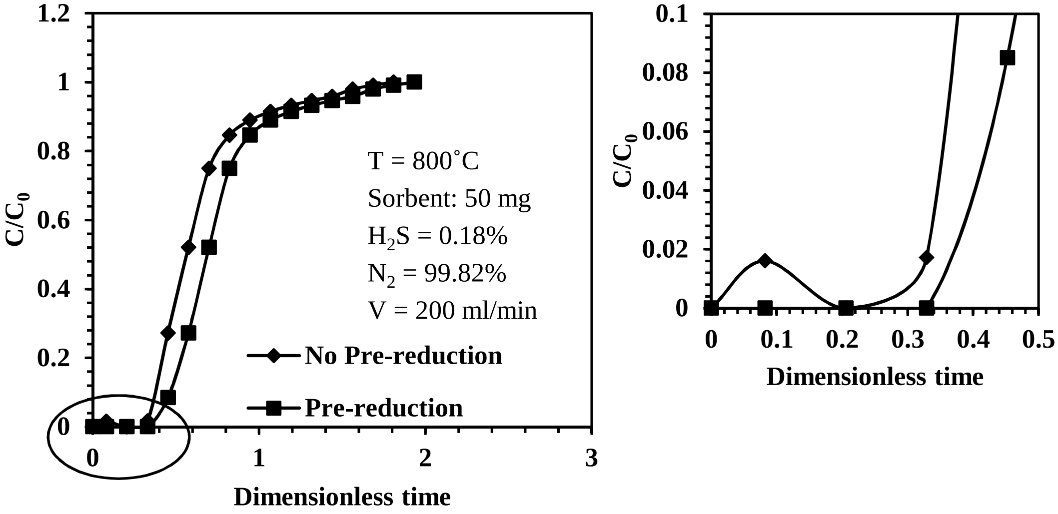

Figure 5.30: Effect of pre-reduction at 800 °C for Cu-Ce (3:1)

It was observed that the H_2S concentration was significantly below the detection limit of the micro-GC using pre-reduced sorbent, while the bumps were observed in early pre-breakthrough region for fresh sorbent sulfidation (without reduction). The initial bumps confirmed that the non-reduced sorbent cannot lead to the concentration requirement of sub-ppmv level. The bumps in the sulfidation of non-pre-reduced sorbents are related to the CeO_2 sulfidation which is in agreement with literature. Zeng et al. (2000) reported that only CeO_2 is capable to reduce the H_2S up to 20 ppmv while CeO_n can reduce the H_2S concentration to sub-ppmv levels. The dimensionless time (or normalized time defined as the actual run time, t, over the theoretical time t^* that is required for the complete conversion of CeO_2 to Ce_2O_2S)) calculation is shown in Appendix D-3. As the temperature increased from 550 to 800 °C the pre-breakthrough time changed from 0.6 to 0.32 respectively which confirms the reduction caused formation of metal copper and subsequent reduction in capacity at higher temperature. The reaction of CuO with H_2 leads to the metallic copper, which has inferior sulfidation efficiency. The explanation for this dramatic change in sulfidation is due to the presence CeO_n in this particular case while without pre-reduction it was only CeO_2. One interesting point to note that at 550 °C the pre-breakthrough ended early for pre-reduced sorbent than non-pre-reduced one, due to slow sulfidation and endothermic reaction of CeO_2 while pre-reduced CeO_n reacts with H_2S rapidly than CeO_2. The CeO_n has faster kinetics as the reaction happens at the surface and the layer of Ce_2O_2S is formed hence the penetration of H_2S inside the sorbent particle is negligible. The pre-breakthrough is early but the superior sulfidation is observed.

5.2.4 Effect of flow rate on sulfidation

To evaluate the effect of H_2S inlet flow rate on the sulfidation performance of the sorbent, 3CuO-1CeO_2 and 3CuO-1Co_3O_4 were selected. The flow rates used for this study were 100 ml/min, 200 ml/min by keeping all other conditions of experiments same as before, and the performance was evaluated at 350 °C, 550 °C as well as 800 °C to check the breakthrough performance. Figure 5.31 show the effect of flow rate on sulfidation at 550 °C for 3CuO-1CeO_2

The sulfidation capacity was observed to be same though the flow rate was changed. At lower flow rate, the extended pre and active-breakthrough regions were observed showing the lower flow of H_2S. This confirms that the sulfidation reaction rate is constant at different flow rates but same temperature conditions.

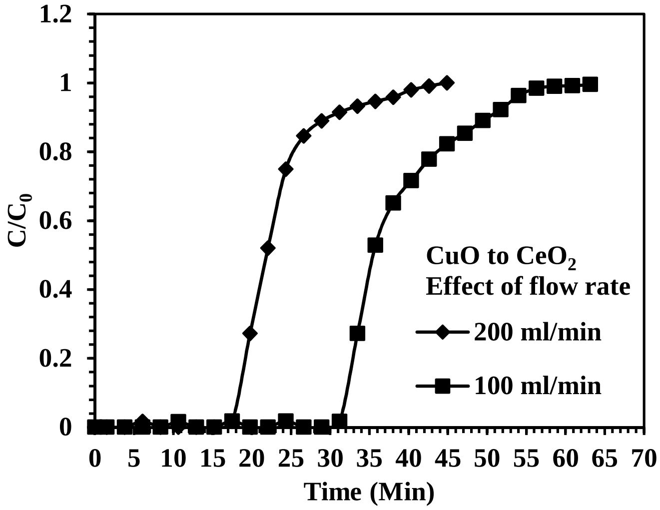

Figure 5.31 Effect of flow rate on sulfidation at 550 °C for CuO to CeO_2

5.2.5 Effect of particle size on sulfidation

In order to study the effect of particle size on the sulfidation performance, 3CuO-1CeO$_2$ was selected. The sulfidation experiments were carried out at 550 °C and 800 °C. The prepared sorbents were sieved by using small size sieves in the size range of 1000 μm to 30 μm. The particle size distribution of the sorbent is as shown in Table 5.15.

Table 5.15: Particle size analysis for 3CuO-1CeO$_2$

No	Size (Micrometer)	% Retained
1	1000	0
2	250	14.34
3	150	16.68
4	63	54.25
5	32	14.73
7	Base	0

Based on the particle size analysis the particles of size between 63 and 1000 μm size were selected for sulfidation experiments and the comparison of sulfidation performance are as shown Figure 5.32.

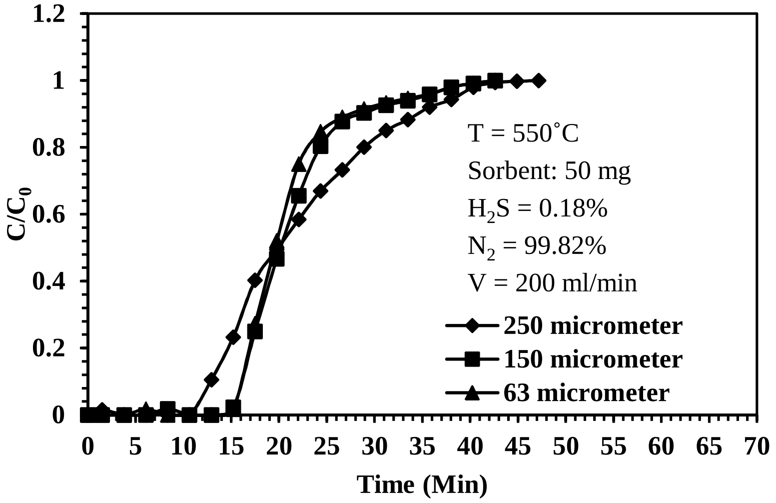

Figure 5.32: Effect of particle size (μm) on sulfidation

As shown in Figure 5.32, the sulfidation breakthrough was independent of particle size between 30 to 250μm, whereas, sorbent with particle size between 250 to 1000 μm showed an extended and early appearance of active-breakthrough region. Moreover, a higher sorption capacity 16.41 g S/100 g sorbent for size between 63 and 250μm and 12.91 g S/100 g sorbent for size 250 μm and better breakthrough performance was found at smaller particle size than at larger particle size. The pre-breakthrough times obtained with this size range (between 63 and 250μm) of sorbent are comparatively higher than those obtained with the large size (between 250 and 1000μm) of sorbent particle. This might be due to the diffusion resistance to the larger particle of sorbent. For smaller particle size, the unreacted core of the particle is small and hence less diffusion resistance for the gas to penetrate in the core. For large particle size sorbent, the unreacted core is bigger and the formation outer sulfide layer provides more diffusion resistance that leads to the extended active and post-breakthrough zones.

5.2.6 Cyclic Sulfidation-Regeneration performance

The synthesized sorbents were evaluated for cyclic sulfidation-regeneration. Three sulfidation and two regeneration runs were performed on the synthesized sorbent. Figure 5.33 shows the comparison of cyclic sulfidation capacity for synthesized sorbents and Table 5.16 lists the sulfidation and regeneration conditions. The comparison for cyclic performance of the sorbents is as discussed below. In case of Cu-Ce mixed metal oxide sorbents, at 550 °C reduction in the sulfidation capacity was noted while at 800°C the capacity remained almost constant. The reduction in capacity in cyclic performance greatly depends upon the regeneration conditions. The effect of regeneration conditions on sorbent behavior is discussed in Section 5.3.The cyclic sulfidation performance of CuO-Co_3O_4 confirmed that at lower temperature the capacity remained same after the cyclic tests. Small reduction in capacity for Cu-Co=1:1 was observed over others. At 550 °C the sulfidation capacities were observed to be constant and not much reduction in capacity was recorded. The cyclic performance of MMS-IZ sorbents was promising over mixed metal oxides. The Cu-Ce MMS-IZ sorbents showed less capacity as compared to mixed metal oxides but the same capacity was observed after multiple cyclic tests. Same observation was made in case of Cu-Co MMS-IZ sorbents. The surface area decrease in case of zeolite is less as compared to mixed metal oxides after sulfidation. The reaction of MMS-IZ sorbents with H_2S is only surface reaction and the regeneration is quiet simple process (Rong et al., 2009).

Table 5.16: Sulfidation and regeneration conditions

No	Type of sorbent	Sulfidation temperature	Regeneration temperature
1	Cu-Ce mixed metal oxide	550 °C	600 °C
2	Cu-Ce mixed metal oxide	800 °C	850 °C
3	Cu-Co mixed metal oxide	350 °C	400 °C
4	Cu-Co mixed metal oxide	550 °C	600 °C
5	Cu-Ce-MMS-IZ	550 °C	600 °C
6	Cu-Ce-MMS-IZ	800 °C	850 °C
7	Cu-Co-MMS-IZ	350 °C	400 °C
8	Cu-Co-MMS-IZ	550 °C	600 °C

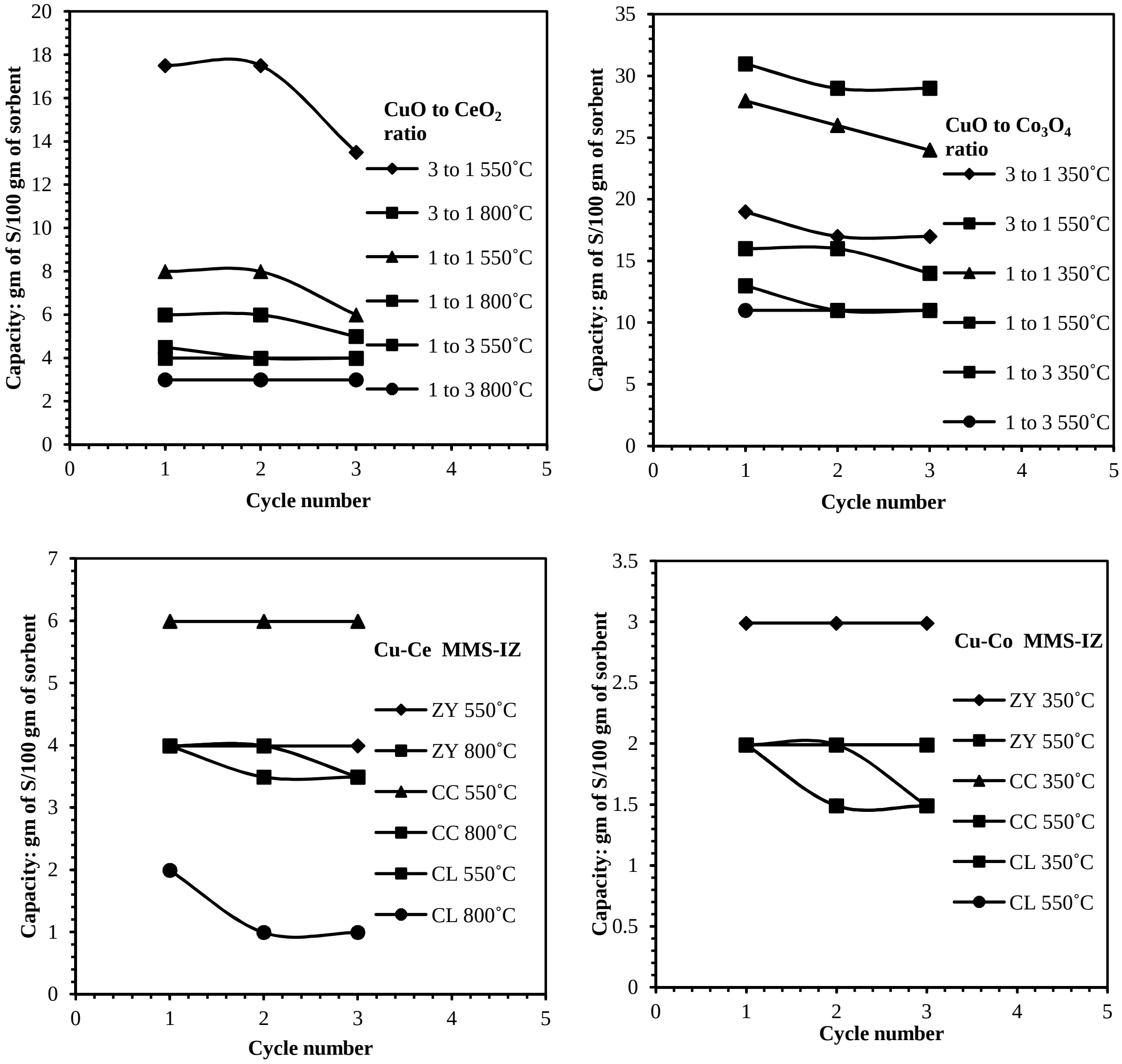

Figure 5.33: Comparison of cyclic sulfidation capacity for sorbents

5.3 REGENERATION OF SULFIDED SORBENT

Regeneration of the sulfided sorbent is an important step when it comes to the cyclic performance of the sorbent. The complete regeneration is necessary in order to have the same sulfidation capacity for the subsequent sulfidation runs. This part of the chapter will discuss the detailed the observations made for the regeneration performance of the mixed metal oxide and MMS-IZ sorbents. The regeneration gas used in this particular study is air. The regeneration performance for $CuO\text{-}CeO_2$ mixed metal oxide sorbents is discussed in details. In order to understand the effect of temperature on regeneration and to check the regeneration path, the sulfided sample of $3CuO\text{-}1CeO_2$ at 800 °C was regenerated by using air at 650 °C, 750 °C and 850 °C. Figure 5.34 shows the regeneration pattern at various temperatures. The general regeneration reaction is as shown below:

$$MeS + 3/2\ O_2 \rightarrow MeO + SO_2$$

The deposition of elemental sulfur at the outlet of the reactor was noticed which concludes that some part of sulfur comes out in the following form of reaction. There is no exact evidence but the deposition formed was supposed to be elemental sulfur. The obvious deposition on the wall of reactor was reported in literature (Xie et al., 2010)

$$2\ MeS + SO_2 \rightarrow 2\ MeO + 3/2\ S_2$$

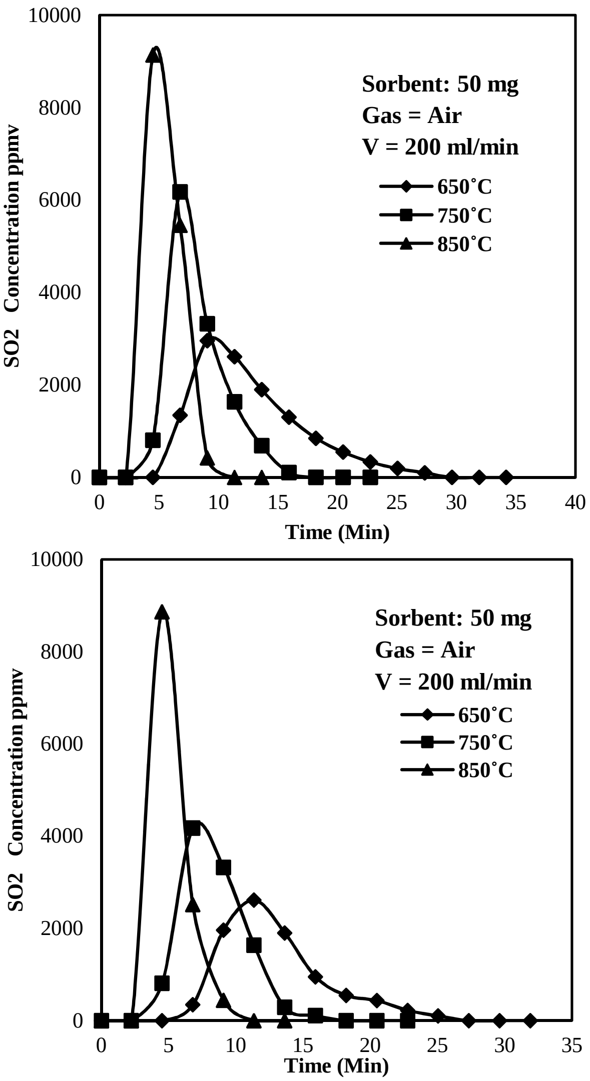

Figure 5.34: Regeneration pattern for Cu-Ce (3:1) mixed metal sulfided sorbent

As shown in Figure 5.34, at higher temperature the regeneration was faster than at lower temperature. More than just regeneration pattern, it was interesting to know the phases formed in regeneration. The regenerated sample was then analyzed by XRD to check the phases present in the sorbent. The analysis showed that there was a formation of $CuSO_4$ and Cu_2SO_4 at lower temperature of 650 °C and some formation was also noted at 750 °C but the sulfate formation was not present at 850 °C. No sulfates of cerium were recorded in XRD but researchers have recorded the stable surface sulfates formation of cerium at lower temperature while at higher temperature CeO_2 has high oxygen mobility which makes the regeneration easy in case of CeO_2 as a sorbent (Wang and Flytzani-Stephanopoulos, 2005; Kampegowda et al., 2007). In this study, the presence of copper oxide initiates different regeneration pattern.

The regeneration pattern is from sulfate to sulfide to oxide at lower temperature. The sulfide formed is quiet stable and leads to decreased sulfidation efficiency in subsequent sulfidation runs. At higher temperatures, the regeneration path is from sulfates to metal oxide form, which shows the stable sulfidation efficiency. The regeneration pattern for $CuO-Co_3O_4$ system was not as complex as copper-cerium pair. The regeneration pattern in case of $CuO-Co_3O_4$ was easy when sulfided at 350 °C the regeneration product was individual oxides but when sulfided at 550 °C there could be formation of some stable sulfides as the regeneration was at 600 °C.

The regeneration of MMS-IZ sorbents was also carried out by using air but after regeneration the structure is intact for zeolite-Y and chabazite but clinoptiolite suffers at higher temperature. Summarizing, MMS-IZ sorbents shows good regeneration behavior. The detailed molecular study is required to understand the regeneration pattern for this kind of sorbent system.

CHAPTER - 6

CONCLUSIONS AND RECOMMENDATIONS

A summary of the important findings and major conclusions of this research work is presented in this chapter. Recommendations for future work in the area are also included.

6.1 CONCLUSIONS

- The main purpose of the addition of cerium oxide to the copper oxide was to study its use as a dispersant but when reduced, CeO_n (n<2) helps to achieve very low level of the H_2S concentration which is observed in reduction and subsequent sulfidation tests. $CuO\text{-}CeO_2$ shows good sulfidation performance at 550 °C as well as 800 °C. More addition of CeO_2 to CuO is not helpful so $3CuO\text{- }1CeO_2$ is the best sorbent in this category.
- The $CuO\text{-}Co_3O_4$ mixed metal oxide sorbent shows the formation of copper-cobalt oxide but no significant effect of the spinel form on the sulfidation is recorded. This pair shows superior sulfidation at lower temperature of 350 °C due to the favorable sulfidation thermodynamics at lower temperature. The cobalt rich sorbent shows better performance at lower temperature while copper rich sorbent at high temperature.

- When a model sorbent (e.g. 3CuO- 1CeO_2) is exposed to the various inlet flow conditions (100 and 200 ml/min) no significant effect is recorded on the sulfidation capacity but the extended pre and active-breakthrough regions are observed.
- The particle size of the sorbent shows the effect on the sulfidation behavior. The particle size of 63 and 125 µm shows almost the same sulfidation capacity but 250 µm shows the less sulfidation capacity. This is attributed due to the unreacted core and increased diffusion resistance.
- The MMS-IZ sorbents show better performance at even higher temperature. The utilization of metal oxide is superior due to better dispersion over the zeolite support. The cyclic tests shows that at higher temperature MMS-IZ sorbents are not suffered by sintering as in case of mixed metal oxides.
- The overall conclusion is though the mixed metal oxide sorbents have higher sulfidation capacity but they are prone to sintering and reduction that leads to reduced sulfidation capacity and complex regeneration. MMS-IZ sorbents shows less capacity but high temperature stability and superior cyclic performance by showing complete utilization of oxides. Both types of sorbents have some advantages and disadvantages but final choice depends upon application and process requirement.

6.2 RECOMMENDATIONS FOR FUTURE WORK

Based on the study done in this work there is a need to explore few more different scenarios for the sorbents

- The performance in actual syngas environment must be studied to check the effect of reducing environment (H_2, CO, H_2O and others) on the sorbents
- The physical and chemical properties (e.g. attrition resistance, sulfide formation etc.) of the sorbents are really the key factors for their performance so these properties development on lab scale will be an important step.
- The regeneration of the spent sorbent is crucial and the effect of different partial pressure of oxygen on regeneration pattern must be studied to see the regeneration performance.
- Fluidized bed study must be performed to check its effect on sulfidation performance.
- Mathematical modeling is required to fit the experimental results and performance prediction. The sulfidation kinetic model will describe the sulfidation process and will help to understand the improvement and optimization required.

REFERENCES

Abbasian J., 1992, “Development of Novel Copper-Based Srobents for Hot Gas Cleanup”, Project Management Report, METC.

Abbasian J., Hill A. H., Flytzani-Stephanopoulos M., Li Z., “Development of Novel Copper-Based Sorbents for Hot-Gas Cleanup”, IGT-Final Technical Report to ICCI/DOE, DE-FC22- 92PC92521, Aug 1994.

Abbasian J., & Slimane R.B., “A regenerable copper-based sorbent for H_2S removal from coal gases”, Industrial and Engineering Chemistry Research, 1998, 37, 2775–2782.

Abbasian J., Slimane R.B., “A regenerable copper-based sorbent for H_2S removal from goal gases”, Ind. Eng. Chem. Res., 1999, 37, 27752782.

Abdul-Majeed, Azad, Martin J. D., “Development of ceria-supported sulfur tolerant nanocatalysts: Rh-based formulations”, Applied Catalysis A: General, 2007, 330, p77–88.

Abu Junaid S.M., Rehman M., Yin H., McCarrrey W. C., Kuznicki S M., “Natural zeolites for oilsands bitumen cracking: Structure and acidity”, Microporous and Mesoporous Materials, 144 (2011), p148-157.

Adachi G.Y., and Masui T., 2001, “Synthesis and Modification of Ceria-based Materials”, Catalysis by Ceria and Related Materials, Imperial College Press, Catalytic Science Series, 2, 15-83.

Akyurtlu J.F., Akyurtlu A., “Behavior of ceria-copper oxide sorbents under sulfation conditions”, Chemical Engineering Science, 1999, 54, p2991-2997.

Alonso L., Palacios J.M., Garcıa E., Moliner R.,“Characterization of Mn and Cu oxides as regenerable sorbents for hot coal gas desulfurization”, Fuel Processing Technology, 2000, 62, p31–44.

Atakul H., Wakker J.P., Gerritsen A.W. and Van den Berg P.J., “Removal of H2S from fuel gases at high temperatures using MnO/Al203”, Fuel ,1995, 74, p187-191.

Akyurtlu J.F., Akyurtlu A., “Behavior of ceria-copper oxide sorbents under sulfation conditions”, Chemical Engineering Science, 1999, 54, p2991-2997.

Aysel T. Atimtay, Douglas P. Harrison, “Desulfurization of hot coal gas”, NATO ASI series, Series G: Ecological sciences, 1999, Vol.42

Auschitzky Boffa A.B., White J.M., Sahin T.,“ Adsorption of H_2O and H_2S on thin film of Cobalt oxide supported on alumina”, Journal of Catalysis, 1990,125, p 325-344.

Bakker J.W., Kapteijn H., Moulijn J.A., “A high capacity manganese-based sorbent for regenerative high temperature desulfurization with direct sulfur production Conceptual process application to coal gas cleaning”, Chemical Engineering Journal, 2003, 96, p223–235.

Ben-Slimane R., Hepworth M.T., “Desulfurization of hot coal-derived fuel gases with manganese-based regenerable sorbents. II. Regeneration and multicycle tests”, Energy and Fuels, 1999, 8, p1184–1191.

Bernal S. Blanco, G. Cauqui M.A., Cifredo G.A., Pintado J.M., and. Rodriguez-Izquierdo G.M., “Influence of reduction treatment on the structural and redox behavior of ceria, La/Ce and Y/Ce mixed oxides”, Catalysis Letters , 1998, 53, p51 – 57

Bernal S., Blanco G., Cifredo G.A., Delgado J.J., Finol D., Gatica J.M., Rodriguez-Izquierdo J.M., Vidal H., “Investigation by means of H_2 adsorption, diffraction and electron microscopy techniques of a cerium-terbium mixed oxide supported on a lanthana-modified alumina”, Chem. Mater., 2002, 14, p844-850

Chrles Rong, Deryn Chu, and John Hopkins, “Test and characterization of some zeolite supported gas phase desulfurization sorbents”, ARL_TR-4859, June 2009.

Clyde S. Brooks, “Syngas desulfurization over metal zeolites”.

Fang-fang Wang, De-xiang Zhang, Hai Zhao, Ting-ting Wu, Jin-sheng Gao, “Research into Kinetics of COS elimination from syngas at moderate temperature”, Fuel 89 (25010), p888-893.

Ferrizz R. M., Gorte R.J., Vohs J.M., “Determining the Ce_2O_2S–CeO_x phase boundary for conditions relevant to adsorption and catalysis”, Applied Catalysis B: Environmental, 2003, 43, p273–280.

Flytzani-Stephanopoulos M., Gavalas G. R., Jothimurugesan K., Lew S., Sharma P. K., Bagajewicz M. J., Patrick V., “Detailed Studies of Novel Regenerable Sorbents for High-Temperature Coal-Gas Desulfurization”, Final Report to DOE, DEFC21- 8-MC22193, Oct 1987.

Flytzani-Stephanopoulos M., Sakbodin M., Wang Z., “Regenerative adorption and Removal of H2S from Hot Fuel Gas Streams by Rare Earth Oxides”, Science, 2006, 312, p1508-1510.

Focht G.D., (1988) “High Temperature Coal-Gas Desulfurization: Kinetic Evaluation of A Zinc Ferrite Sorbent,” A dissertation, The Department of Chemical Engineering, Louisiana State University.

Focht G.D., 1988, "High Temperature Desulfurization Using Zinc Ferrite: Reduction and Sulfidation Kinetics," Chemical Engineering Science, 43, p3005-3013.

Gangwal S.K. et al., "Testing of Novel Sorbents for H2S Removal from Coal-Gas," Environmental Progress, 8(1), 1989, p26-34.

Guo-Hui Li, Li-zhen Dai, Da-shun Lu, Shao-yi peng,"Characterization of Copper Cobalt mixed oxide", Journal of solid state chemistry 89, 1990, p167-173.

Gupta Puneet, "Regenerable metal oxide composite and their use in novel chemical processes", A Dissertation, The Ohio state university, 2006.

Haneda M., Mizushima T., Kakuta N., Ueno A., Sato Y., Matsuura S., Kasahara K. and Sato M., "Structural characterization and catalytic behavior of Al2O3-supported cerium oxides", Bull. Chem., Soc. Jpn., 1993, 66, p1279-1288.

Jae Bin Chung, Jong Shik Chung, "Desulfurization of H_2S using cobalt-containing sorbents at low temperatures", Chemical Engineering Sciemve, 60, 2005, p115-1523.

Jiancheng Wang, Yunpeng Zhang, Lina Han, Liping Chang, Weiren Bao, "Simultaneous removal of hydrogen sulfide and mercury from simulated syngas by iron based sorbents", Fuel xxx, 2011, pxxx-xxx.

Kwang Bok Yi, Podlaha E. J., Douglas P. Harrison, "Ceria-zirconia high temperature desulfurization sorbents", Ind. Eng. Chem. Res., 2005, 44, p7086-7091.

Lee D. Gasper-Galvin, Aysel T. Atimtay, Raghubir P. Gupta, “Zeolite-Supported Metal Oxide Sorbents for Hot Gas Desulfurization”, Ind. Eng. Chem. Res., 1998, 37, p4157-4166.

Makoto Kobayashi, Flytzani-Stephanopoulos M., “Reduction and sulfidation kinetics of cerium oxide and Cu-modified cerium oxide”, Ind. Eng. Chem. Res., 2002, 41, p3115-3123.

Meng X.M., De Jong W., Verkooijen A. H. M.,“Therodynamic analysis and kinetic model of H_2S sorption using different sorbents”, AIchE, 2009, Wiley interscience (2009) , DOI 10.1002/ep. 10386.

Oguz Karvan, Husnu Atakul, “Investigation of Cuo/mesoporous SBA-15 sorbents for hot gas desulfurization”, Fuel processing technology, 89, 2008,p908-915.

Parveen Kumar, Chun Yi Sung, Oki Muraza, Matteo Cococcioni, Saleh Al Hashimi,“H_2S adsorption by Ag and Cu ion exchanged faujasites”, Microporous and Mesoporous Materials, 146, 2011, p127-133.

Philip R. Westmoreland, Douglas P. Harrison, “Evaluation of candidate solids for high-temperature desulfurization of low-btu coal gas”, 1976.

Rajesh S. Kempegowda, Navadol Laosiripojana, Suttichai Assabumrungrat, “High temperature desulfurization over nano-scale high surface area ceria for application in SOFC”, Korean J. Chem. Eng., 25 (2), 2008, p223-230.

Shaheen W. M., Alo A. A., “Characterization of solid-solid interactions and physiochemical properties of copper-cobalt mixed oxides and $Cu_xCo_{3-x}O_4$ spinels”, Materials research bulletin, 36, 2001, p1703-1716.

Tamhankar S.S., Bagajewicz M., Gavalas G. R., “Mixed-oxide sorbents for high temperature removal of hydrogen sulfide”, Ind, Eng. Chem. Process Des. Dev.,1986, 25, p429-437.

Vamvuka D., Arvanitidis C., Zachariadis D., “Flue gas desulfurization at high temperature: A review”, Environmental engineering science, 21, 2004, p525-547.

Wei Xie, Liping Chan, Dehai Wang, Kechang Xie, Terry Wall, Jianglong Yu, “Removal of sulfur at high temperatures using iron based sorbents supported on fine coal ash”, Fuel, 89, 2010, p868-873.

Xiangmei Meng, Weibren de Jong, Ranadeep Pal, Adrian H. M. Verkooijen, “In bed and downstream hot gas desulfurization during solid fuel gasification: A review”, Fuel processing technology, 91, 2010, p964-981.

Yasyerli S., Irfan Ar, Dogu G., Dogu T., “Removal of hydrogen sulfide by clinoptiolite in a fixed bed adsorber”, Chemical engineering and processing, 41, 2002, p785-792.

Zeynep Ozaydin, Sena Yasyerli, Gulsen Dogu, “Synthesis and activity of copper-incorporated MCM-41-type sorbents prepared by one-pot and impregnation procedures for H_2S removal,” Ind. Eng. Chem. Res., 47, 2008, p1035-1047.

Zhijiang Li, Flytzani-Stephanopoulos M., “Cu-Cr-O and Cu-Ce-O regenerable oxide sorbents for hot gas desulfurization”, Ind. Eng. Chem. Res., 36, 1997, p187-196.

Zeng Y., Zhang S., Grives F. R., Harrison D. P., “High temperature desulfurization with elemental sulfur production”, Chemical engineering science, 54, 1999, p3007-3017.

Zheng wang, Flytzani-Stephanopoulos M., "Cerium oxide-based sorbents for regenerative hot reformate gas desulfurization", Energy and Fuels, 19, 2005, p2089-2097.

Zeng Y., Kaytakoglu, Harrison D. P., "Reduced cerium oxide as an efficient and durable high temperature desulfurization sorbent", Chemical Engineering science, 55, 2000, p4893-4900.

APPENDIX – A

QUARTZ REACTOR DETAILS

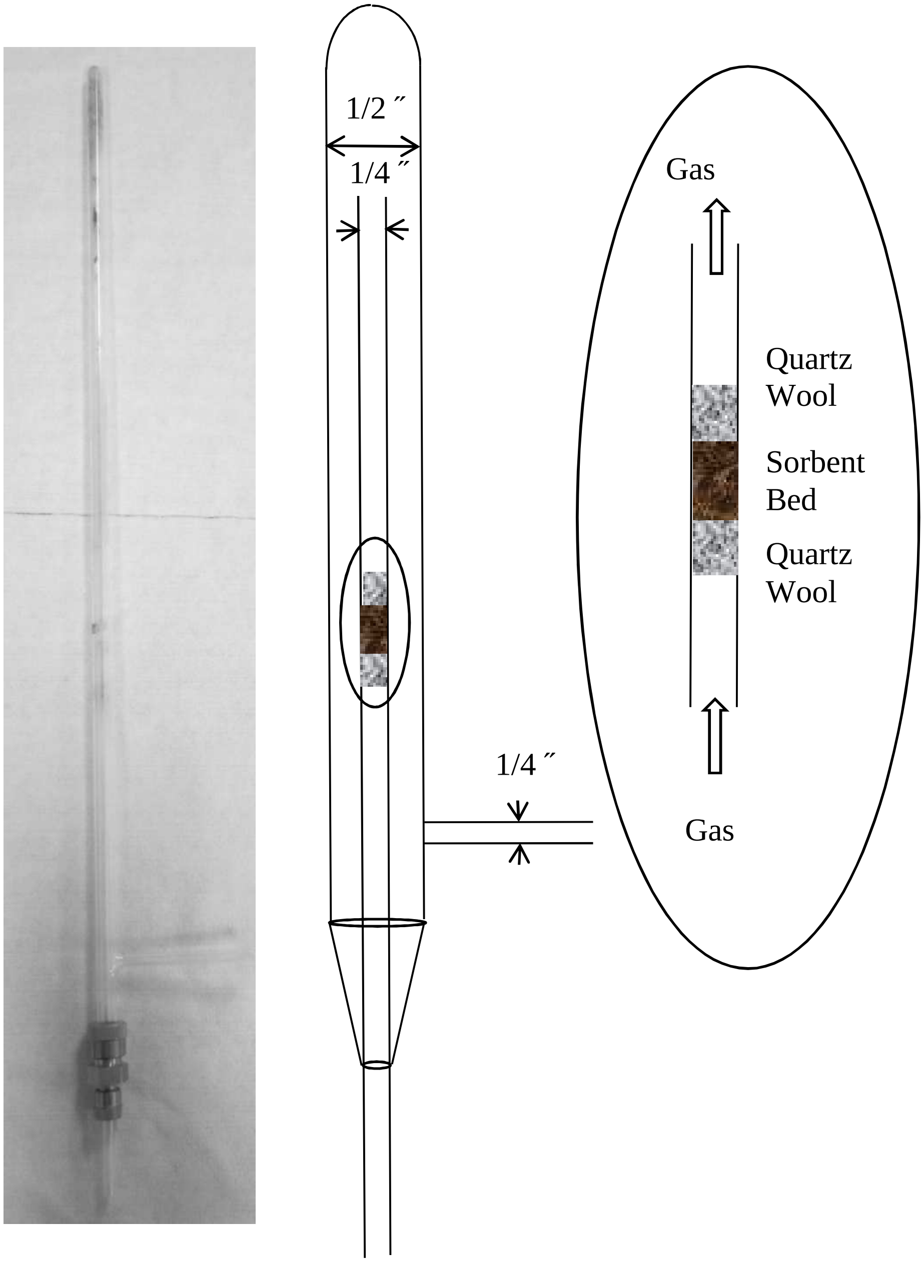

Figure A-1: Quartz packed bed reactor

APPENDIX – B

GAS CHROMATOGRAPHY DETAILS

Method Details

Table B.1: The test method used for gas analysis

CHANNEL 1		CHANNEL 2	
Item	**Specification**	**Item**	**Specification**
Column Temperature	75°C	Column Temperature	100°C
Injector Temperature	110°C	Injector Temperature	110°C
Inject Time	40 m sec	Inject Time	100 m sec
Backflush Time	7 sec	Backflush Time	0 sec
Initial pressure	25 Psi	Initial pressure	25 Psi
Run time	90 Sec	Run time	90 Sec

The Varian CP-4900 (Micro GC) is equipped with two detectors. The second installed channel, which is PPU (MGC BF MOD PPU 10m Hi, Field R) is mainly used for detecting the H_2S and SO_2 concentrations in this study in the outlet gas.The PPU channel was calibrated for H_2S as well as SO_2. The figures below show the linear calibration curve. The carrier or reference gas used for Channel 1 is Argon while for Channel 2 is Helium.

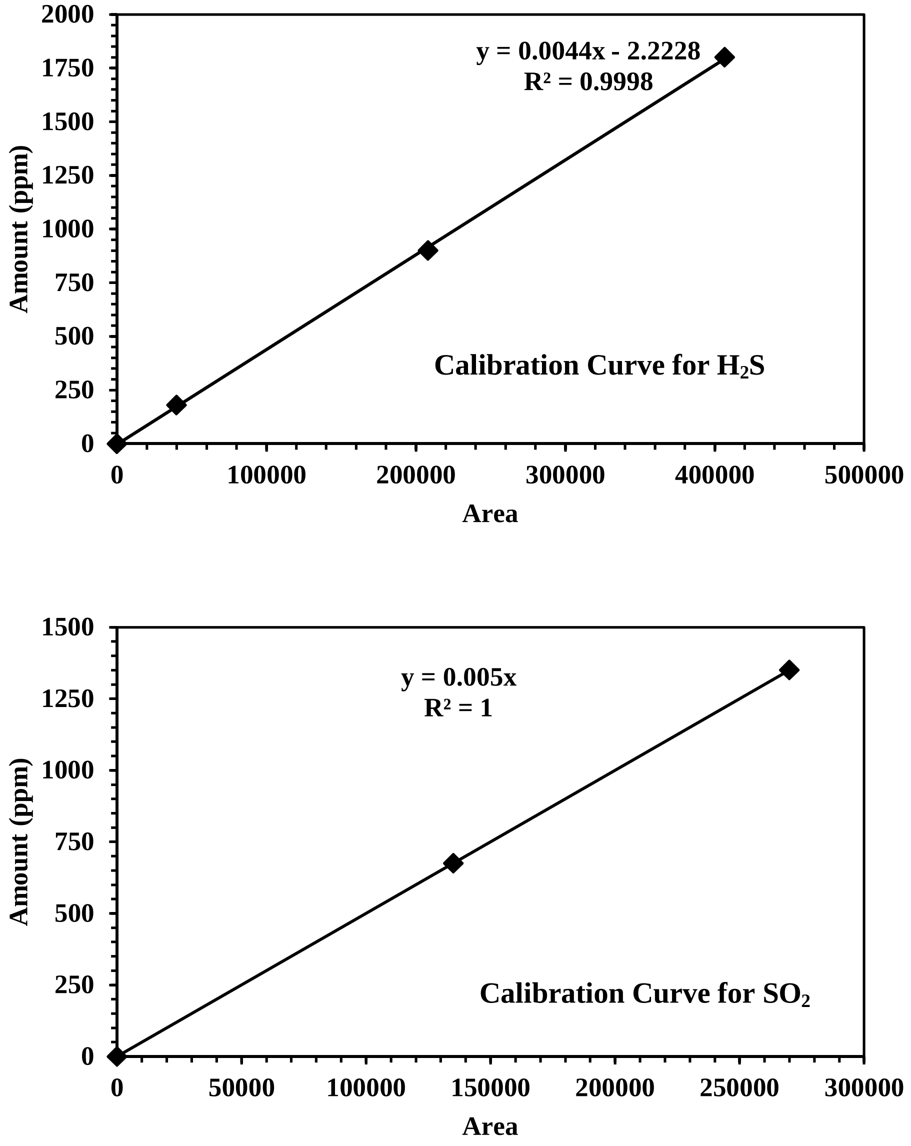

Figure B.1: Calibration Curves for GC

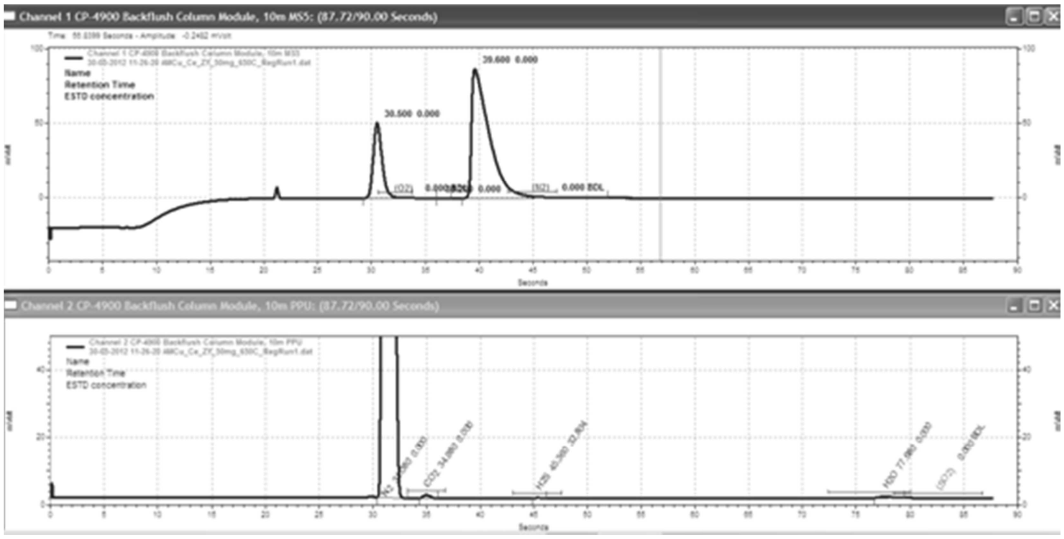

Figure B.2: Sample chromatograph for low H_2S concentration

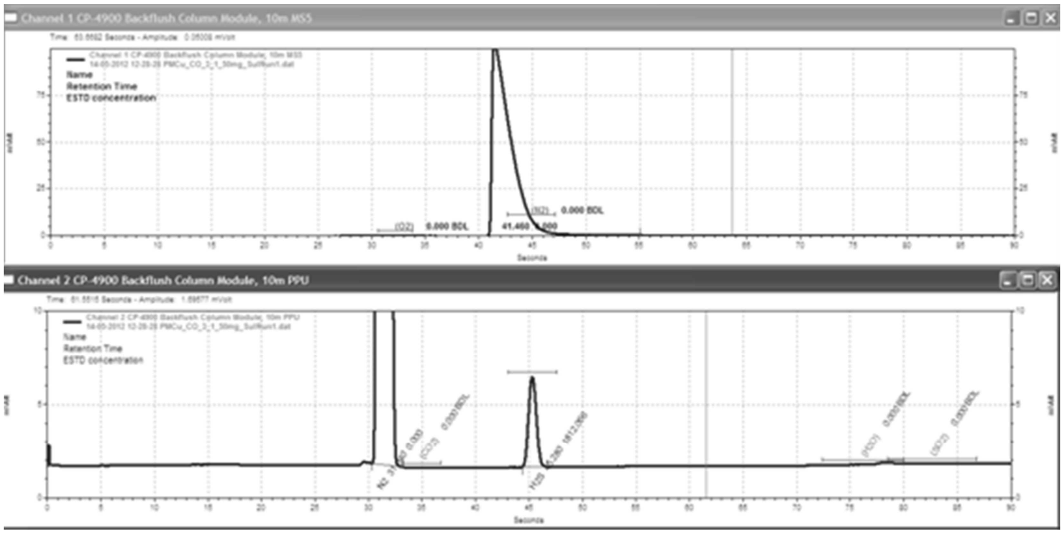

Figure B.3: Sample chromatograph for high H_2S concentration

APPENDIX – C

FACTSAGE 6.1 DATA

Phase stability diagrams for mixed metal oxide systems

Phase stability diagrams from Factsage helps to understand the regeneration and product phases formation with variation in the partial pressure of the gaseous components. The Cu-Ce-S-O and Cu-Co-S-O phase diagrams are received at various temperatures from Factsage. Figures B-2 and B-3 are the corresponding phase diagrams.

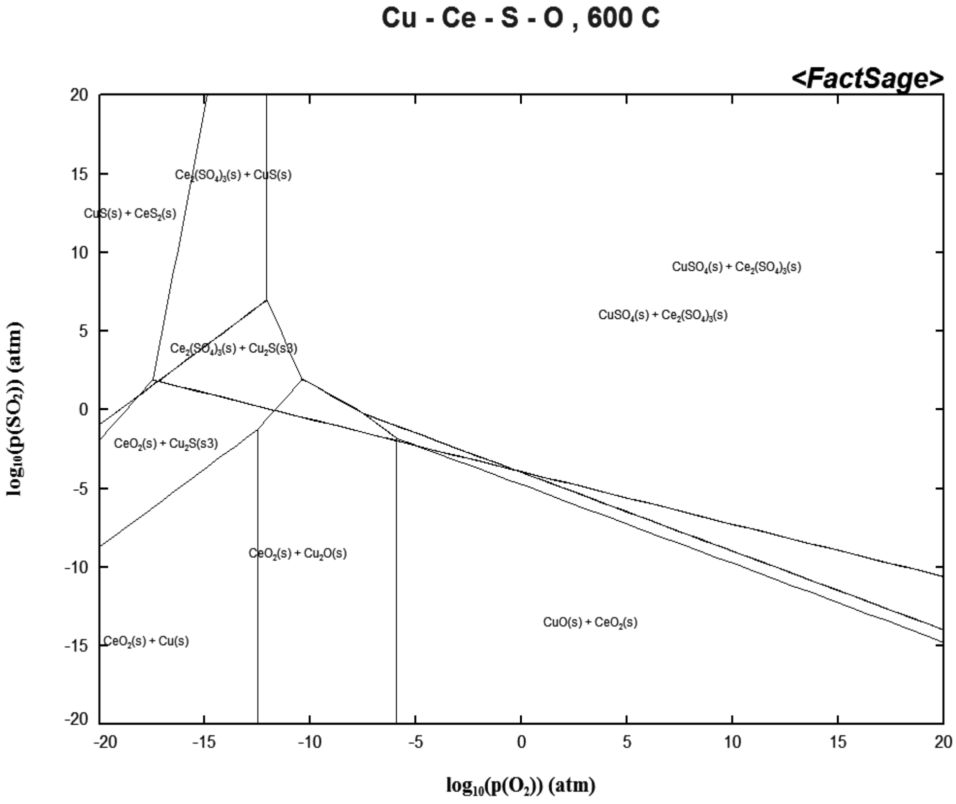

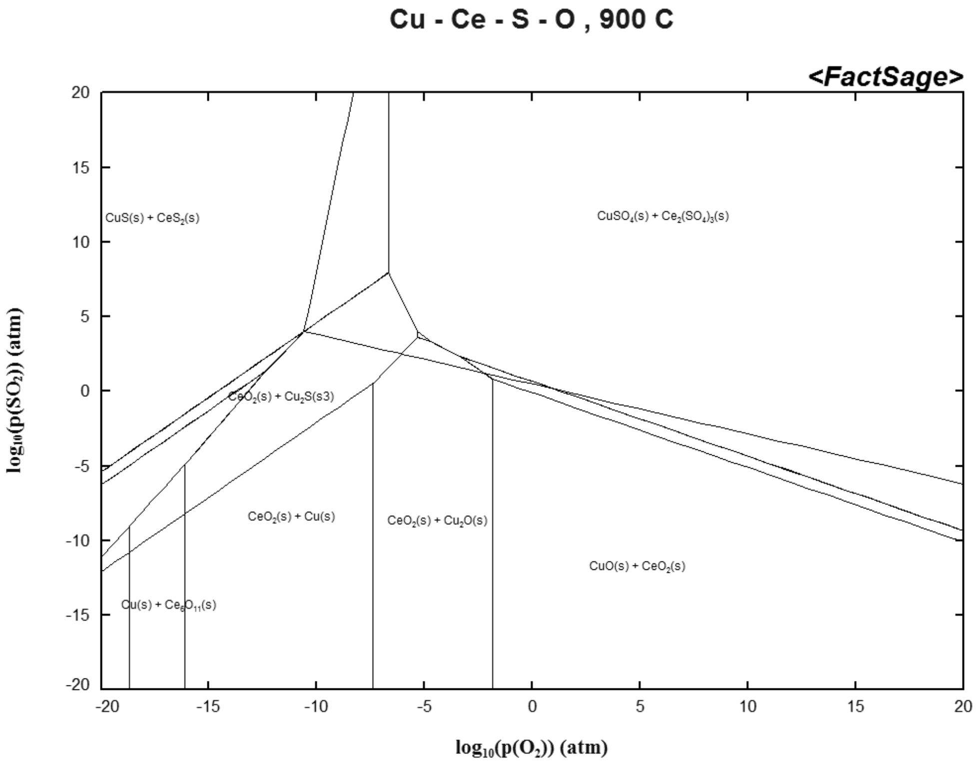

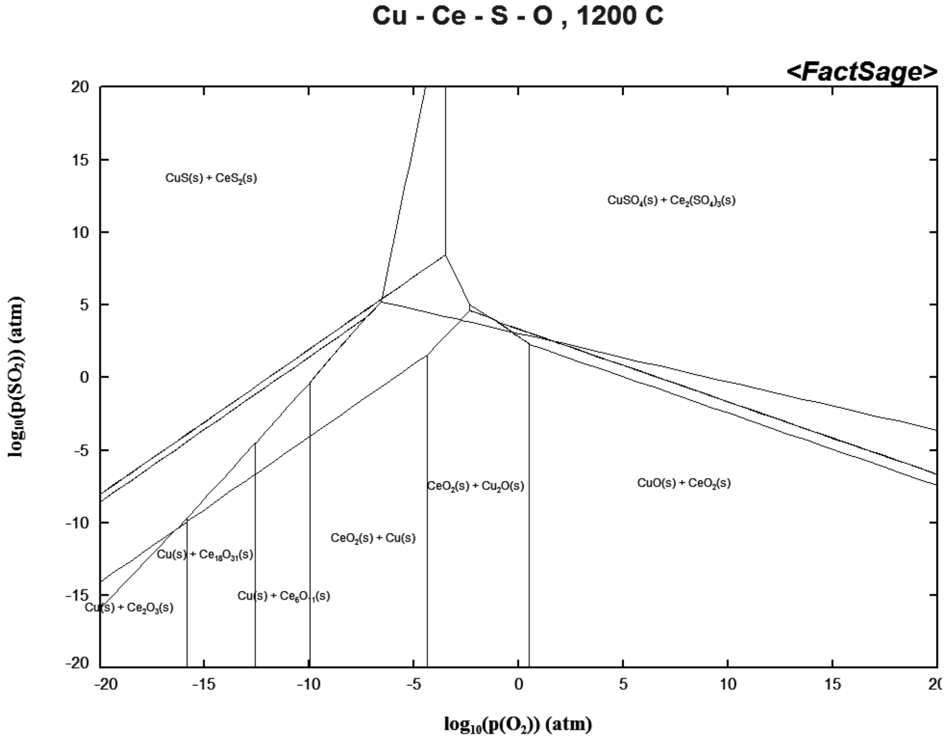

Figure C-1: Phase stability diagrams for Cu-Ce mixed metal oxide systems over a wide temperature range (600 to 1200 °C)

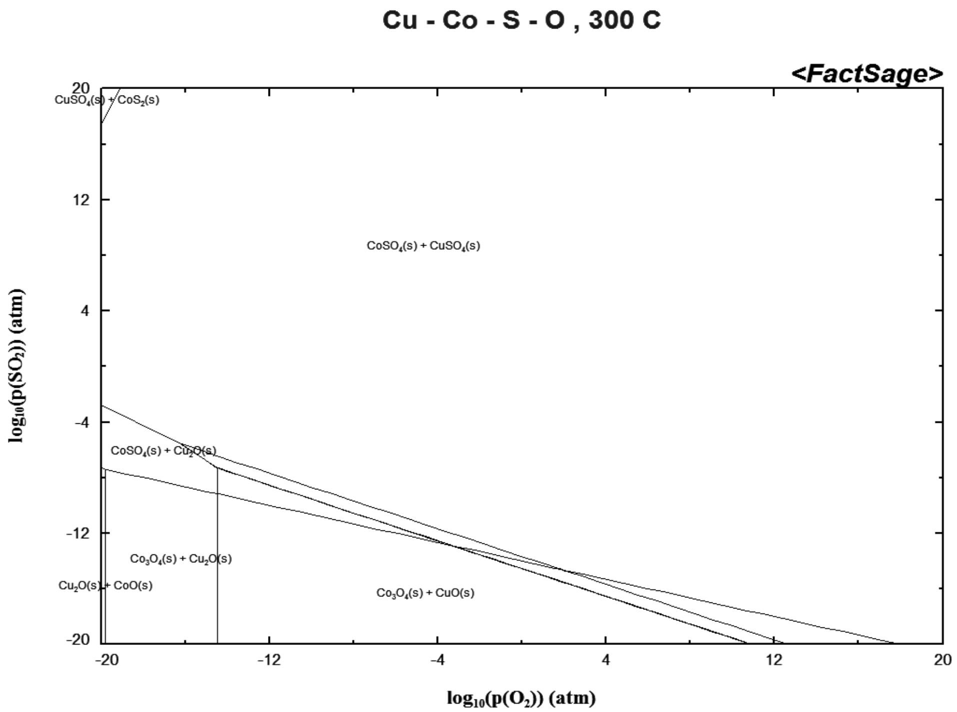
Cu - Co - S - O , 300 C
<FactSage>
$CuSO_4(s) + CoS_2(s)$
$CoSO_4(s) + CuSO_4(s)$
$CoSO_4(s) + Cu_2O(s)$
$Co_3O_4(s) + Cu_2O(s)$
$Cu_2O(s) + CoO(s)$
$Co_3O_4(s) + CuO(s)$
20
12
4
-4
-12
-20
-20
-12
-4
4
12
20
$\log_{10}(p(SO_2))$ (atm)
$\log_{10}(p(O_2))$ (atm)

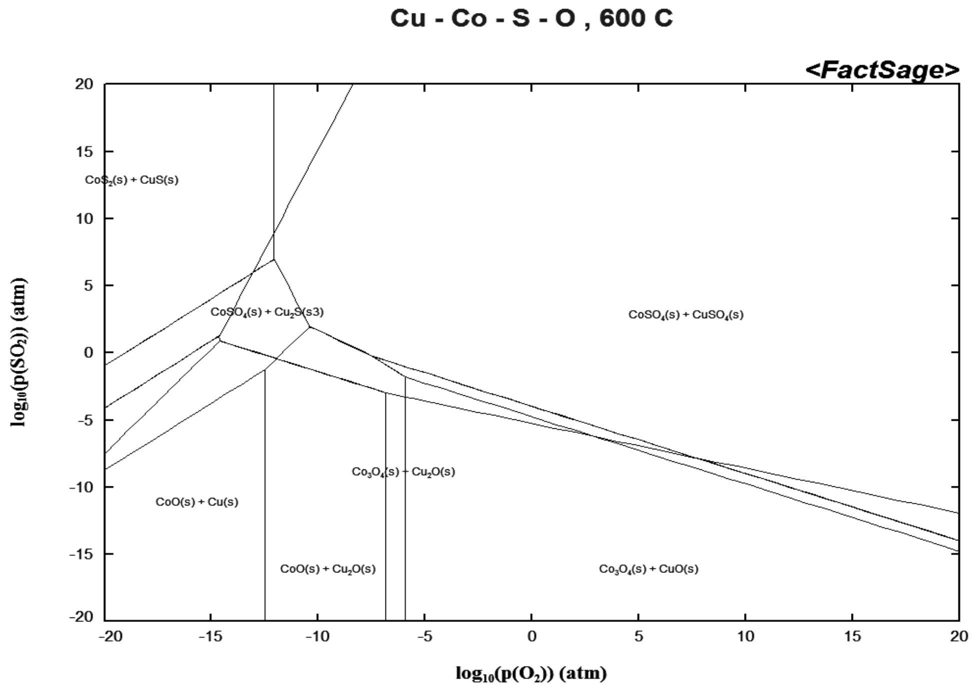
Cu - Co - S - O , 600 C
<FactSage>
$CoS_2(s) + CuS(s)$
$CoSO_4(s) + Cu_2S(s3)$
$CoSO_4(s) + CuSO_4(s)$
$Co_3O_4(s) + Cu_2O(s)$
$CoO(s) + Cu(s)$
$CoO(s) + Cu_2O(s)$
$Co_3O_4(s) + CuO(s)$
20
15
10
5
0
-5
-10
-15
-20
-20
-15
-10
-5
0
5
10
15
20
$\log_{10}(p(SO_2))$ (atm)
$\log_{10}(p(O_2))$ (atm)

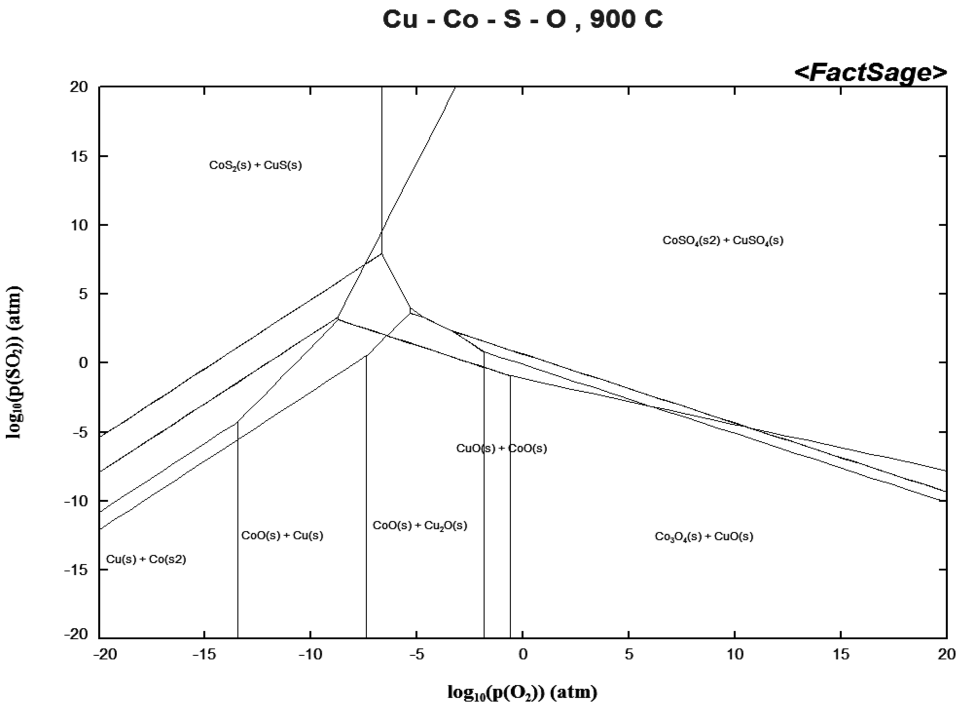

Figure C-2: Phase stability diagrams for Cu-Co mixed metal oxide sorbents over a wide temperature range (300 to 900 °C)

APPENDIX – D

Sample calculations

D-1: Calculation of n in CeO_n

The run was done at 550 °C with 15 % H_2, remaining N_2 and amount of sample taken was about 30 mg and the reduction level observed was 0.53% i.e. 0.159 mg loss.

Sorbent Charged in TGA = 30 mg

Moles of O in 30 mg of CeO_2 = $(30\times10^{-3}) / (172.115) \times 2 = 3.48 \times10^{-4}$

Weight loss in reduction = 0.159 mg

Equivalent mole of O = $(0.159\times10^{-3}) / (16) = 9.9375\times10^{-6}$

$n = ((3.48 \times10^{-4} - 9.9375\times10^{-6}) / 3.48 \times10^{-4}) \times 2= 1.942 = 1.94$

The value of n is 1.94

D-2: Calculation of sulfidation capacity

Gas flow rate: 200 sccm

Gas composition: 0.18 % H_2S and balance N_2

Amount of sorbent = 50 mg

H_2S in gas: 1800 PPM = $1800 \times 10^{-6} = 0.0018$ litre

= $0.0018 / 24.465 = 7.4 \times 10^{-5}$ Mols

= $7.4 \times 10^{-5} \times 34.1 = 0.00251$ gs of H_2S

Gas flow rate = 200 sccm

= 200 / 1000 = 0.2 l/min

The gas composition is 0.18 % H_2S and balance N_2

H_2S flow rate = 0.2 × (0.18/100) = 0.00036 l/min

= 0.00036/ 24.465 = 1.5×10^{-5} moles/min

= $1.5 \times 10^{-5} \times 34.1$ = 0.0005 g/min

H_2S flow rate = 0.0005 g/min

The content of sulfur = $1.5 \times 10^{-5} \times 32$ = 0.00047 g/min

The breakthrough (100 ppmv H_2S concentraion) observed for 3CuO-1CeO_2 sorbent at 550 °C is **17.50** mins (from Figure 4.19)

The sulfidation capacity = 0.00047 × 17.50 **= 0.00821** g of S

The sulfidation capacity for a bed of 50 mg is 0.00821 g of S

The sulfidation capacity for 100 g of sorbent = 0.00821 × (100 / 0.05)

= 16.42 g of S

The sulfidation capacity is 16.41 g of S per 100 g of sorbent

D-3: Calculation of dimensionless time

Calculation Hypothesis: Considering that, only Ce_2O_2S and Cu_2S were formed as the sulfidation product.

$2\ CeO_2 + H_2S + H_2 \rightarrow Ce_2O_2S + 2\ H_2O$

$2\ CuO + H_2S + H_2 \rightarrow Cu_2S + 2\ H_2O$

0.0125 g of CeO_2 = 7.2625×10^{-5}

Equivalent moles of H_2S = 3.6262×10^{-5}

H_2S flow rate = 1.47×10^{-5} moles/min

Reaction Time: 2.466 min ~ 2.5 min

0.0375 g of CuO = 4.7142×10^{-4}

Equivalent moles of H_2S = 2.3571×10^{-4}

H_2S flow rate = 1.47×10^{-5} moles/min

Reaction Time: 16.034 min ~ 16 min

Total reaction time = 16 min + 2.5 min = 18.5 min (=1 dimensionless time)

APPENDIX – E

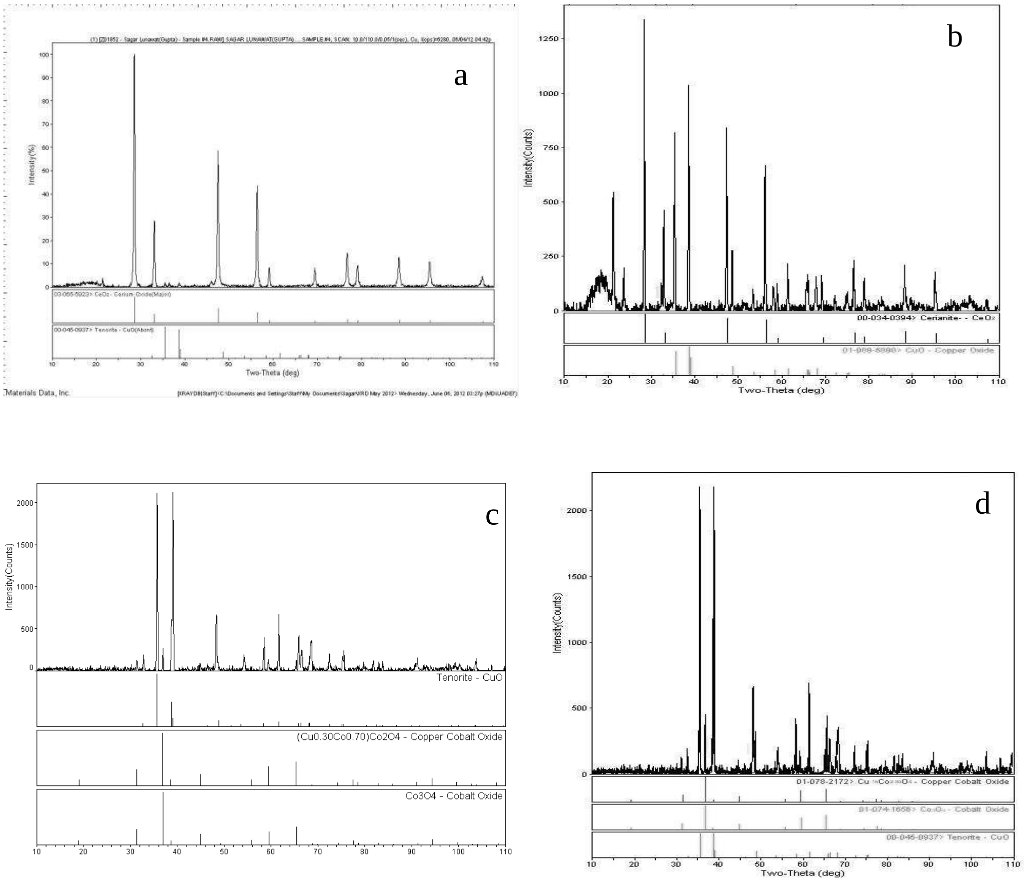

Figure E-1: XRD analysis of sorbent, (a = 3:1, b=1:3) CuO-CeO$_2$ and (c= 3:1, d=1:3) CuO-Co$_3$O$_4$ mixed metal oxide sorbents

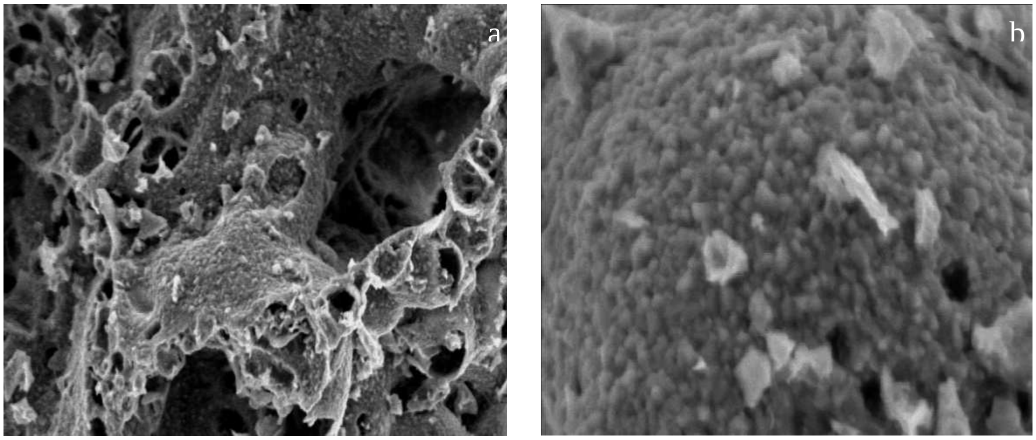

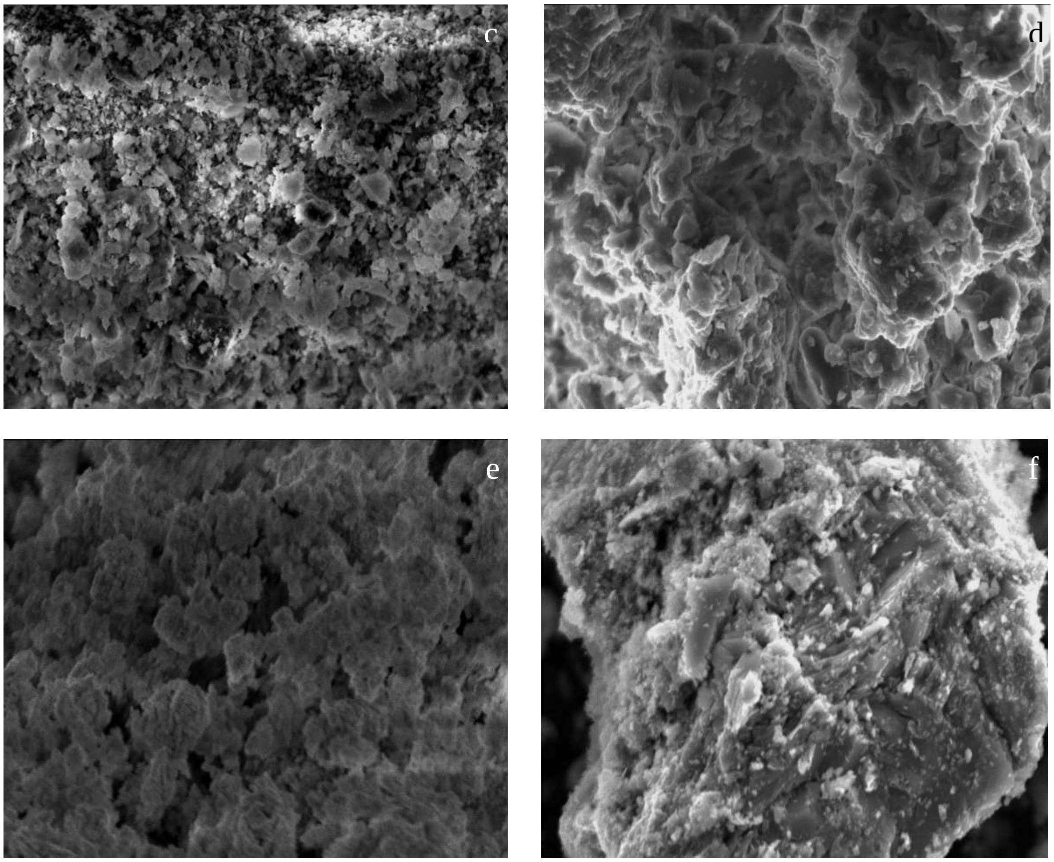

Figure E-2: SEM analysis of fresh sorbent, (a) 3CuO-1CeO$_2$, (b) 1CuO-3CeO$_2$, (c) Cu-Ce-CC, (d) Cu-Ce-CL, (e) Cu-Ce-ZY, (f) Ce-Co-CC

```
University of Alberta
Fsc: 3943  LSec: 30  18-Jul-2012  1:42 PM     kV: 40   uA: 500    (Rh)   2000um-Spot    Atm:Vacuum
A | C:\Documents and Settings\Administrator\Desktop\data\Sagar Lunawat(CME-Dr. Raj Gupta)\July 18 2012 - Sag
  | ar (Gupta) - #1 - Cu-Ce--CC.spc
```

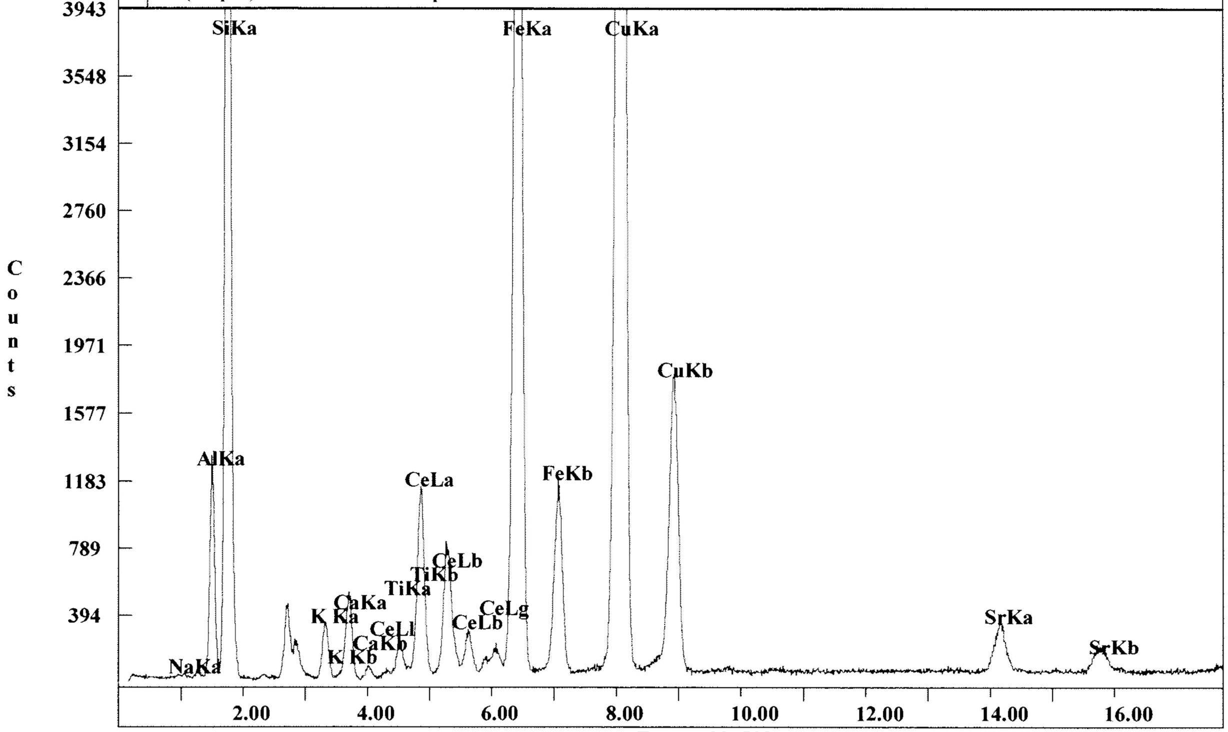

```
         Quantitative Results

 Element    Inte   Weight%  Atomic%
 NaK        5.97     4.40     6.04
 AlK      334.40    13.67    15.99
 SiK     2279.40    59.30    66.64
 K K      109.33     1.62     1.31
 CaK      167.00     1.69     1.33
 TiK       72.13     0.35     0.23
 CeL      412.30     4.92     1.11
 FeK     2979.87     5.91     3.34
 CuK     5134.83     7.93     3.94
 SrK      197.60     0.22     0.08

Stage X: 49.00 Y: 61.00 Z: 97.64
```

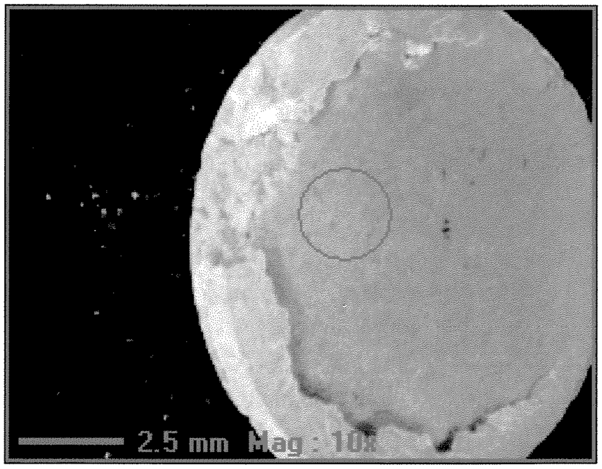

University of Alberta

Fsc: 5653 LSec: 30 18-Jul-2012 2:17 PM kV: 40 uA: 500 (Rh) 2000um-Spot Atm:Vacuum

A C:\Documents and Settings\Administrator\Desktop\data\Sagar Lunawat(CME-Dr. Raj Gupta)\July 18 2012 - Sagar (Gupta) - #3 - Cu-Ce--CL.spc

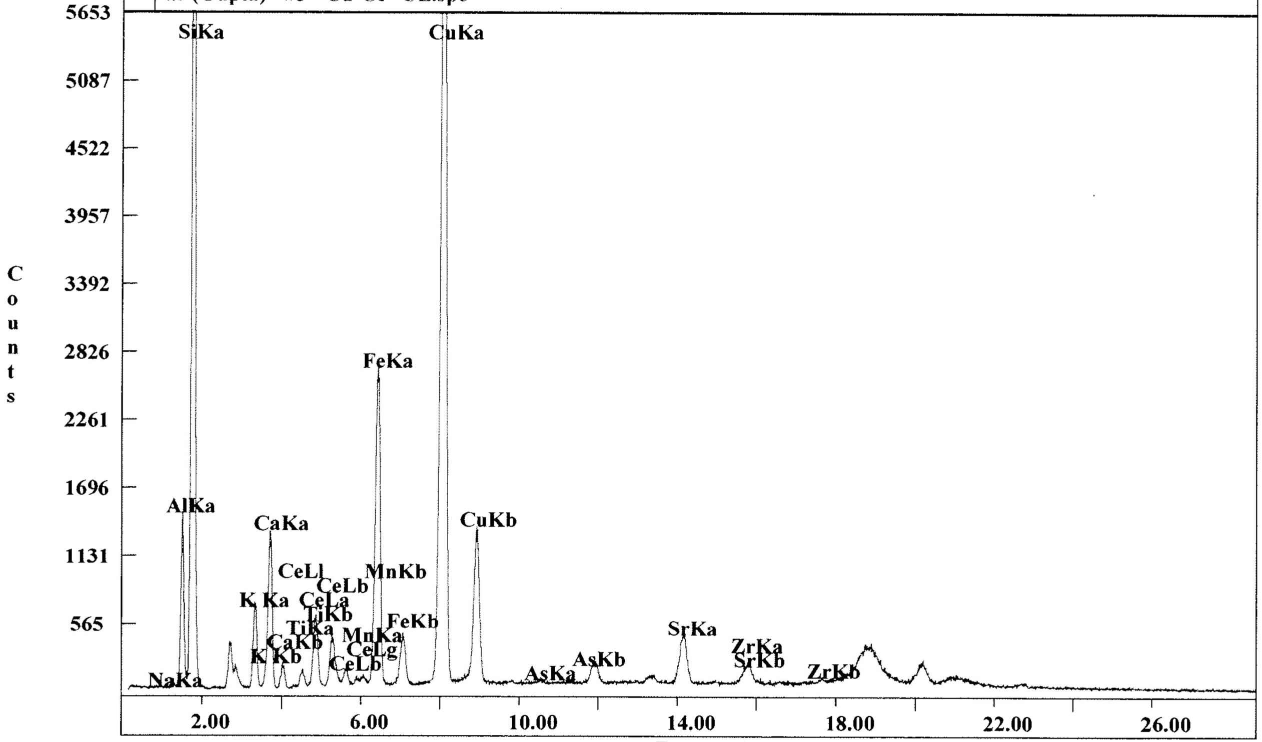

```
                Quantitative Results

  Element      Inte   Weight%   Atomic%
  NaK          2.07      1.39      1.86
  AlK        372.47     13.49     15.38
  SiK       2662.07     64.81     71.02
  K K        234.00      3.67      2.89
  CaK        455.77      5.10      3.92
  TiK         54.56      0.31      0.20
  CeL        224.90      3.09      0.68
  MnK         19.03      0.05      0.03
  FeK       1139.53      2.39      1.32
  CuK       3660.33      5.32      2.58
  AsK         21.00      0.02      0.01
  SrK        284.57      0.27      0.10
  ZrK         96.40      0.09      0.03

Stage X: 55.00 Y: 67.00 Z: 97.69
```

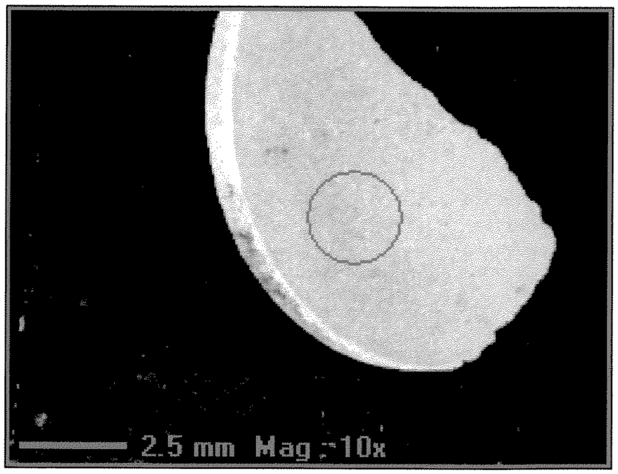

University of Alberta

Fsc: 5646 LSec: 30 18-Jul-2012 1:56 PM kV: 40 uA: 500 (Rh) 2000um-Spot Atm:Vacuum

A C:\Documents and Settings\Administrator\Desktop\data\Sagar Lunawat(CME-Dr. Raj Gupta)\July 18 2012 - Sagar (Gupta) - #2 - Cu-Ce--ZY.spc

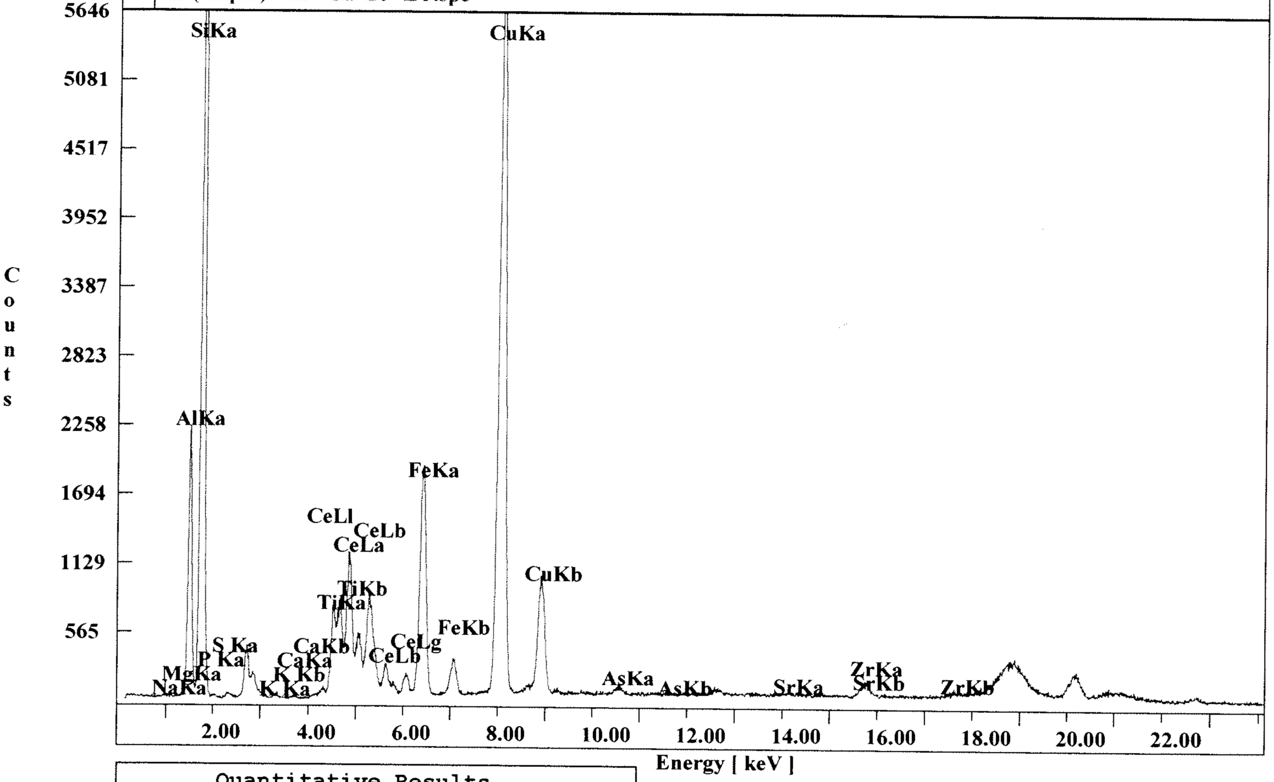

Quantitative Results

Element	Inte	Weight%	Atomic%
NaK	5.97	3.96	5.15
MgK	2.87	0.53	0.65
AlK	577.27	22.76	25.23
SiK	2013.57	59.48	63.35
P K	7.80	0.35	0.34
S K	12.63	0.29	0.27
K K	10.73	0.18	0.14
CaK	6.87	0.08	0.06
TiK	262.83	1.37	0.86
CeL	400.17	5.10	1.09
FeK	808.57	1.69	0.91
CuK	2837.07	4.06	1.91
AsK	40.33	0.04	0.02
SrK	23.83	0.02	0.01
ZrK	87.00	0.08	0.03

Stage X: 55.00 Y: 60.00 Z: 97.54

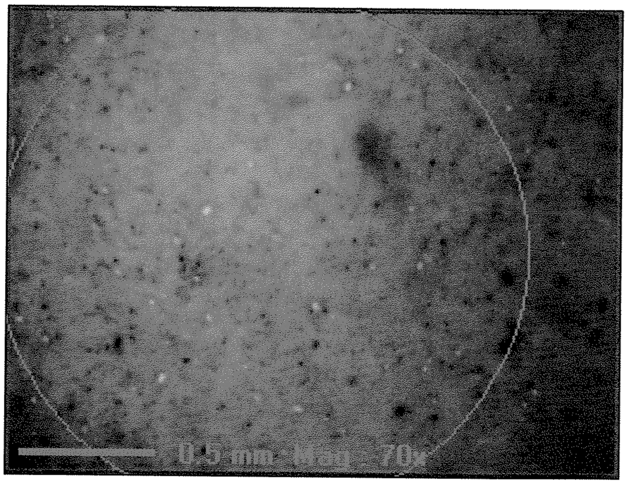

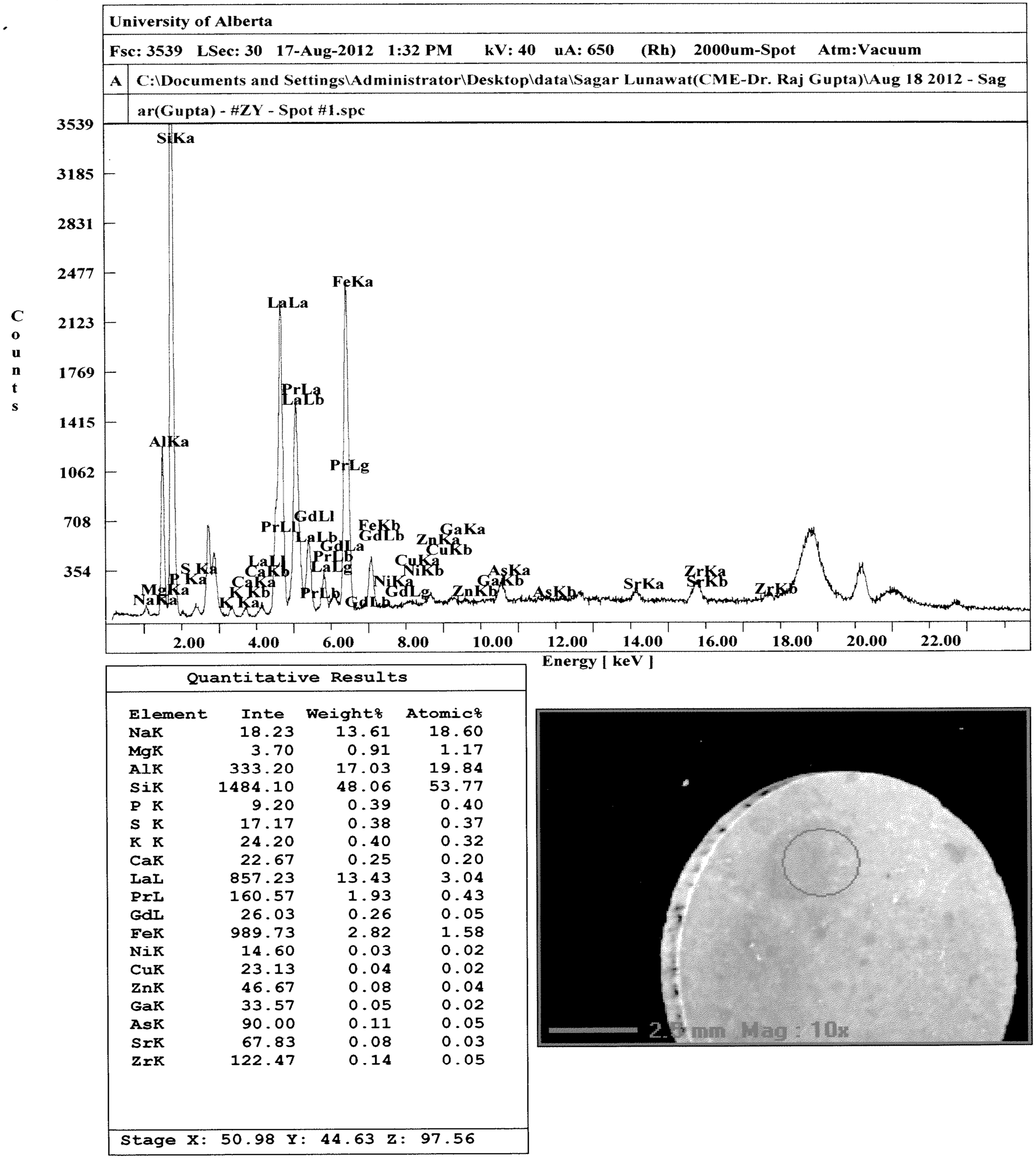

University of Alberta

Fsc: 3539 LSec: 30 17-Aug-2012 1:32 PM kV: 40 uA: 650 (Rh) 2000um-Spot Atm:Vacuum

A C:\Documents and Settings\Administrator\Desktop\data\Sagar Lunawat(CME-Dr. Raj Gupta)\Aug 18 2012 - Sagar(Gupta) - #ZY - Spot #1.spc

Quantitative Results

Element	Inte	Weight%	Atomic%
NaK	18.23	13.61	18.60
MgK	3.70	0.91	1.17
AlK	333.20	17.03	19.84
SiK	1484.10	48.06	53.77
P K	9.20	0.39	0.40
S K	17.17	0.38	0.37
K K	24.20	0.40	0.32
CaK	22.67	0.25	0.20
LaL	857.23	13.43	3.04
PrL	160.57	1.93	0.43
GdL	26.03	0.26	0.05
FeK	989.73	2.82	1.58
NiK	14.60	0.03	0.02
CuK	23.13	0.04	0.02
ZnK	46.67	0.08	0.04
GaK	33.57	0.05	0.02
AsK	90.00	0.11	0.05
SrK	67.83	0.08	0.03
ZrK	122.47	0.14	0.05

Stage X: 50.98 Y: 44.63 Z: 97.56

Figure E-3: XRF analysis of MMS-IZ sorbents

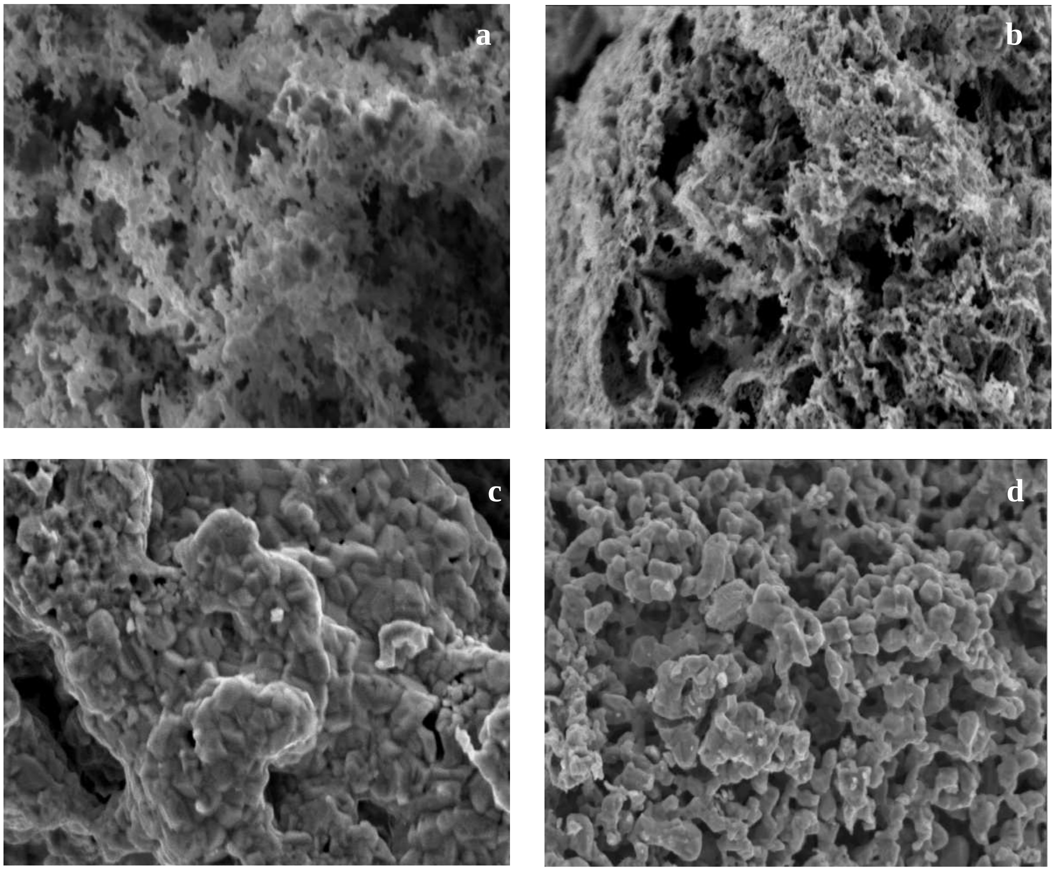

Figure E-4: SEM analysis of sulfided sorbents (a) 3CuO-1CeO$_2$, (b) 1CuO-3CeO$_2$, (c) 3CuO-1Co$_3$O$_4$, (d) 1CuO-3Co$_3$O$_4$

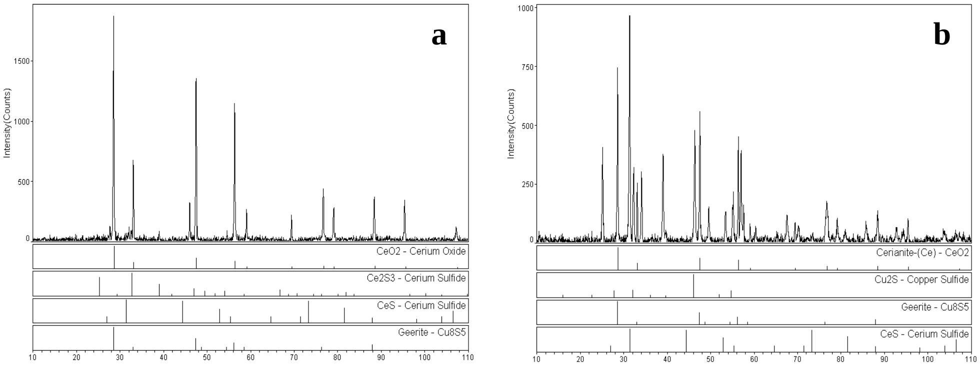

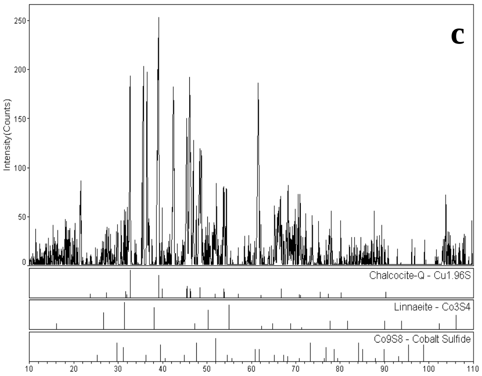

Figure E-5: XRD analysis of sulfided sorbents (a) 1CuO-1CeO$_2$, (b) 1CuO-3CeO$_2$, (c) 1CuO-1Co$_3$O$_4$

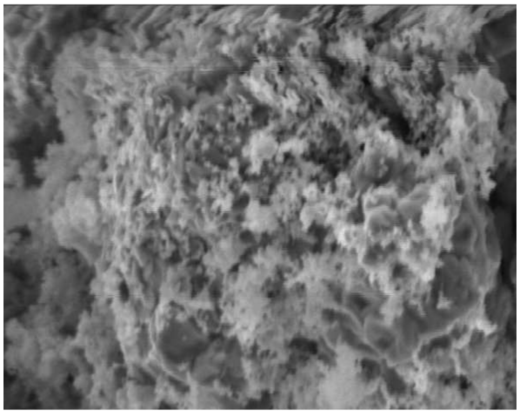

Figure E-6: SEM analysis of regenerated 3CuO-1CeO$_2$ sorbent

VITA

Sagar Narendra Lunawat was born to Narendra and Chhaya Lunawat, in Pune, India. He completed his high school education in Pune in 2004. He was accepted by University of Pune (AISSM's COE) into the Department of Chemical Engineering and earned a Bachelor of Engineering in 2008. In his curriculum, he participated and won various prizes at national level in India. He hosted various shows and starred on a television show in 2009. Upon graduation, he worked as a Process Engineer at Praj Industries Limited, Pune. He continued his education in the graduate program of University of Alberta, Department of Chemical Engineering (2010). He was elected as the Vice president Student services at Graduate student's association - University of Alberta in 2011 and served on various committees. This thesis completes his requirements to receive the degree of Master of Science in Chemical Engineering.